COMPUTER AIDED DESIGN FOR ROBUST CONTROL USING THE QFT METHOD

By

ARGYRIOS ZOLOTAS

Supervisor: Dr G D Halikias

Assessor: Dr H J Strangeways

The University of Leeds

Department of Electronic and Electrical Engineering

April, 30, 1998

Dedicated to my beloved parents
and sister

Αφιερωμένο στους αγαπημένους μου γονείς
και στην αγαπημένη μου αδελφή

TABLE OF CONTENTS

ACKNOWLEDGEMENTS

I would like to express my gratitude to my supervisor, Dr G D Halikias for all his help, guidance encouragement and interest throughout my work. I extend my thanks to all my close friends also for their patience and support.

I am grateful to the University of Leeds, which provided me with the necessary support for completing the final year project.

I should also like to thank my parents for their financial support throughout my time at Leeds.

OBJECTIVES OF THE PROJECT

- To develop software tools for robust control design of highly uncertain systems involving the QFT method.

- To carry out a comprehensive case study and illustrate the method via appropriate examples.

- To automate the control design (loop shaping) stage using optimisation techniques

ABSTRACT

This report outlines the full work on the final year project. The project's title is 'CAD for robust control using the QFT design method '. The aim of the project is to develop software tools, suitable for the robust control design of highly uncertain SISO systems. The design of these systems is based on I Horowitz' s QFT method. This is a frequency domain loop-shaping design technique, which is fully described in Chapter 2. The report is a step-by-step guide to the design. It includes an introduction to control and robust systems, an explanation of the QFT method, and the problem definition of the design using an illustrative example. It continues with designs of phase lead and lag compensators via graphical techniques. Next the application of optimisation methods for the design of optimal PD and PID controllers is discussed. Designing an appropriate pre-filter completes the design procedure. Finally, a number of simulations show that the design technique was successful and meets the given specifications. The report concludes with a summary of the project work and its results and suggests future directions, which can be followed in order to improve certain aspects of the design. The Appendix summarises aspects of the theories used for the purposes of the project and a list of Matlab files created and used.

LIST OF FIGURES

Appendices

LIST OF TABLES AND FLOW DIAGRAMS

LIST OF SYMBOLS

$K(s)$	controller (s-domain)
$G(s)$	plant (s-domain)
$G_o(s)$	nominal plant (s-domain)
$F(s)$	of pre-filter (s-domain)
$L(s)$	open loop (s-domain)
$L_o(s)$	nominal open loop (s-domain)
$R(s)$	reference input (s-domain)
$D(s)$	disturbance (s-domain)
$Y(s)$	output signal (s-domain)
P	parameter space
T_R	input-output tracking bounds
T_D	disturbance bounds
$T_R(s)$	tracking control ratio
$\delta_R(j\omega)_{HF}$	spread of tracking bounds at high frequencies
M_p	peak overshoot
t_s, t_x	settling time
t_p	peak time
B_u	upper tracking bound
B_l	lower tracking bound
ω_i	i-th frequency element
M_D	disturbance rejection model
ω_n	natural frequency
p_u	percent undershoot
$|x|$	absolute value of x, magnitude of x
$|x|_{dB}$	magnitude of x in dBs
A	matrix $A=[a_{ij}]$ $n\times m$
A^T	transpose of matrix A
$R(A), \mathfrak{R}(A)$	range of matrix A
$R^{n\times m}$	real vector space of real $n\times m$ vectors
R^n	real vector space of real n-vectors
0	zero scalar, matrix or vector
a_{ij}	i-th, j-th element of a matrix

rank(A)	rank of matrix A
$S^{\perp}$	S perp. (perpendicular to S)
ζ	damping factor
$\sigma_i(A)$	i-th singular value of matrix A

ABBREVIATIONS AND ACRONYMS

CL	Closed Loop
ES	Error Signal
GUI	Graphical User Interface
HF	High Frequency(-ies)
LHP	Left Hand Plane
LHS	Left Hand Side
LTI	Linear Time Invariant
MATLAB	MAtrix LABoratory
MIMO	Multi-input, Multi-output
MISO	Multi-input, Single-output
NC	Nichols Chart
NP	Nyquist Plane
OL	Open Loop
PD	Proportional plus Derivative
PI	Proportional plus Integral
PID	Proportional plus Integral plus Derivative
QFT	Quantitative Feedback Theory
RHP	Right Hand Plane
RHS	Right Hand Side
RI	Reference Input
SISO	Single-input, Single-output
SVD	Singular Value Decomposition
TDF	Two Degrees of Freedom
TF	Transfer Function
UHFB	Universal High Frequency Bound

CHAPTER ONE

INTRODUCTION TO CONTROL SYSTEMS, UNCERTAINTY AND ROBUST CONTROL

1.1 Control Systems

There are two types of Control Systems, Open Loop & Closed Loop Systems illustrated in figure 1.1.A:
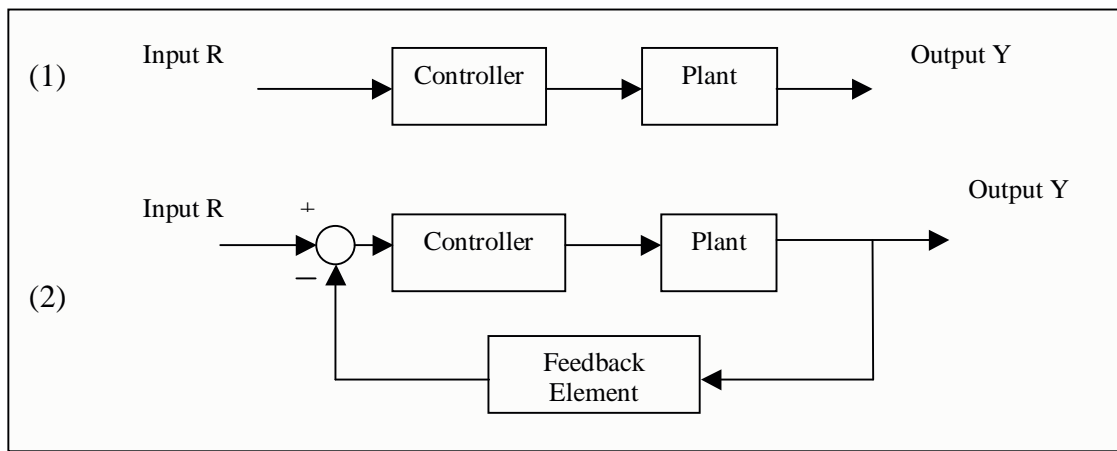
Figure 1.1.A: (1) Open loop and (2) Closed Loop Systems

In the case of open loop systems, the output has no effect on the input signal. In the case of closed loop systems, however the output through the feedback element affects the input signal, ideally '*in such a manner as to maintain the desired output value*' [Ref.1]. The feedback element '*provides the means for feeding back the output signal, in order to compare it with the reference input signal*' [Ref.1]. Often, undesirable external input signals can enter the feedback loop and they have effects on the output (Open-Loop systems) or on both the output and the input (Closed-Loop systems). One type of such signals, are external disturbances. Figure 1.1.B, shows an external step disturbance signal entering at the plant's output:
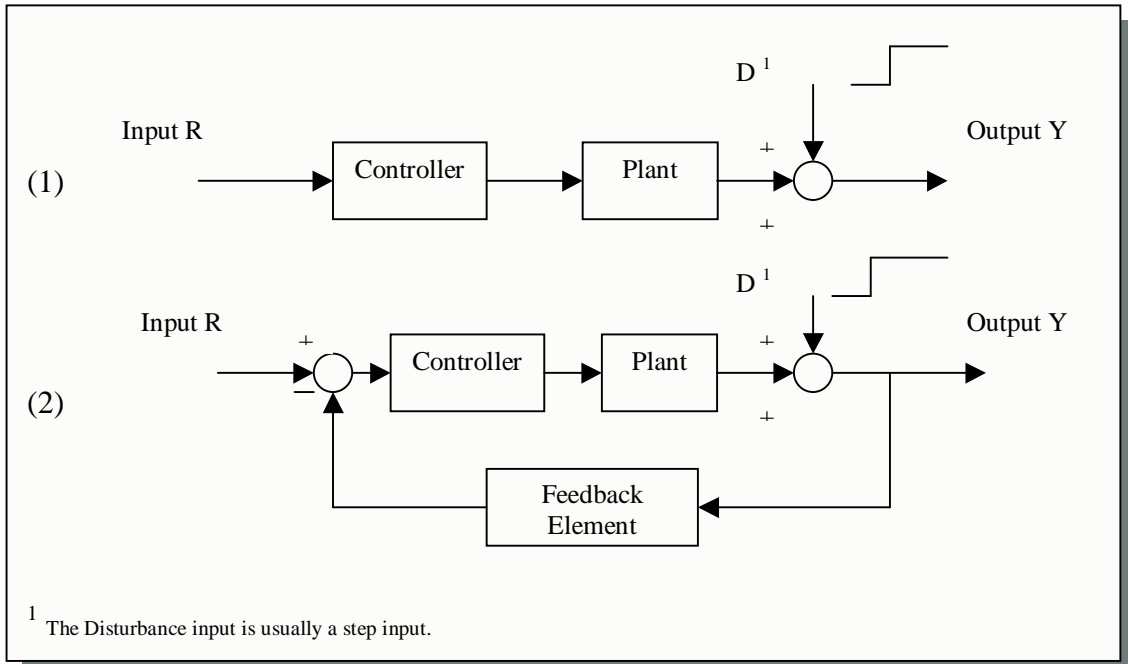
Figure 1.1.B: (1) Open loop and (2) Closed loop systems, with external disturbance

From the above figure, in the Open loop system, the disturbance appears directly on the output and as a result it cannot be attenuated by means of the controller. In the Closed loop system however, the disturbance affects both the output and the input signals. It is thus possible to reduce its effect on the output by designing a controller *K(s)* appropriately.

In addition to disturbance rejection the control system should also have good tracking properties (the output should follow the reference input fast and accurately with small steady state errors {s.s.e}) and also good stability margins.

1.2 Uncertainty and Robust Control

The design of a control system according to classical methods assumes full knowledge of the plant and the controller. In practical systems, however, the plant model will always be an inaccurate representation of the actual physical system due to:

- *Parameter changes*

- *Unmodeled dynamics*

- *Unmodeled time delays*

- *Changes in equilibrium point (operating point)*

Table 1.2.a: Reasons of inaccurate representation of a practical physical system, by a plant model

Robust Control methods address the problem of uncertainty systematically. They aim to maintain adequate performance and stability margins despite the presence of uncertainty in the dynamics of the plant. For the purposes of this project QFT was used in the design and analysis of control systems characterised by significant uncertainty and undesired external inputs [Ref.1,2,3,4]. A robust control system has the following characteristics:

- Low sensitivities to parameter changes

- Closed loop stability is maintained within the range of parameter change

- Its performance does not deteriorate rapidly with parameter change

Table 1.2.b: Characteristics of a Robust Control System

The meaning of the above terms is illustrated in the example of figure 1.2.A:
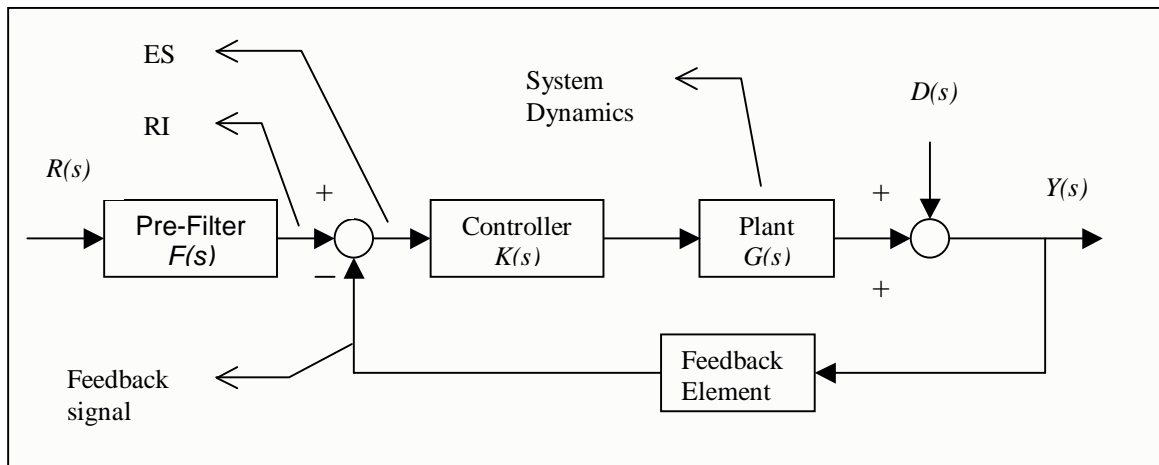
Figure 1.2.A: TDF control system plus external disturbance at the output of the plant.

The main example of a plant model[2] that considered in this report is taken as the following second order system:

$$G(s) = \frac{ka}{s(s+a)}, \text{ where } k \in [1,10] \text{ and } a \in [1,10] \tag{1}$$

This model is simply used to illustrate the design method. The software developed was written with general SISO plants in mind [Ref.1]. In equation (1), k and a are uncertain but constant parameters varying in the given ranges. The region of plant uncertainty is shown in figure 1.2.B:
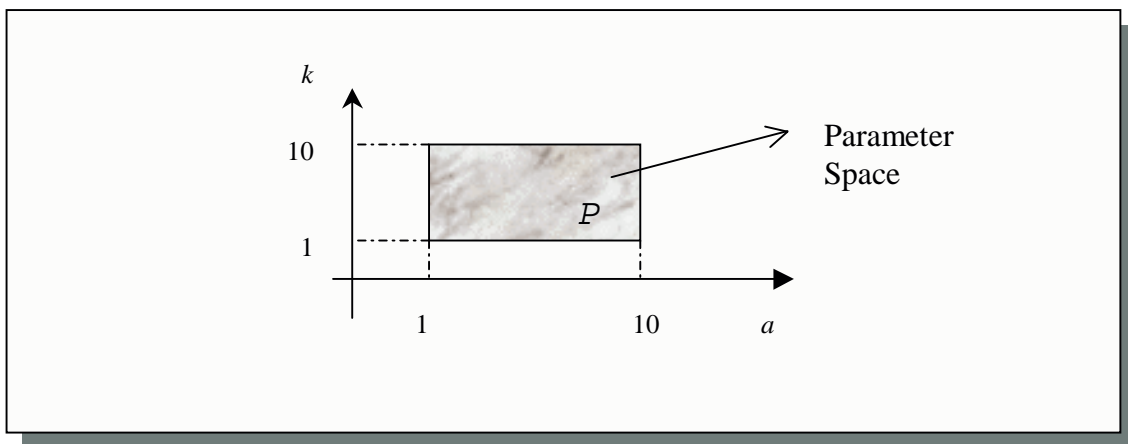
Figure 1.2.B: Region of plant uncertainty (known as *Parameter Space*)

Note that this plant has significant uncertainty due to the range of its uncertain parameters. Since the parameters a and k can vary simultaneously, the plant exhibits both gain and phase uncertainty in the frequency domain. The main objective of robust control in this case is to maintain the stability and performance properties of the closed loop system, as a and k vary in the indicated ranges.

---

[2] In Chapter Four, other plant models are used to illustrate the performance of the design methods.

CHAPTER TWO

QUANTITATIVE FEEDBACK THEORY

2.1 The Development of QFT

QFT is a frequency domain loop shaping design method [Ref.1,2,3,4]. I M Horowitz proposed this method in 1969 and since then it has been developed for SISO, MISO and MIMO LTI uncertain plants. In addition, the method has also been extended to non-linear and time-varying systems. QFT is a systematic design methodology for systems characterised by significant parameter uncertainty.[3]

2.2 Design method (Problem Definition)

QFT emphasises the use of feedback in order to achieve adequate robust system performance tolerances despite the presence of plant uncertainty and disturbance signals. It formulates, by *quantitative means*, the design objectives in terms of the following sets [Ref.1]:

1. $\boldsymbol{T_R}$ = {T_R} and $\boldsymbol{T_D}$ = {T_D}, acceptable tracking input-output bounds and acceptable disturbance output bounds, respectively, typically defined in the frequency domain (i.e. in terms of magnitude Bode plots).
2. $\boldsymbol{P}$ = {P}, possible uncertain plants, defined either in the frequency domain ('*uncertainty templates')* or in the *parameter-space.*

The objective is to guarantee that the control ratio T_R (between the reference input and the system's output) will exist within the bounds $\boldsymbol{T_R}$; and that the ratio T_D (between the disturbance input and the system's output) will exist within the bounds $\boldsymbol{T_D}$, for all P in $\boldsymbol{P}$. Thus, the technique proposes that the designed system has to meet the tracking specifications and has to reject the disturbance input for all possible plants. For the purposes of this project, QFT theory is applied to a SISO system, which includes external disturbance input.[4] For illustration purposes the TDF unity feedback cascade compensated system of figure 1.2.A will be used. The plant model is given by equation (1) and the parameter space is shown in figure 1.2. The reference and the disturbance signals are both unit step inputs {R_o=1, D_o=1}.

---

[3] There are alternative techniques with the same aim, i.e. H_∞ optimal control

[4] The system can be described as a pseudo-MISO system due to the existence of the external disturbance, although MISO systems are normally characterised by the presence of multiple reference inputs

2.3 Design specifications (Tracking Models)

The closed loop system has to satisfy a number of specifications. These correspond to the closed loop time responses to specific reference or disturbance input signals. For the purpose of QFT these are first translated in the frequency domain. The tracking control ratio models are based on a simple second order system and are synthesised in order to specify time and gain tolerance responses (under-damped and over-damped conditions) [Appendix A] [Ref.1]. In this case the upper and lower bounds of the tracking control ratios {$T_R(s)$} are shown below:

Upper tracking bound, under-damped with peak gain M_P=1.2 (approx. 20% overshoot) and with settling time t_s=2 sec.

$$T_{R_U}(s) = \frac{0.6584(s+30)}{(s+2\pm j3.969)} \tag{2}$$

Lower tracking bound, over-damped with settling time t_s=2 sec.

$$T_{R_L}(s) = \frac{8400}{(s+3)(s+4)(s+10)(s+70)} \tag{3}$$

The zero at *s=-30* {term *(s+30)*} in (1) and the pole at *s=-70* {term *(s+70)*} in (2), were introduced because the difference between the upper and the lower tracking bounds at high frequencies $\delta_R(j\omega_i)_{HF}$ needs to be wider compared to the high frequency model uncertainty. Figures 2.3.A and 2.3.B show the time domain step responses and the frequency domain responses, of the upper and lower bounds, respectively.
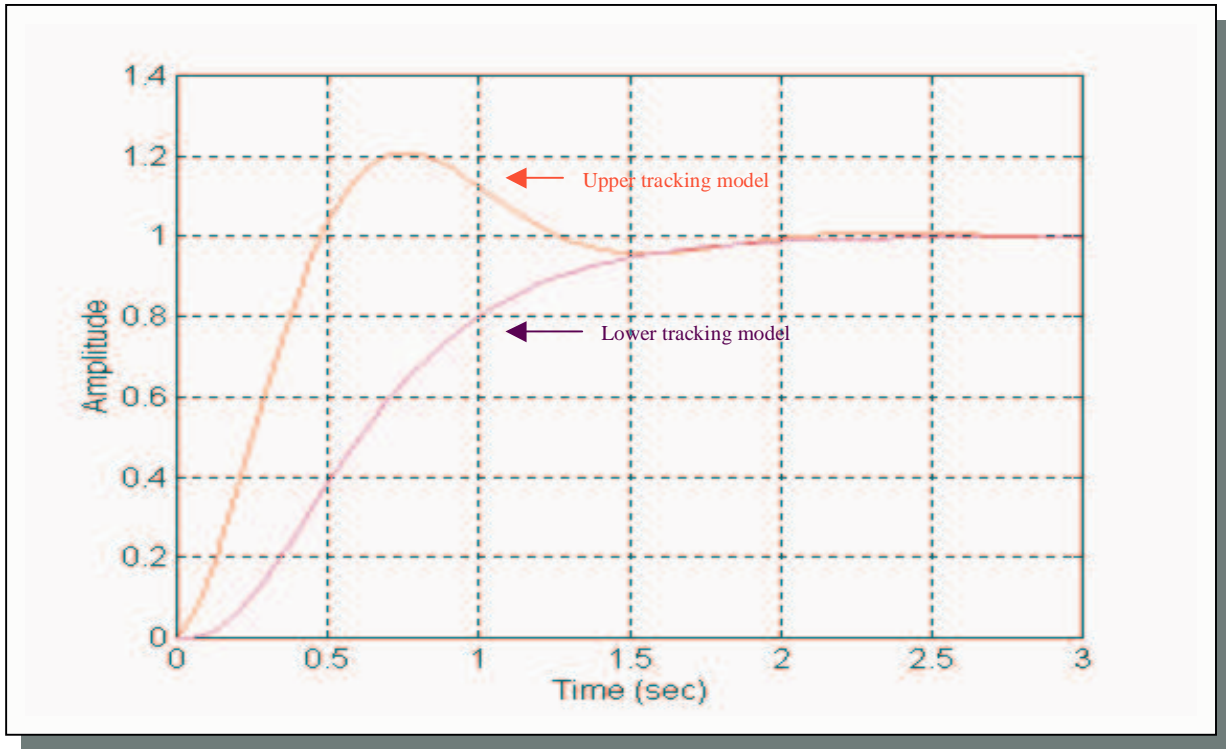
Figure 2.3.A: Time domain step responses of upper and lower tracking models
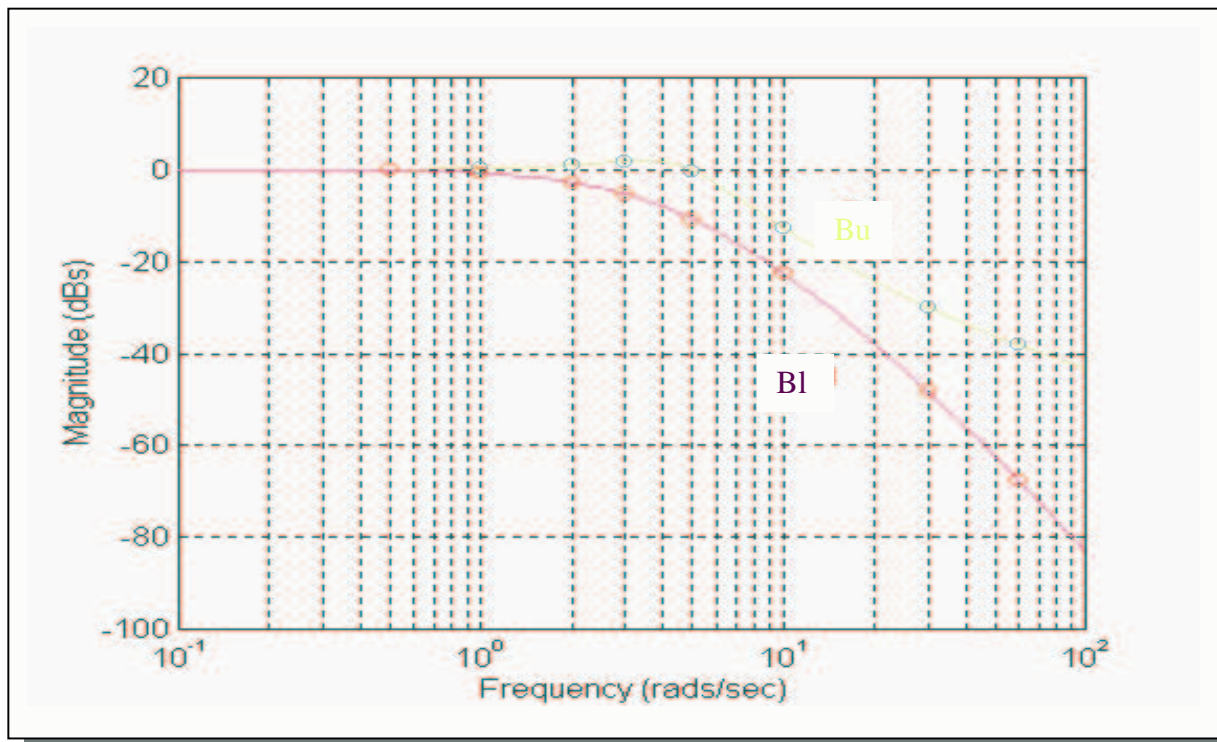
Figure 2.3.B: Frequency response of upper and lower tracking bounds Bu and Bl, respectively

The difference between the upper and lower bounds $\delta_R(j\omega_i)$ in figure 3.2.B, for eight chosen frequencies is given in Table 2.3.a.

Frequencies (rads/sec)	0.5	1.0	2.0	3.0	5.0	10.0	30.0	60.0
Difference $\delta_R(j\omega_i)$ (dBs)	0.26	1.03	3.72	7.14	10.57	9.85	18.30	29.45

Table 2.3.a: Tracking specifications $\delta_R(j\omega_i)$, i = 1,2,3,… (in dBs)

Function **track_ul()** was used to produce the frequency and time domain step responses of the upper and lower models.

2.4 Translation of Parameter Space Uncertainty into Uncertainty Templates

QFT assumes that the plant uncertainty can be represented by a set of templates on the complex plane, known as *uncertainty templates* [Ref.1]. Each template encloses all the possible frequency responses of the plant for a specific frequency ω_i. As an example, eight frequencies are considered $\omega_i=\{0.5, 1\ 2, 3, 5, 10, 30, 60\}$ rads/sec and as a result eight uncertainty templates will be formed. The complex plane, on which the uncertainty templates are displayed, is known as the Nichols Chart (NC). It represents the open loop gain of a system in dBs versus the open loop phase of the system in degrees, in the frequency domain. One uncertainty template, in this case for $\omega_5=5$ rads/sec, is shown in figure 2.4.A:
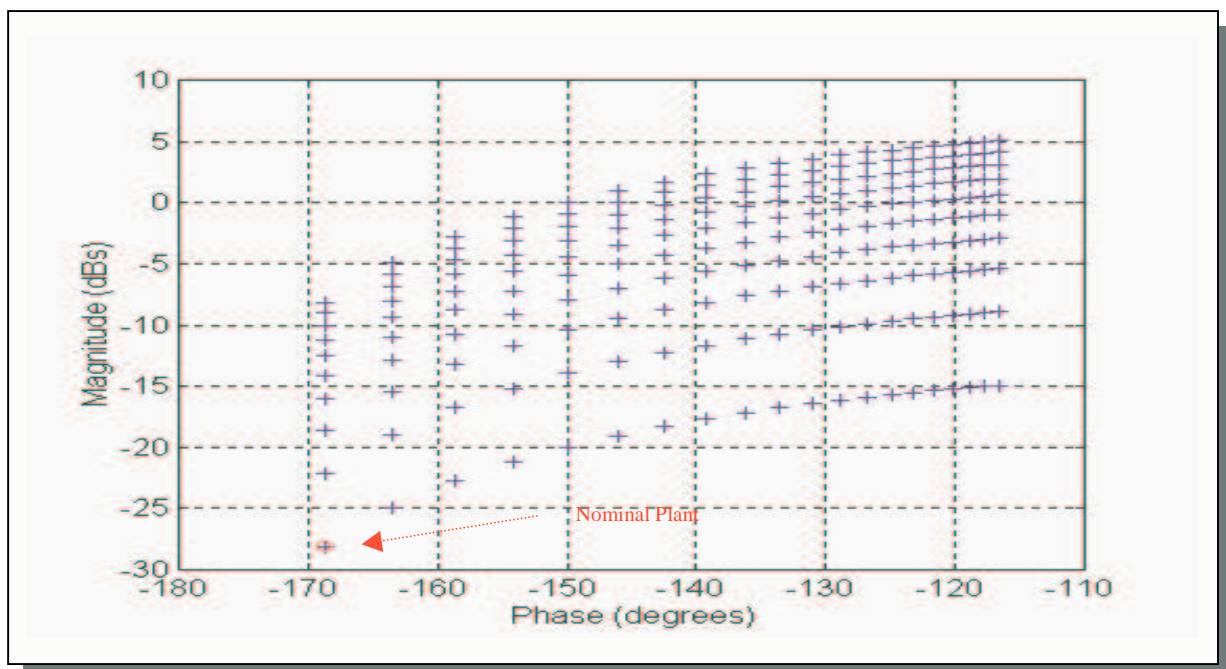
Figure 2.4.A: Uncertainty template for $\omega_5=5$ rads/sec and Nominal plant, on the NC.

Generally, uncertainty templates on the NC can be translated to the open loop transmission function of the system, $L(j\omega)=G(j\omega)K(j\omega)$ via the controller $K(s)$. The variation of $L(j\omega)$ can be assumed to be the same as the variation of $G(j\omega)$ for all its possible values at any specific frequency. This is because the compensator $K(j\omega)$ is assumed to be fixed. The nominal $L(j\omega)$, indicated by $L_o(j\omega)$, arises from a controller $K(s)=1$ and the substitution for $k=1$ and $a=1$ which corresponds to our choice of nominal plant. Although this choice is arbitrary (any fixed a and k combination would be acceptable) it is considered good practice to select the nominal plant which has its NC template point at the lower left corner for all frequencies for which the templates were obtained.

To find the uncertainty templates for the model given in (1), function **templ_cs()** was used. To reduce the computational burden of the algorithm, function **c_hull1()** was used to reduce the number of the points representing each template. Figure 2.4.B shows the convex hull of the template of figure 2.4.A.
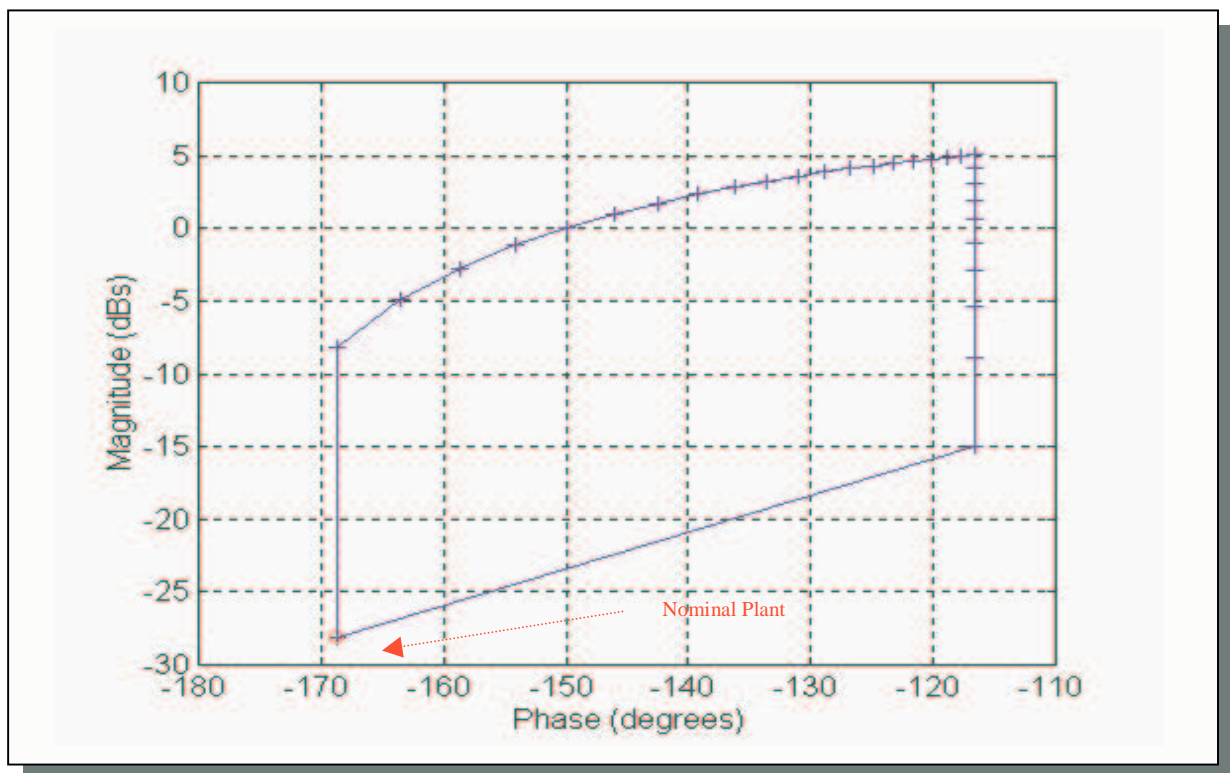
Figure 2.4.B: Convex Hull of uncertainty template for $\omega_5=5$ rads/sec

The eight uncertainty templates (one for each of the eight selected frequencies) on the NC are shown in figure 2.4.C. Moreover, the nominal open loop $L_o(j\omega_i)$ for $K(s)=1$ is shown in figure 2.4.D.
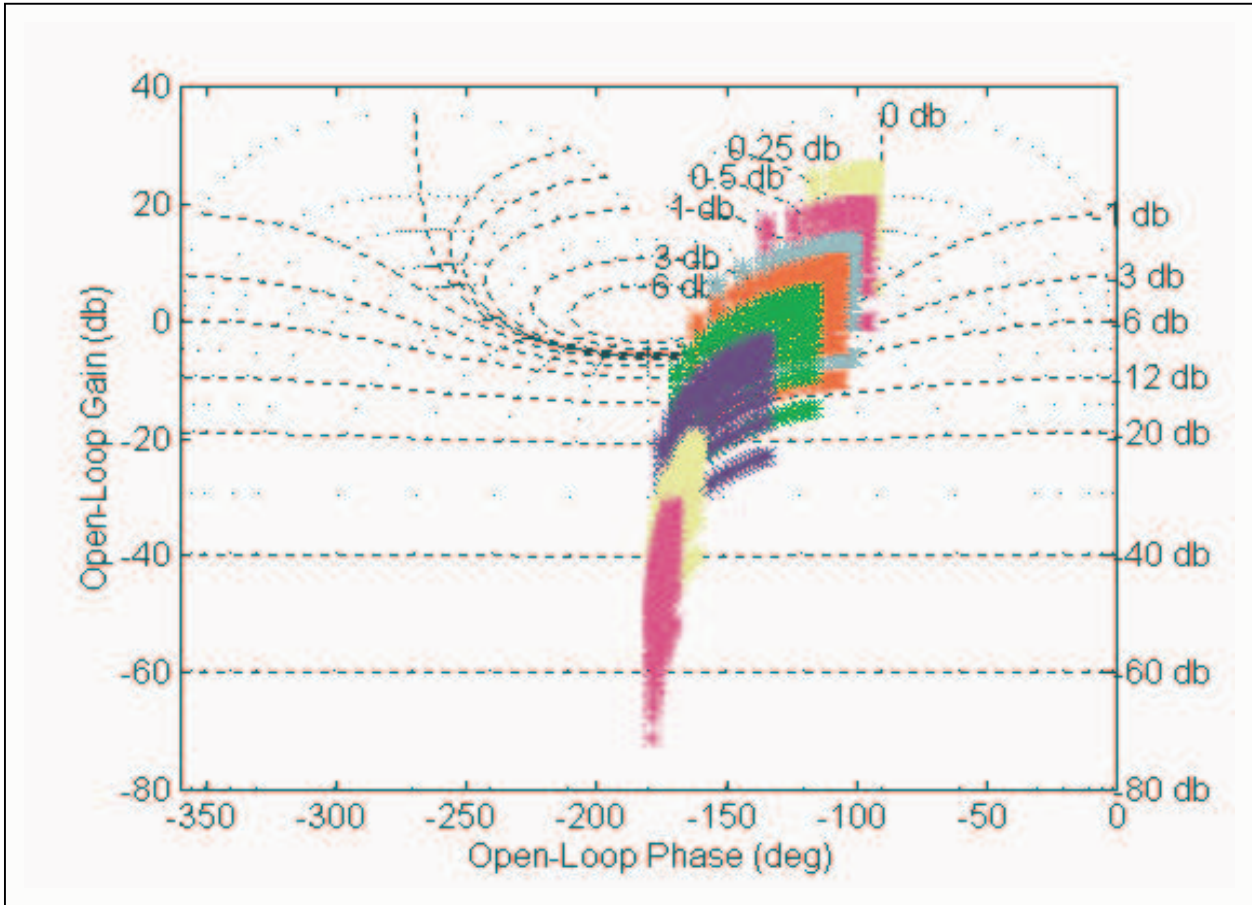
Figure 2.4.C: NC with uncertainty templates for ω_i={0.5, 1, 2, 3, 5, 10, 30, 60} rads/sec
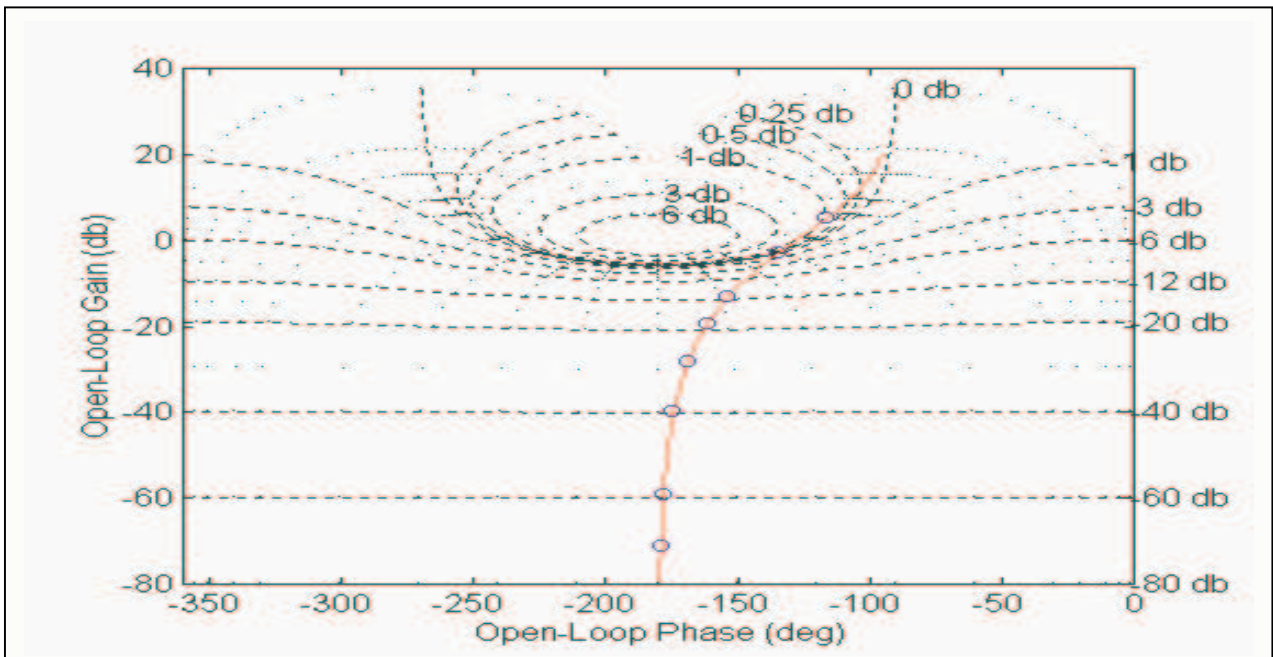
Figure 2.4.D: NC with nominal open loop $L_o(j\omega)$

2.5 Stability Bound or U-Contour

The stability bound or U-contour (sometimes referred to as Universal High Frequency Boundary UHFB), defines the region of the NC which should not be penetrated by the nominal open loop system $L_o(j\omega)=G_o(j\omega)K(j\omega)$ at high frequencies. The reason for this is as follows:

To establish minimum damping for the nominal closed loop system it is well known that $L_o(j\omega)=G_o(j\omega)K(j\omega)$ should not enter an appropriately chosen M-circle (in this case $M=1.2$) [Appendix B]. Since,

(a) at high frequencies the uncertainty template becomes a vertical line and

(b) we want to enforce the minimum damping requirement for all plants,

the lowest point of the M-circle must be extended downwards by a gain V which is equal to the gain uncertainty spread at high frequencies. For example, consider a general system as the one in figure 2.5.A. In this example the uncertainty template is a vertical line of length V dBs and the nominal open loop response is represented by its lowest point. Then for all uncertain L's to lie outside the $M=1.2$ circle at high frequencies, the nominal open loop response must lie on or below the U-contour.
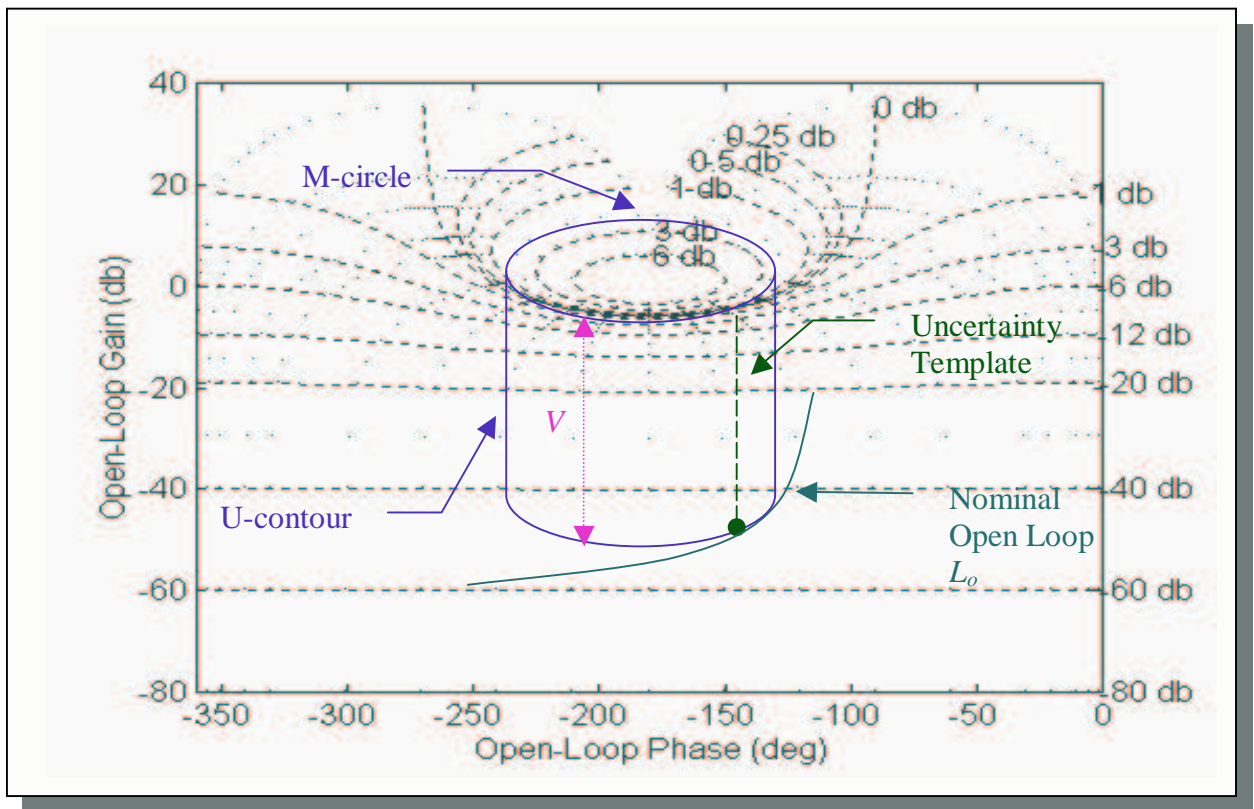
Figure 2.5.A: NC with U-contour, example for illustration

In general, gain V is obtained as:

$$V = \Delta \log_{10} |L(j\omega)|$$

or

$$V = \Delta \log_{10} |G(j\omega)| = \lim_{\omega \to \infty} \left[20\log_{10} |G_{max}(j\omega)| - 20\log_{10} |G_{min}(j\omega)| \right] \tag{4}$$

For the model given in (1), V is found using (4) as:

$$V = \Delta \log_{10} |G(j\omega)| = \lim_{\omega \to \infty} \left[20\log_{10} |G_{max}(j\omega)| - 20\log_{10} |G_{min}(j\omega)| \right]$$

thus

$$V = \Delta \log_{10} |G(j\omega)| = \lim_{\omega \to \infty} \left[20\log_{10}(k \times a)_{max} - 20\log_{10}(j\omega)^2 - 20\log_{10}(k \times a)_{min} + 20\log_{10}(j\omega)^2 \right]$$

which implies

$$V = 20\log_{10}(10 \times 10) - 20\log_{10}(1 \times 1) \Rightarrow V = 40 - 0 \Rightarrow V = 40 \text{ dBs}$$

Function **hf_bound()** was used to produce the U-contour for the system in (1), which is shown in figure 2.5.B
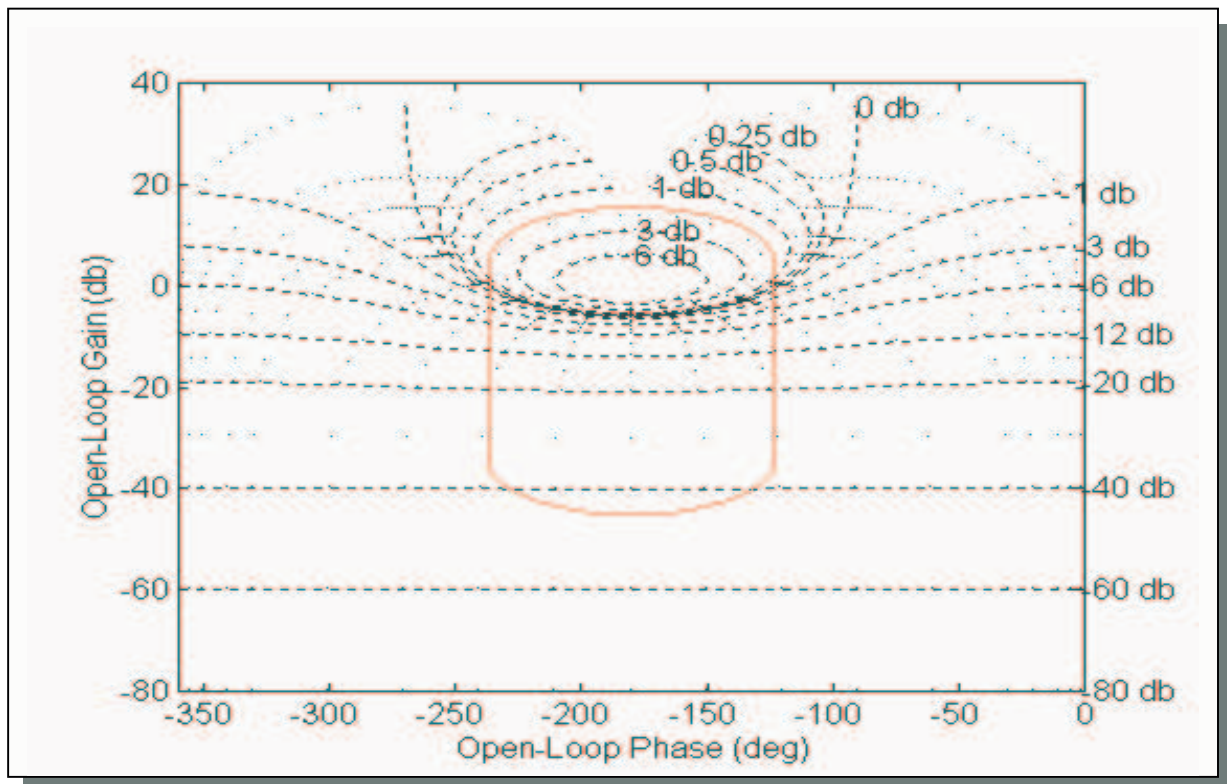
Figure 2.5.B: NC with U-contour (m-circle value, $M=1.2$)

2.6 Tracking bounds (Horowitz templates)

In order to achieve the closed loop specifications, the plant templates must lie on or above specific areas on the NC. These areas are in the forms of contours and they are known as *Tracking bounds* or *Horowitz templates* [Ref.1,2,3]. They specify the minimum open loop gain for the system to achieve the desired robust performance. In the case of the model given in (1) and for the selected eight frequencies ω$_i$, eight tracking bounds will be plotted on the NC. Functions **hr_bnds1()** and **trk_bnds()**. Figure 2.6.A displays the tracking contours for our system.
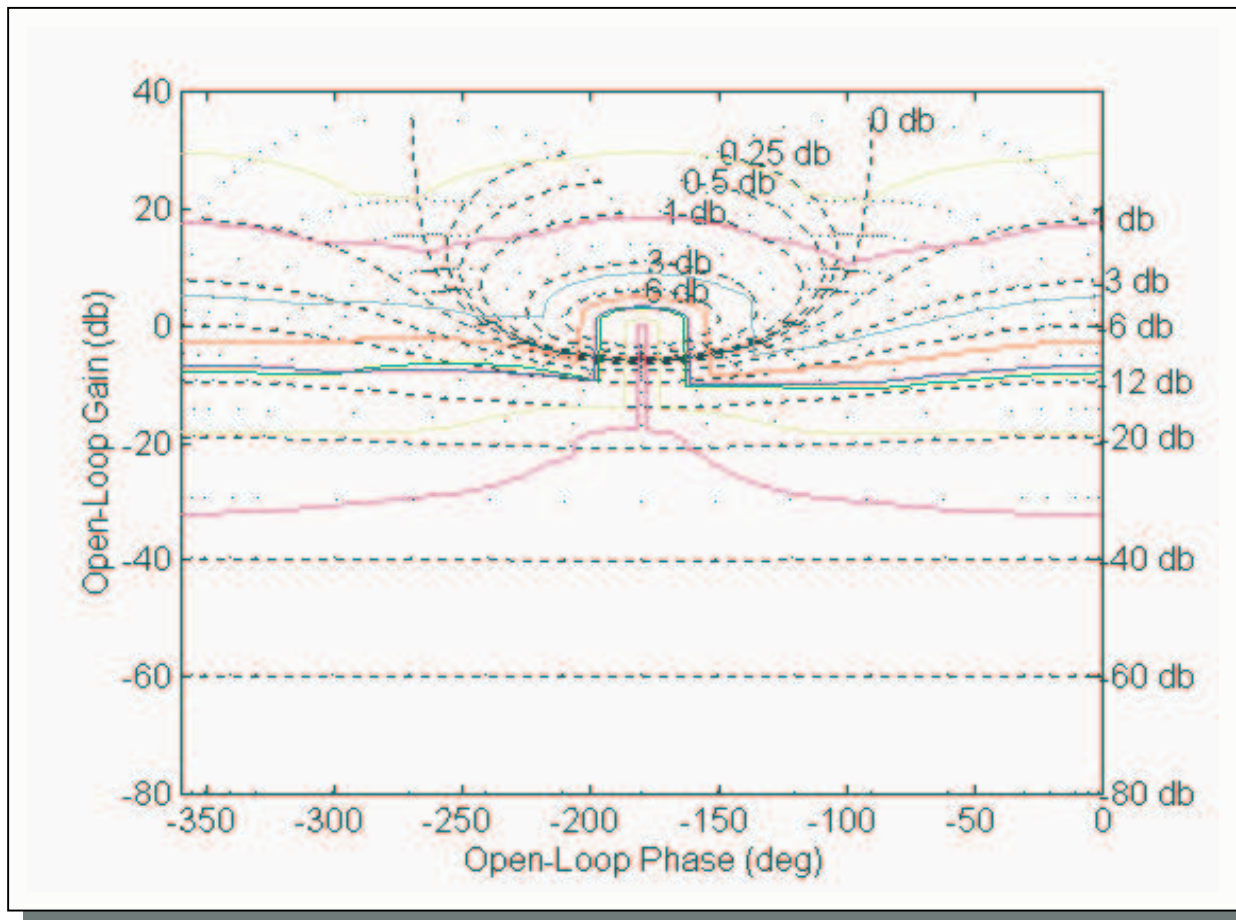
Figure 2.6.A: NC with Horowitz templates (for eight frequencies)

The Horowitz templates can be obtained from the following considerations:
The control ratio of the system without the presence of the pre-filter is:

$$T_R(j\omega) = \frac{L(j\omega)}{1+L(j\omega)}, \quad \text{where } L(j\omega) = G(j\omega)K(j\omega) \tag{4}$$

13

The locus of all points $|T_R|=M$, is known as an M-circle [Appendix B] [Ref.5]. The grid lines shown in figure 2.6.A, represent the M-circles for different values of M. For each uncertainty template, the corresponding tracking specification require that:

$$\max_{p \in P}\left\{\left|T_{\max}(j\omega)\right|_{dBs} - \left|T_{\min}(j\omega)\right|_{dBs}\right\} \leq \delta(j\omega) \tag{5}$$

With the plant templates placed at any location on the NC, the above condition is equivalent to

$$\left|M_{\max} - M_{\min}\right| \leq \delta(j\omega) \tag{6}$$

where M_{max} and M_{min} denote the maximum and the minimum M-value among all points of the templates, respectively. Consequently, if at its current location condition (6) is not satisfied, the open loop gain must be increased. The points defining the Horowitz template (for each phase) represent the gain at which condition (6) is met with equality. In practice, the Horowitz templates are calculated in software via a simple bisection algorithm over a finite phase grid.

2.7 Disturbance Rejection

In the presence of external disturbance inputs, the system must not only satisfy the tracking specifications but also the disturbance rejection specifications in order to have the desired performance. The disturbance rejection models used are either first or second order systems [Ref.1]. In this case a second order disturbance rejection model is needed to reject the unit step disturbance input at the output of the plant in figure 1.2.A. The requirement is:

$$\left|y(t)\right| \leq a_p, \text{ for } t \geq t_x \tag{7}$$

where a_p and t_x are design parameters. For a second order model, the disturbance response in the time domain is of the form,

$$y(t) = D_o e^{-at} \cos bt \tag{8}$$

The corresponding disturbance rejection model is:

$$M_D(s) = \frac{s(s+a)}{(s+a)^2 + b^2} \tag{9}$$

where $a = \zeta\omega_n$ and $b = \omega_n(1-\zeta^2)^{-1/2}$, in which ω_n is the natural frequency and ζ is the damping factor of the model. The model parameters can be obtained from the initial value of the disturbance input D_o, the percent undershoot p_u, the settling time t_x and the maximum gain α_p of the disturbance response. It can be easily shown that for this model:

$$\omega_n = -\frac{1}{\zeta \times t_x} \ln\left(\frac{a_p}{D_o}\right) \tag{10}$$

ζ can be obtained from a look up table and is related to its percent undershoot.

The model in equation (9) also contains a non-dominant zero, which ensures that the final model is compatible with the degree of the control ratio of the system. Note also that the zero $s=0$ in (9) enforces asymptotic rejection to step disturbance inputs.

I the example considered in this project, a second order model is needed with $D_o=1$, $p_u=25\%$, $\alpha_p=0.1$ and $t_x=2$sec. The following parameters were obtained using function **dop_md2a()**:

$$\omega_n=2.65 \text{ rad/sec}$$
$$\zeta=0.43$$
$$\alpha=1.15$$
$$b=2.39$$

The disturbance model obtained is:

$$M_D(s) = \frac{s(s+1.15)}{(s+1.15)^2 + 2.39^2} \tag{11}$$

The above model rejects the disturbance input (the step response of the disturbance model stays within the region [-0.1,0.1]) after 2 sec with an undershoot of approximately 25%, as verified from the simulation shown in figure 2.7.A. Figure 2.7.B shows the magnitude-frequency response of $M_D(s)$.
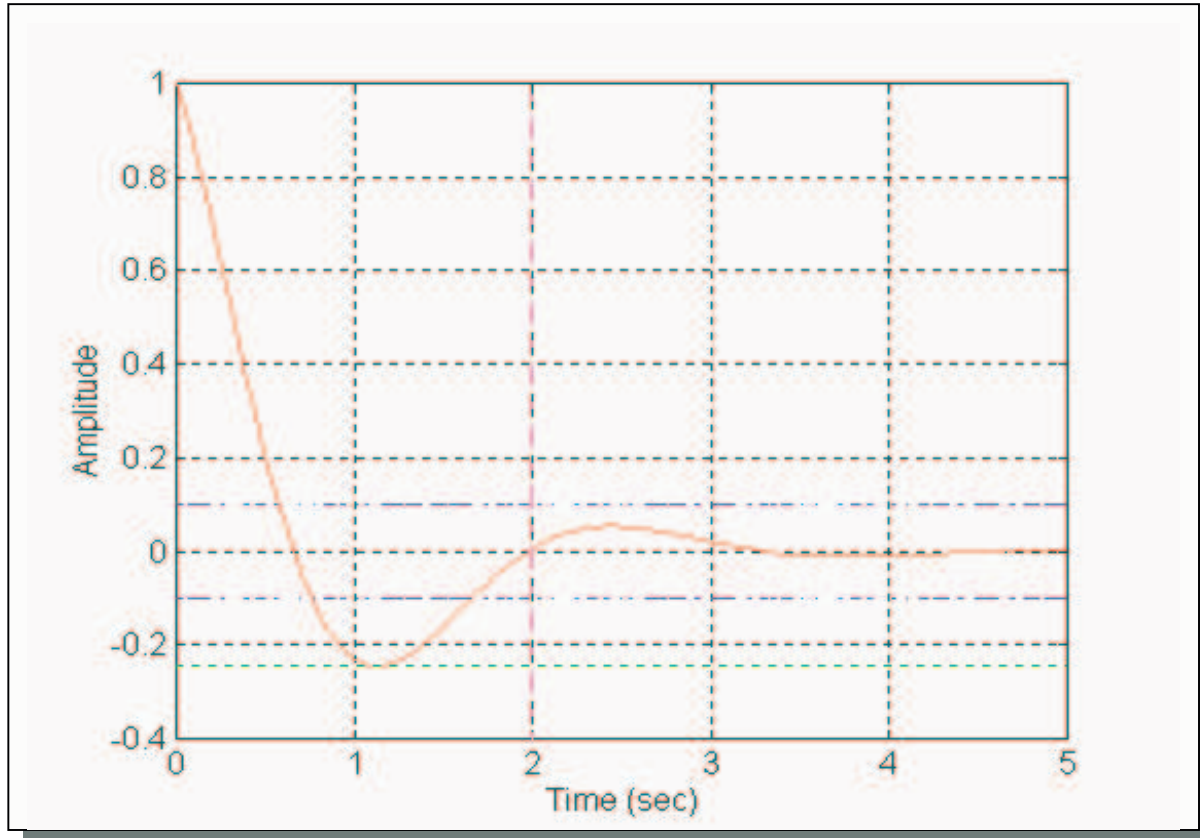
Figure 2.7.A: Second order Disturbance rejection model

In the frequency domain the magnitude bode plot of the model is the following:
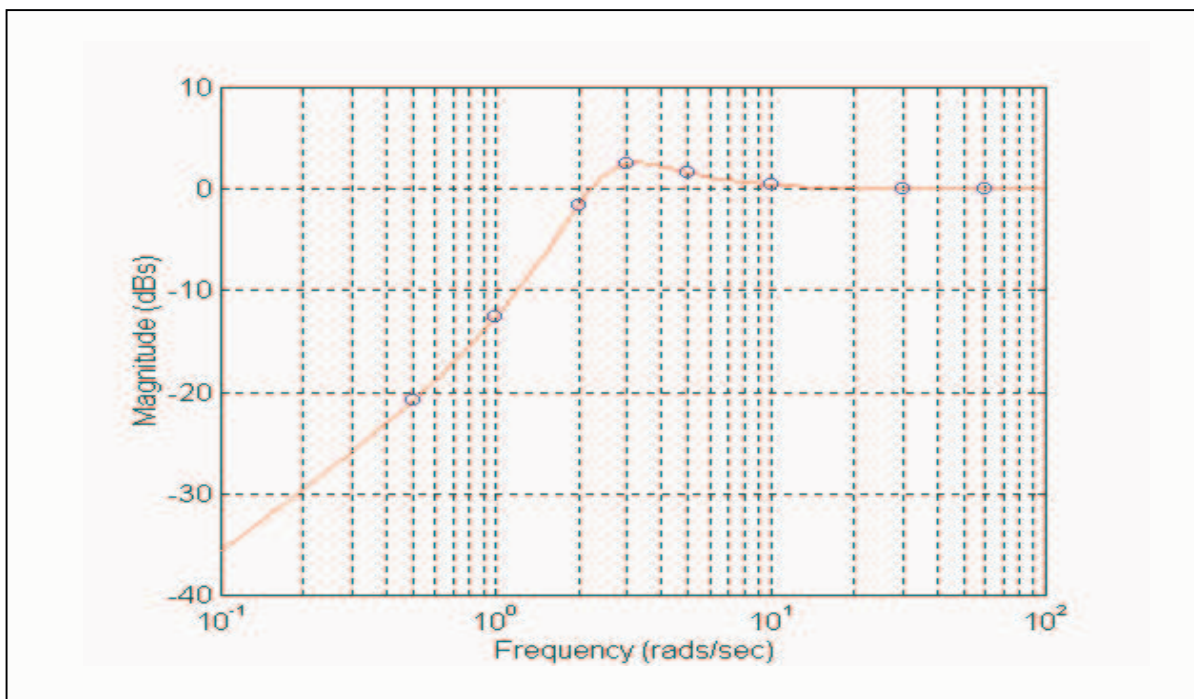
Figure 2.7.B: Magnitude Bode plot of the second order disturbance rejection model

The blue circles in figure 2.7.B represent the gain at each of the eight specified frequencies {0.5, 1, 2, 3, 5, 10, 30, 60} rads/sec. The results are summarised in table 2.7.a.

Frequencies (rads/sec)	0.5	1.0	2.0	3.0	5.0	10.0	30.0	60.0
Gain *A* (dBs) (in absolute terms)	**20.78**	**12.5**	**1.54**	**2.55**	**1.59**	**0.43**	**0.05**	**0.01**

Table 2.7.a: Disturbance rejection gain (A_i, i=1,2,3,..,8)

2.8 Disturbance Bounds

When an external disturbance input is present, the design must satisfy both tracking and disturbance rejection specifications in order to be characterised as successful. For disturbance rejection the nominal open loop $L_o(j\omega)$ must lie on or above specific regions on the NC to ensure that the closed loop disturbance rejection specifications will be successfully met. These areas are known as the *disturbance bounds* and they are formed in a similar way to the tracking bounds. They specify the minimum open loop gain of the system required to meet the disturbance rejection specifications for all uncertain plants. These are obtained as follows:

The disturbance-modelling ratio of the system in figure 1.2.A is:

$$T_{YD}(j\omega) = \frac{1}{1 + G(j\omega)K(j\omega)} = \frac{1}{1 + L(j\omega)} \tag{12}$$

For the disturbance bounds on the NC the requirement for fulfilling the disturbance rejection specifications is that:

$$|T_{YD}(j\omega_i)| \leq A_i, \quad \text{for all } i \tag{13}$$

where A_i is the corresponding gain in dBs of the Bode plot in table 2.7.a, at each frequency.

According to the above, the disturbance bounds for the example considered here were found using functions **dis_bnds()** and **dist_bnd1()**.Figure 2.8.A shows the disturbance bounds on the NC:
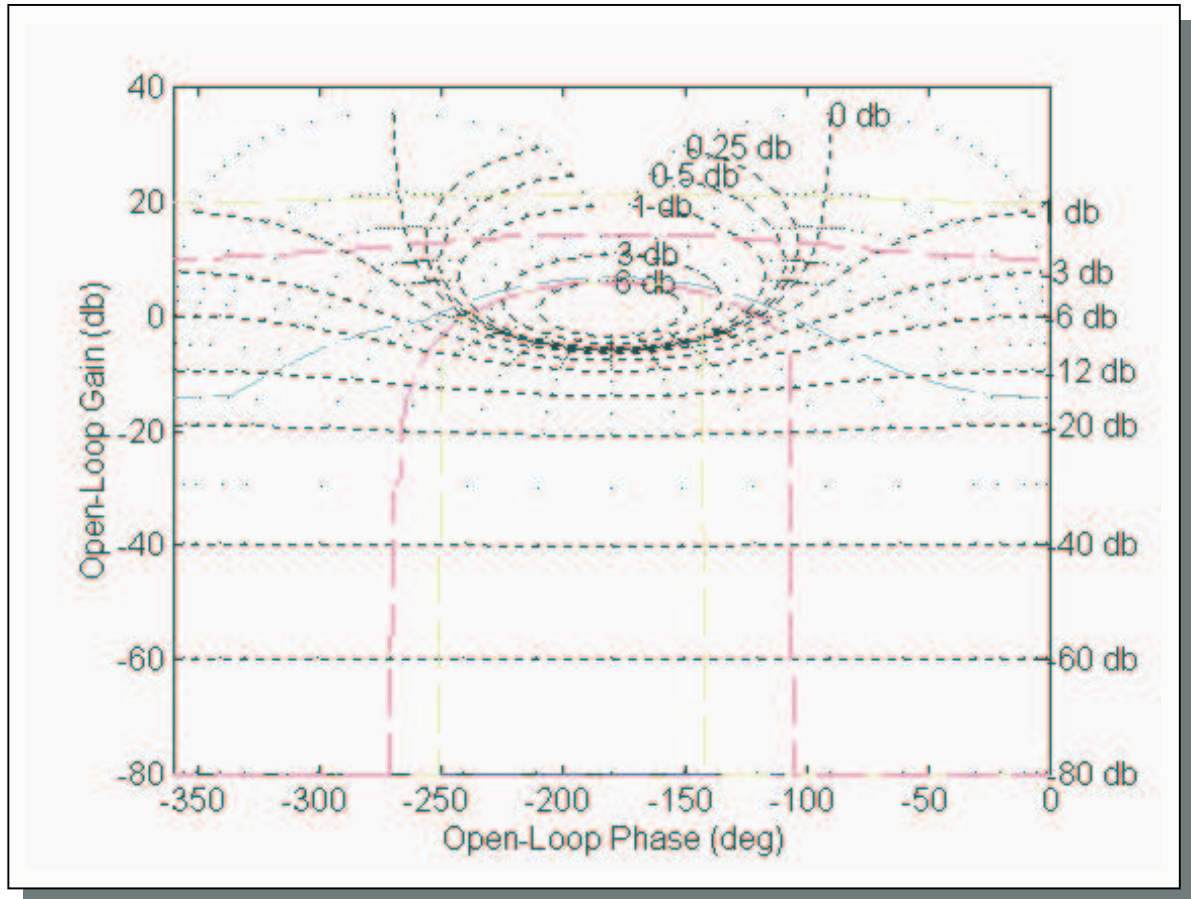
Figure 2.8.A: NC with disturbance bounds

The nominal open loop must lie on or above the disturbance bounds in figure 2.8.A for the corresponding frequencies, in order to meet the disturbance rejection specifications.

The system must lie above the disturbance bounds and the tracking bounds in order to meet simultaneously the disturbance rejection and the tracking specifications. Moreover, it must not penetrate the U-contour in order to establish a minimum damping for the nominal closed loop system. Figure 2.8.B shows the NC with the Horowitz templates, the disturbance bounds, the U-contour, and the nominal open loop. In addition, figure 2.8.C shows the maximum bounds that the nominal open loop must lie on or above, so that the system will meet the disturbance and tracking specifications simultaneously.
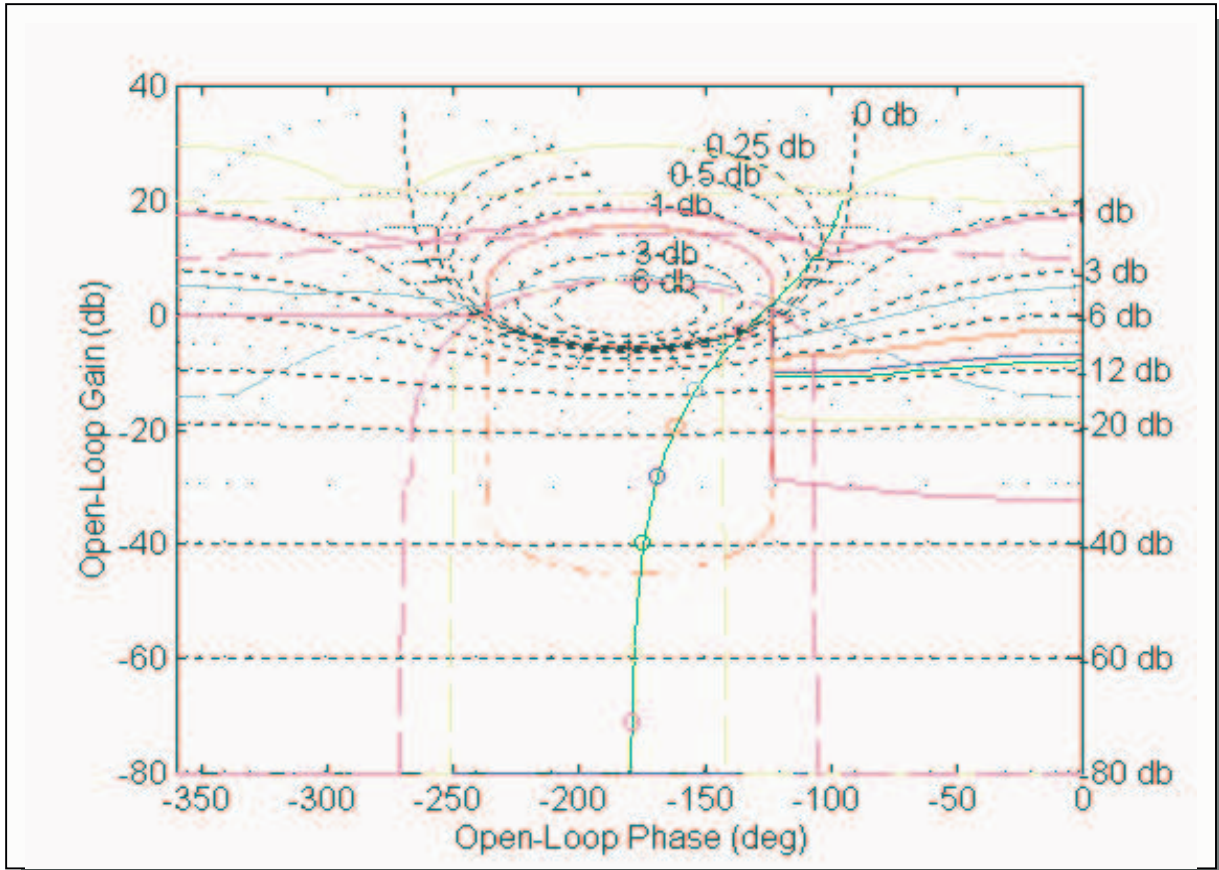
Figure 2.8.B: NC with Horowitz templates, disturbance bounds, U-contour, and nominal open loop
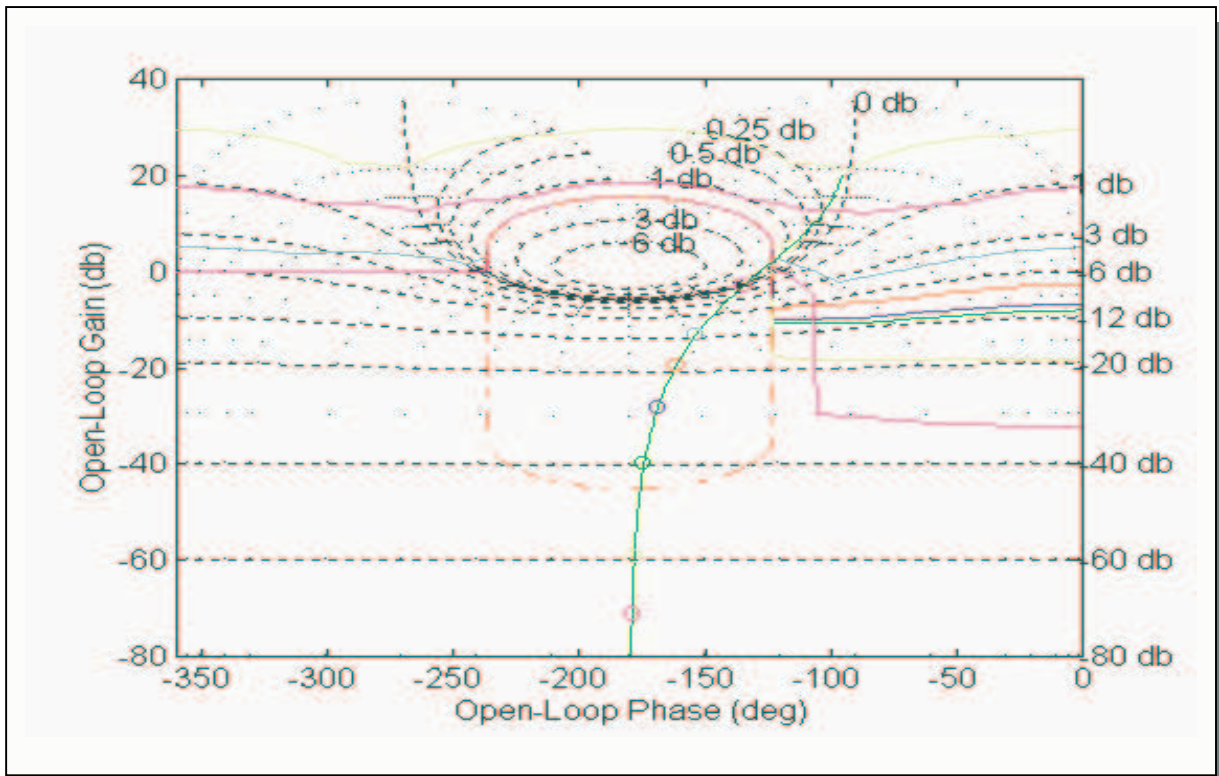
Figure 2.8.C: NC with maximum bounds, U-contour, and nominal open loop

19

From figure 2.8.C, note that in the left region of the NC (region of phases from -360° until the first phase at which the U-contour starts forming) the nominal open loop (if it exists in this region) must lie on or above the bound at 0 dBs (straight line) to ensure stability. It is also a good practice to consider the U-contour as a performance bound; this helps with the implementation of the algorithms given later in this project.

2.9 Loop shaping

So far we have seen that in order to attain the desired closed loop specifications the following requirements must be fulfilled:

(a) $L(j\omega)$ must not penetrate the U-contour to ensure stability and minimum damping.

(b) The nominal open loop must lie on or above the tracking and disturbance bounds on the NC (for each corresponding frequency) to achieve robust tracking performance and disturbance rejection. If it happens to exist in the left region of the NC, it must also lie on or above the 0 dB bound to ensure stability.

Therefore the open loop response will be shaped with the aim to satisfy (a) and (b) above.

Open loop shaping can be achieved using compensator design. A compensator or controller is a dynamic system that is used in cascade with the plant to achieve the desired open loop characteristics. In the next chapter four types of controllers are discussed, phase lead, phase lag, PD, and PID. The first two controllers are used for loop shaping using a graphical design. The PD and PID controllers are designed via optimisation methods to find the *'best'* solution to the design problem.

CHAPTER THREE

CONTROLLER DESIGN

3.1 Introduction

This chapter discusses the design of appropriate controllers, which are used so that the system will achieve desired open loop characteristics. Four types of controllers are considered, *phase lead*/*phase lag*, *PD*, and *PID* [Ref.5,7]. The first two types are used to shape the loop suitably via a graphical design. The *PD* and *PID* controllers are designed to give the optimal solution to a suitably defined optimisation problem. The process and the results are illustrated using appropriate examples.

3.2 Graphical design using Phase Lead and Phase lag controllers

In order to shape the loop appropriately (see Section 2.9), gain, phase lead or phase lag need to be injected at each frequency of interest so that the design will give an acceptable result according to the given specifications [Ref.5,7].

3.2.1 Phase Lead Controller

A *phase lead* controller has a transfer function of the form:

$$K(s) = \frac{1 + \dfrac{s}{\omega_1}}{1 + \dfrac{s}{\alpha \omega_1}} \tag{14}$$

where $\alpha > 1$. The *phase lead* controller injects positive phase in the system for all frequencies. The maximum phase shift is given by:

$$\phi_m = \sin^{-1}\left(\frac{\alpha - 1}{\alpha + 1}\right) \tag{15}$$

and occurs at frequency:

$$\omega_m = \omega_1 \sqrt{\alpha} \tag{16}$$

Figure 3.2.1.A, shows the Bode plots of the following phase lead controller:

$$K(s) = \frac{1 + \dfrac{s}{15}}{1 + \dfrac{s}{30}}$$

where ω_l=15 rads/sec, α=2 and, using formulae (15) and (16), φ_m=19.47^o at ω_m=21.2 rads/sec.
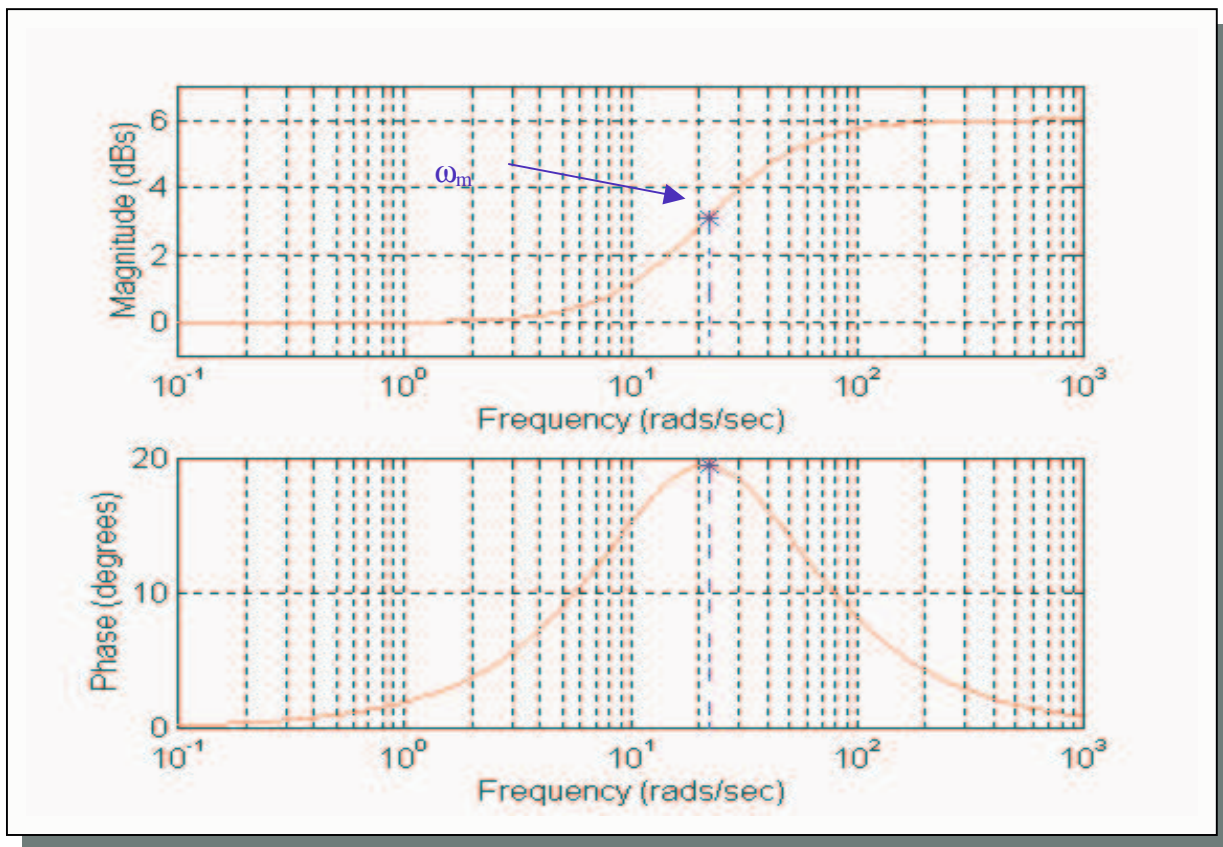
Figure 3.2.1.A: Bode plots (magnitude and phase) of phase lead controller

As it can be seen from the Bode plots, the *phase lead* controller acts as a high pass filter because it increases the gain at high frequencies relative to the gain at low frequencies. As an example, figure 3.2.1.B shows a loop shaping using one *phase lead* controller:
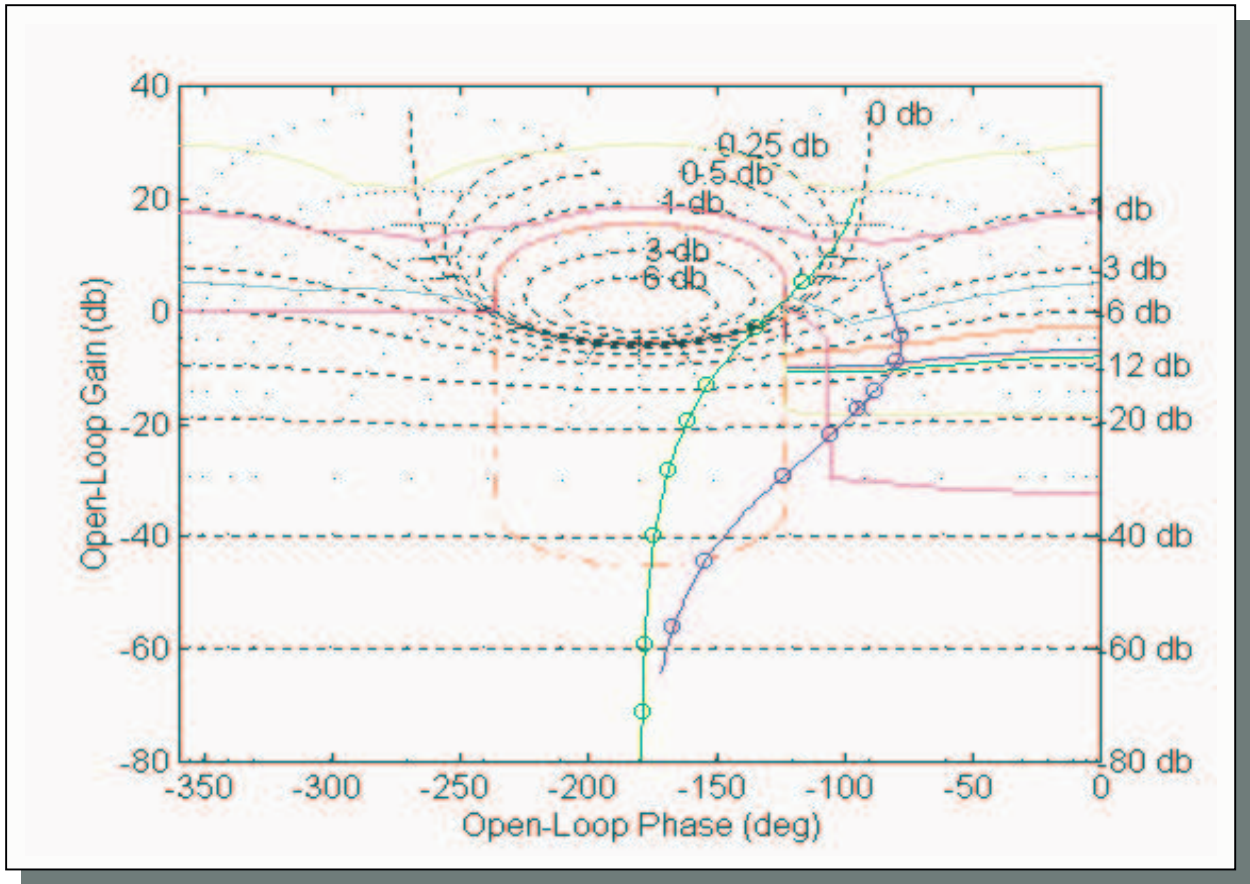
Figure 3.2.1.B: NC with overall bounds, initial nominal open loop (green line) and new nominal open loop using one phase lead controller (blue line)

From figure 3.2.1.B we can see that the use of a phase lead controller introduces high gain at high frequencies and attenuates low frequencies. Moreover, the nominal open loop moves outside the U-contour at the frequency at which maximum phase was injected.

3.2.2 Phase Lag Controller

The transfer function of a *phase lag* controller is:

$$K(s) = \frac{1 + \dfrac{s}{\alpha \omega_1}}{1 + \dfrac{s}{\omega_1}} \qquad\qquad (17)$$

where $\alpha > 1$. The *phase lag* controller injects negative phase to the system for a specific range of frequencies. The maximum phase shift is given by equation (15) and it occurs at ω_m given by

equation (16). Figure 3.2.2.A shows the Bode plots of a *phase lag* controller with the following transfer function:

$$K(s) = \frac{1 + \dfrac{s}{30}}{1 + \dfrac{s}{15}}$$

where ω_l=15 rads/sec, α=2 and, using formulae (15) (we also have to introduce a minus sign due to phase lag) and (16), φ_m=-19.47^o at ω_m=21.2 rads/sec.
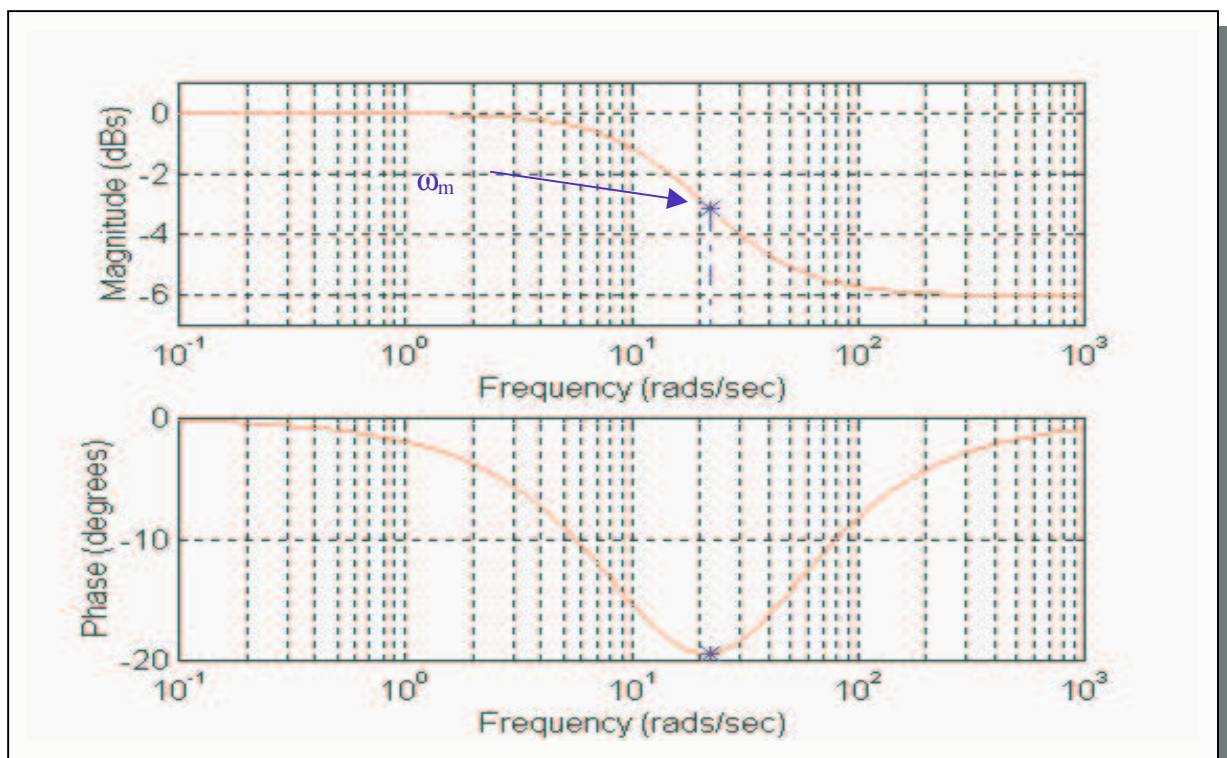
Figure 3.2.2A: Bode plots (magnitude and phase) of phase lag controller

As can be seen from the above figure, the *phase lag* controller acts as a low pass filter as it increases gain at low frequencies relative to the gain at high frequencies. Therefore it can be used in cascade with a phase lead controller to give a reasonable design. Figure 3.2.2.B shows the shaping of the loop after the use of one *phase lead* controller (from figure 3.2.1.B) and one *phase lag* controller in cascade.
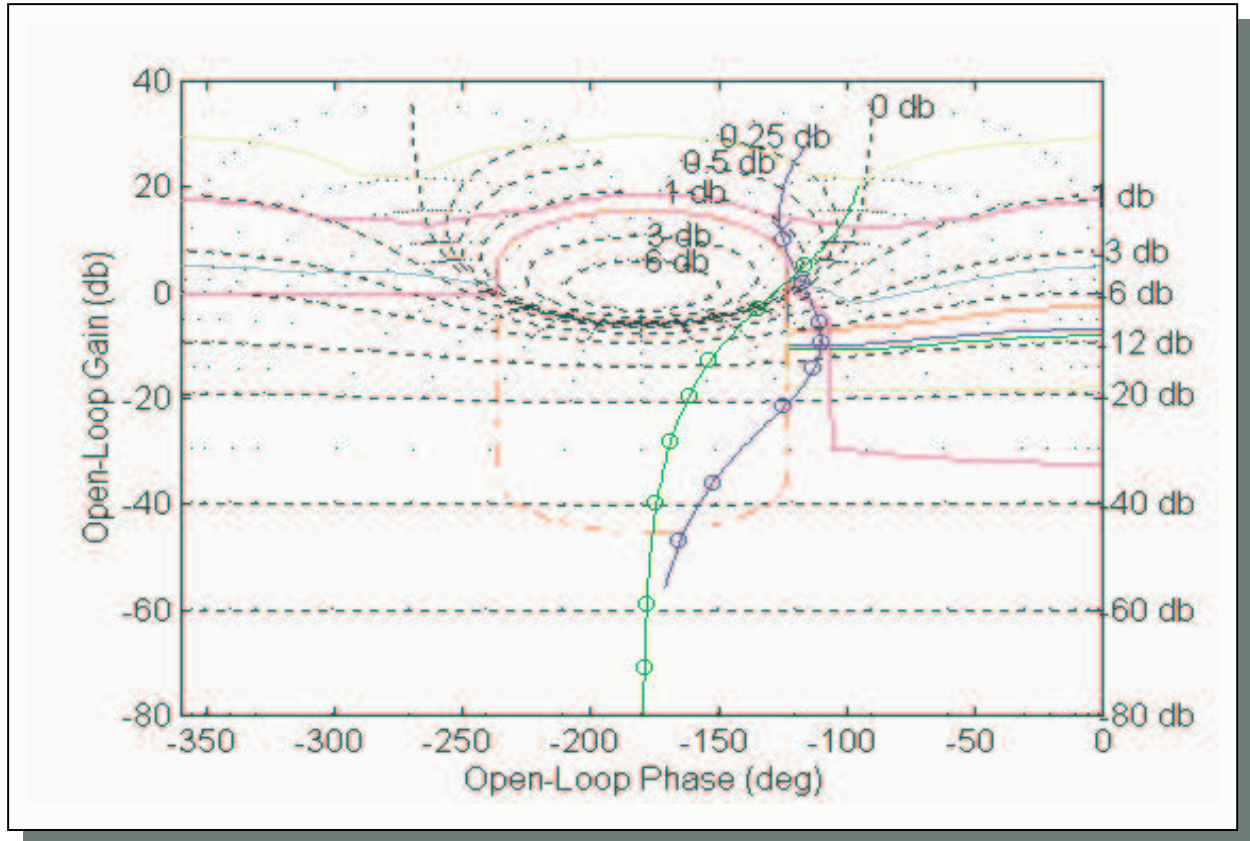
Figure 3.2.2.B: NC with initial nominal open loop, and new nominal open loop after using one phase lead controller (from figure 3.2.1.B) and one phase lag controller.

Thus, by using appropriate designed phase lead and phase lag controllers in cascade, a solution to the loop-shaping problem can be obtained. This is shown in figure 3.2.2.C (next page), where a number of phase lead and phase lag controllers are used to give the best performance.
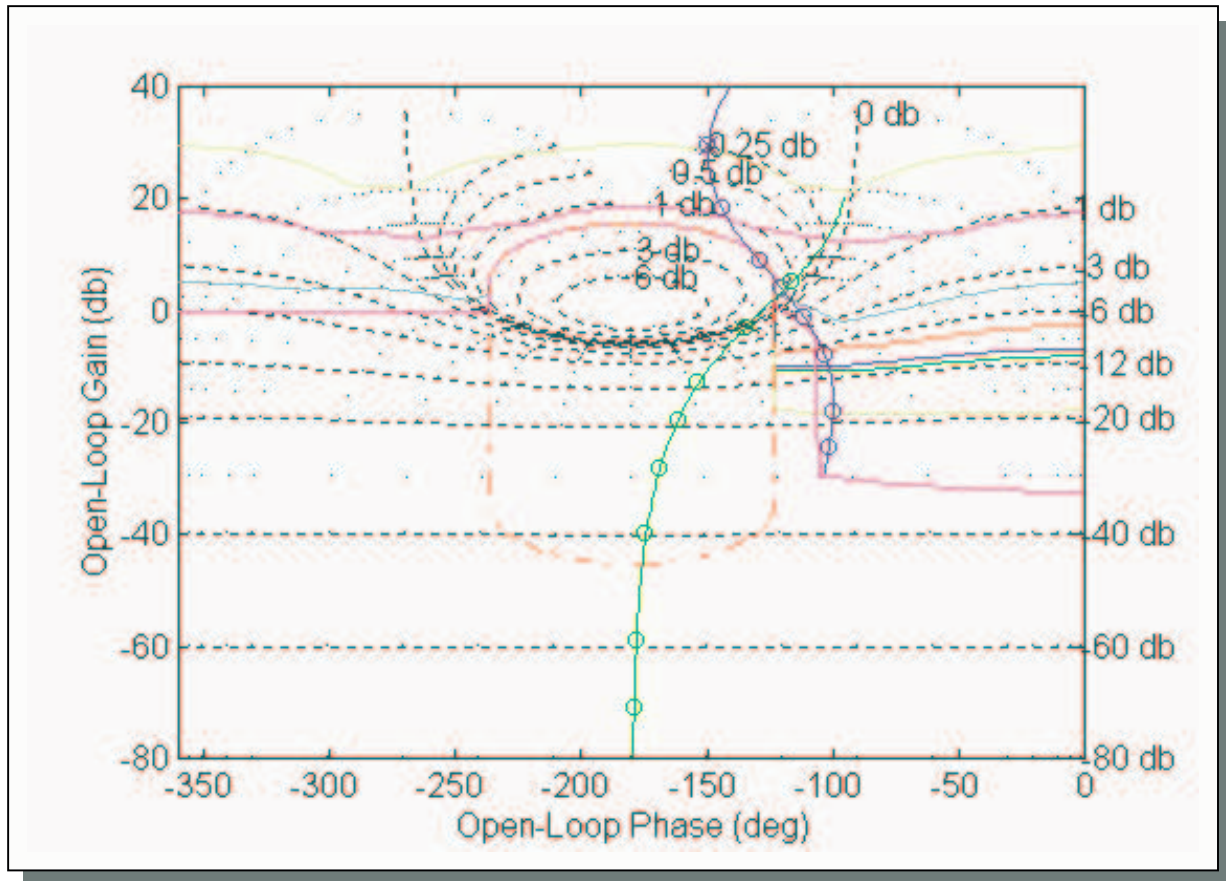
Figure 3.2.2.C: NC with initial nominal open loop and final nominal open loop (the controller obtained helps the system to satisfy all given specifications)

3.2.3 User Graphical Program

Since a number of 1st order controllers are required to shape L_o appropriately, a user friendly graphical program was designed to make this design task easier.

For this purpose function **gr_des()** was written. The procedure for the design is the following:

By clicking on a point (desired frequency at which the max phase shift will be injected) on the NC, **gr_des()** returns the point's co-ordinates (magnitude and phase). From these co-ordinates, **gr_des()** estimates the nearest point on the L_o (nearest exact frequency of interest) and the true magnitude and phase are obtained. Then by clicking on a second point, the required phase (lead or lag) and gain are estimated and the appropriate controller is selected via the functions **ph_lead()** and **ph_lag()**. This procedure has been implemented in such a way (with the use of a loop), which offers the designer the following capabilities:

1. *Design new controller*
2. *Connect new controller in cascade with old controller*
3. *Remove the last designed controller*
4. *Exit when design is completed and save all data information*

The loop is shown by means of the following logic diagram:
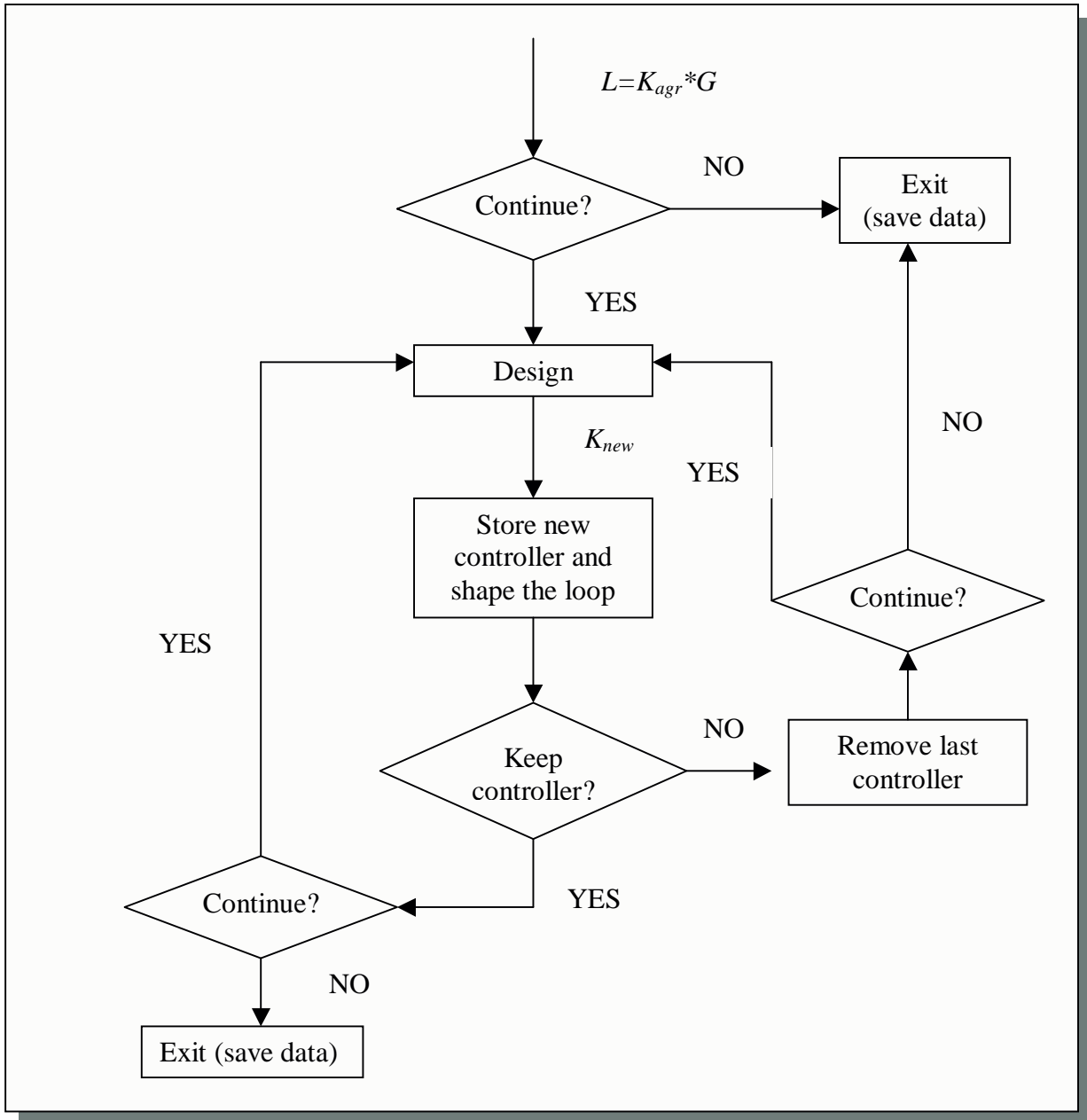
Flow Diagram 3.2.3.f: Procedure of graphical design

The final design is illustrated using function **maintest()**. This function returns the overall controller obtained from the design.

3.3 Controller Design using Optimisation Methods

In the previous section the design of a controller consisting of phase lag and lead cascade terms was discussed. This section presents *optimisation methods* for designing *proportional* and *derivative* (*PD*) and *proportional, integral* and *derivative* (*PID*) controllers. The first part is an introduction to *optimisation methods* in general, while the next two parts discuss the application of these methods to the design of a *PD* and a *PID* controller, respectively. Two simulations – one for each type of controller – show that the methods work appropriately.

3.3.1 Optimisation methods

Optimisation according to Fletcher [Ref.6] is '*the science of determining the "best solutions" to certain mathematically defined problems, which are often models of physical reality*'. *Optimisation* and its hybrid methods can be applied to a great range of problems and practical applications. The solution obtained by these methods is typically simpler, more accurate, and cost effective. For the purposes of this project, *optimisation* is used in order to determine algorithmic solutions to the problem of designing optimal *PD* and *PID* controllers for highly uncertain plants. The procedure is described below and the simulations are mainly based on the plant given in equation (1).

3.3.2 Proportional plus Derivative (PD) Controller

The first type of controller, which can be used to give a solution to the design problem, is the *PD* controller. Here, both the error and the derivative of the error are used for control, and its transfer function is the following:

$$K_{pd}(s) = k_p + k_d s \qquad (18)$$

The *PD* controller, effectively adds a zero at $s = -k_p/k_d$ to the OL_{TF}. Both the transient response and the steady state error (s.s.e) are improved, because the *PD* anticipates large errors and tries to correct them before they occur [Ref.5,7].

In frequency domain terms, the *PD* controller adds phase lead to the nominal open loop, reaching a maximum additional phase lead of 90° at high frequencies (this is due to the dominant nature of the derivative at high frequencies). At low frequencies the dominant part is the proportional term which only adds gain to the nominal OL. The phase is always positive due to the derivative term (the proportional term has 0° phase). For example, figure 3.3.2.A shows the Bode plots of a *PD* controller with the following transfer function:

$$K_{pd}^1(s) = 1 + 2s$$
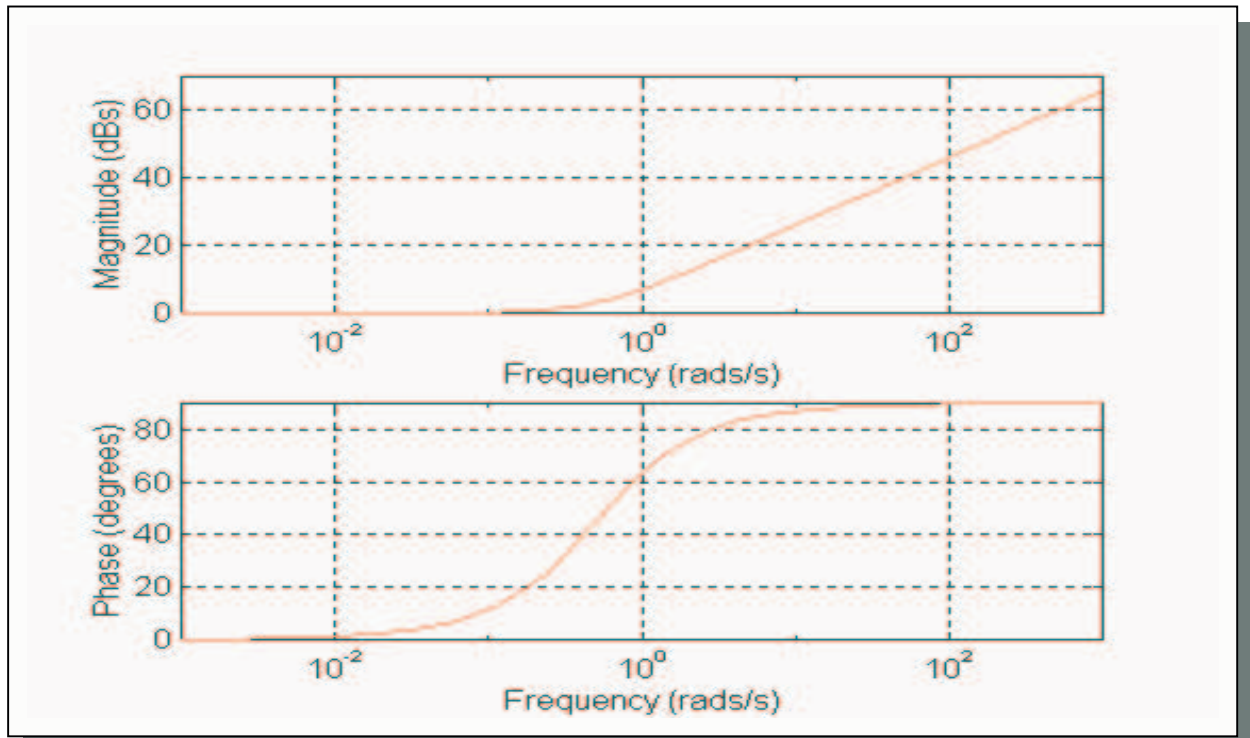
Figure 3.3.2.A: Bode plots of a *PD* controller

In order to optimise the controller the following considerations were made:

The frequency response ($s=j\omega$) of the *PD* controller (from equation (18)), in terms of magnitude and phase is:

$$K_{pd}(j\omega) = k_p + k_d j\omega \tag{19}$$

Magnitude (linear): $$m(\omega) = |K_{pd}(j\omega)| = \sqrt{k_p^2 + (k_d\omega)^2} \tag{20}$$

Phase: $$\phi(\omega) = \tan^{-1}\left(\frac{k_d\omega}{k_p}\right) \geq 0 \tag{21}$$

Suppose that $\phi(\omega_o)$ is fixed at any specified frequency ω_o, i.e. $\phi(\omega_o)=\phi_o$. Then by using equation (21), ϕ_o is given by:

$$\phi(\omega_o) = \phi_o = \tan^{-1}\left(\frac{k_d \omega_o}{k_p}\right)$$

which implies

$$\tan(\phi_o) = \frac{k_d}{k_p}\omega_o \Rightarrow \frac{k_d}{k_p} = \frac{\tan(\phi_o)}{\omega_o} := \gamma_o \tag{22}$$

where γ_o is a constant which fixes the relation between k_p and k_d.

Moreover, using (22) the phase of the controller at any frequency ω is:

$$\phi(\omega) = \tan^{-1}\left(\frac{k_d \omega}{k_p}\right) = \tan^{-1}\left[\tan(\phi_o)\frac{\omega}{\omega_o}\right] = \tan^{-1}(\gamma_o \omega) \tag{23}$$

It follows from the analysis above that if the phase of the compensator is fixed at any specified frequency (i.e. $\phi(\omega_o) = \phi_o$) then the phase ϕ of the compensator at all other frequencies is also fixed.

Under these conditions the magnitude (linear) of the controller can be expressed as:

$$m(\omega) = |K(j\omega)| = \sqrt{k_p^2 + k_d^2 \omega^2} = |k_d|\sqrt{\left(\frac{k_p}{k_d}\right)^2 + \omega^2} = |k_d|\sqrt{\frac{1}{\gamma_o^2} + \omega^2} \tag{24}$$

i.e. $m(\omega) \propto |k_d|$. Now consider the nominal plant model G_o and the nominal OL system $L_o = G_o K$. Then the phase of the nominal OL is:

$$\angle L_o(j\omega) = \angle G_o(j\omega) + \angle K(j\omega)$$

or,

$$\psi(\omega) = \beta(\omega) + \tan^{-1}(\gamma_o \omega) \tag{25}$$

where the phase of the nominal plant model $\beta(\omega)$ is fixed and known. Also, the magnitude of the nominal open loop in dBs is:

$$|L_o(j\omega)|_{dB} = |G_o(j\omega)|_{dB} + |K(j\omega)|_{dB}$$

i.e.,

$$|L_o(j\omega)|_{dB} = A|_{dB} + 20\log_{10}(|k_d|) + 20\log_{10}\left(\sqrt{\frac{1}{\gamma_o^2} + \omega^2}\right) \qquad (26)$$

where, $A/_{dB}$ is the gain of the nominal plant G_o at any frequency ω in dBs. Now, consider the Nichols chart with *Horowitz templates* $\{f(\omega_1, \varphi), f(\omega_2, \varphi), \ldots\ldots\ldots, f(\omega_N, \varphi)\}$ and U-contour B:
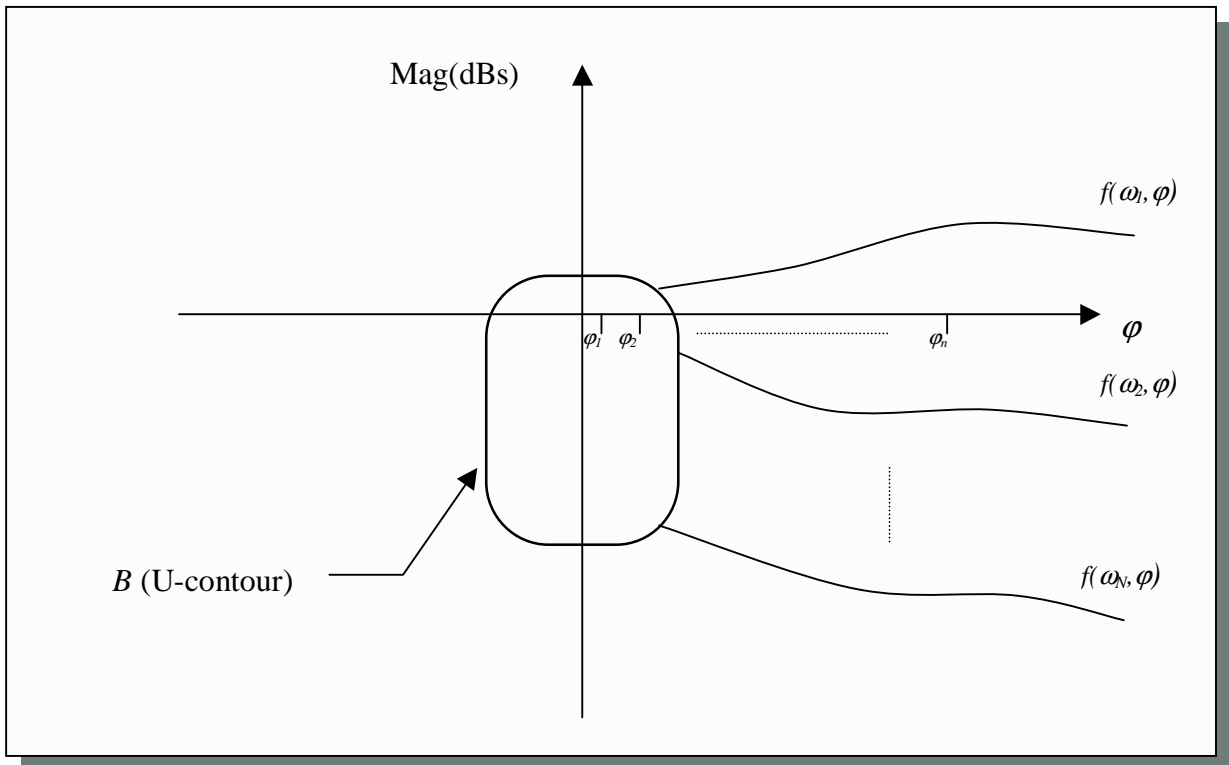
Figure 3.3.2.B: NC with Horowitz templates and U-contour, discrete phases φ_i (*PD* controller)

The design constraints that the *PD* controller has to satisfy are:

1. $|L(j\omega_i)|_{dB} \geq f(\omega_i)$, for all $i=1,2,3,\ldots\ldots,N$

2. $L(j\omega_i) \notin B$,   for all $i=1,2,3,\ldots\ldots,N$

According to QFT theory [Ref.2,3], the asymptotic gain of the open loop system must be a minimum (subject to satisfying the Horowitz and U-contour constraints). This is to avoid '*over-designing*' the system (e.g. resulting in a closed loop bandwidth larger than is absolutely necessary) which could imply measurement noise amplification and possible instability due to un-modelled dynamics. The asymptotic gain of the nominal open loop system is given by:

$$\lim_{\omega \to \infty}\left\{ \left| \left(k_p + k_d\, j\omega\right) \times G_o(j\omega) \right| \right\} \tag{27}$$

Suppose that:

$$\left|G_o(j\omega)\right| \sim \frac{A}{\omega^p}$$

at very high frequencies. (Assume that $p \geq 2$, where p is the pole/zero excess of the nominal plant). Then the asymptotic gain of the nominal open loop is:

$$\left|L_o(j\omega)\right| \sim \frac{A}{\omega^{p-1}} \times \left|k_d\right|$$

at high frequencies. Since A and p are fixed from the plant, $|L_o(j\omega)|_{\omega=high}$ is minimised by minimising $|k_d|$. Hence the following optimisation problem is formulated:

Minimise k_d subject to the following constraints:

$$\left|L(j\omega_i)\right| \geq f(\omega_i, \psi), \quad \text{for all } i=1,2,3,\ldots\ldots,N$$

$$(\text{where } \psi = \angle L(j\omega_i))$$

$$\text{AND} \quad L(j\omega_i) \notin B, \quad \text{for all } i=1,2,3,\ldots\ldots,N$$

This suggests an algorithm for minimising $|k_d|$. First assume that the axis representing the phase angle of the NC has been discretised into a linearly spaced array $\{ \psi_1, \psi_2, \psi_3, \ldots\ldots, \psi_n \}$ (n can take any value but 100 is suitable)[6].

Suppose that we fix the phase at the nominal open loop at the first frequency of interest, i.e. $\angle L_o(j\omega_l) = \psi_1$. Then:

$$\angle K(j\omega) = \angle L_o(j\omega_1) - \angle G_o(j\omega_1)$$

or

$$\angle K(j\omega_1) = \psi_1 - \beta(\omega_1) = \tan^{-1}\left(\frac{k_d}{k_p} \times \omega_1 \right) \tag{28}$$

Hence

$$\frac{k_d}{k_p} = \frac{1}{\omega_1} \times \tan^{-1}\left(\tan(\psi_1 - \beta(\omega_1)) \right) \tag{29}$$

is fixed. Thus

$$\left| K(j\omega_i) \right| = \left| k_d \right| \sqrt{\frac{1}{\gamma_o^2} + \omega_i^2}$$

or

$$\left| K(j\omega_i) \right|_{dB} = 20 \log_{10}(\left| k_d \right|) + 10 \log_{10}\left(\frac{1}{\gamma_o^2} + \omega_i^2 \right) \tag{30}$$

and hence

---

[6] The result depends on the discretisation of the phases, if the discretised phases comply with the phases of the bounds then the result is nearly accurate.

$$\left|L_o(j\omega_i)\right|_{dB} = 20\log_{10}(k_d) + 10\log_{10}\left(\frac{1}{\gamma_o^2} + \omega_i^2\right) + 20\log_{10}\left(\left|G_o(j\omega_i)\right|\right) \qquad (31)$$

$|k_d|$ should be large enough to satisfy the Horowitz specifications (including disturbance bounds if applicable), i.e.:

$$\left|L_o(j\omega_i)\right|_{dB} \geq f(\omega_i, \psi_i) \qquad (32)$$

where $\psi_i = \angle L_o(j\omega_i)$, for all $i=1,2,3,......,N$. This implies (from equation (31)) that

$$20\log_{10}(|k_d|) \geq f(\omega_i, \psi_i) - 20\log_{10}\left(\left|G_o(j\omega_i)\right|\right) - 10\log_{10}\left(\frac{1}{\gamma_o^2} + \omega_i^2\right) \qquad (32a)$$

The above is equivalent to:

$$20\log_{10}(|k_d|) \geq \max_{i\in\{1,2,3,.....,N\}}\left\{f(\omega_i, \psi_i) - 20\log_{10}\left(\left|G_o(j\omega_i)\right|\right) - 10\log_{10}\left(\frac{1}{\gamma_o^2} + \omega_i^2\right)\right\}$$

or

$$|k_d| \geq 10^{\wedge}\left(\frac{\max\limits_{i\in\{1,2,3,.....,N\}}\left\{f(\omega_i, \psi_i) - 20\log_{10}\left(\left|G_o(j\omega_i)\right|\right) - 10\log_{10}\left(\frac{1}{\gamma_o^2} + \omega_i^2\right)\right\}}{20}\right) \qquad (33)$$

In order to minimise the asymptotic gain of $L_o(j\omega)$ we must choose k_d equal to the *RHS* of equation (33). Note, that $\psi_i = \angle L_o(j\omega_i)$ is fixed for all $i=1,2,3,......,n$. Specifically:

$$\psi_1, \text{ is fixed by assumption}$$

$$\psi_2 = \angle L_o(j\omega_2) = \angle G_o(j\omega_2) + \tan^{-1}(\gamma_o\omega_2), \qquad \text{where } \gamma_o = [tan(\varphi_1)/\omega_1]$$

$$\vdots$$

$$\psi_N = \angle L_o(j\omega_N) = \angle G_o(j\omega_N) + \tan^{-1}(\gamma_o\omega_N)$$

The following algorithm was implemented in *MATLAB*:

Algorithm PD₁

1. Initialise an array to store the local minimum variable k_d for each value of $\angle L_o(j\omega_l)$.

2. Initialise an array to store the relevant values of k_p.

3. Outer loop (runs n times, where n is the number of discretised fixed phases for the first frequency of interest)

  3.1 Find constant γ_o using the following expression:

$$\gamma_o = \frac{1}{\omega_1} \times \tan\left(\phi_k - \angle G_o(j\omega_1)\right)$$

where, ϕ_k is the value of the fixed phases for k=1,2,3,……,n for the first frequency ω_l.

  3.2 Initialise an array to store phases of nominal open loop for all frequencies of interest (it initialises every time the value of fixed phase is changed).

  3.3 Initialise an array to store the values of k_d obtained for all frequencies each time the outer loop runs (it also initialises every time the outer loop runs, and this helps to identify the minimum local k_d for each k)

  3.4 Inner loop (runs a total of N times, where N is the number of frequencies of interest).

    3.4.1 For the first frequency (when i=1) ω_l, the phase of the nominal open loop is fixed by assumption.

    3.4.2 For the rest of the frequencies (when i runs from 2 until N) find the phase of the nominal open loop using the following expression:

$$\psi_i = \angle G_o(j\omega_i) + \tan^{-1}(\gamma_o \omega_i)$$

which is fixed because every time the loop runs the phase of the nominal plant is fixed and known, the frequency is known and the constant γ_o is also known (obtained from the outer loop). The OL phase for the first frequency is exactly the same as the phase of the bounds. For all other frequencies the magnitude of the bounds is obtained approximately via linear interpolation.

    3.4.3 For each i find k_d using formula (33) (met with equality) that satisfies the requirements and temporary store it.

    End of Inner loop.

    3.5 Find the local minimum k_d that satisfies the requirements for each k, and store it.

    3.6 Find the relevant k_p using formula (22) (first solve for k_p) and also store it.

End of Outer loop

4. Obtain the value of the global minimum k_d (optimal solution) and the corresponding index.

5. Use the index obtained in step 4 to find the relevant value of k_p.

END OF ALGORITHM

The above algorithm (which was implemented in Matlab function **cpd_opti**()), works as expected and finds the optimal controller which gives the solution to the design problem. In order to illustrate the procedure, consider the following two examples:

- Example 1:

Consider the plant given in equation (1) and the specifications for tracking requirements and disturbance rejection given in Sections 2.3 and 2.7. Figure 3.3.2.C shows the nominal open loop with the frequencies of interest, the U-contour and the corresponding maximum bounds. It also shows the new nominal open loop corresponding to the designed optimal *PD* controller.
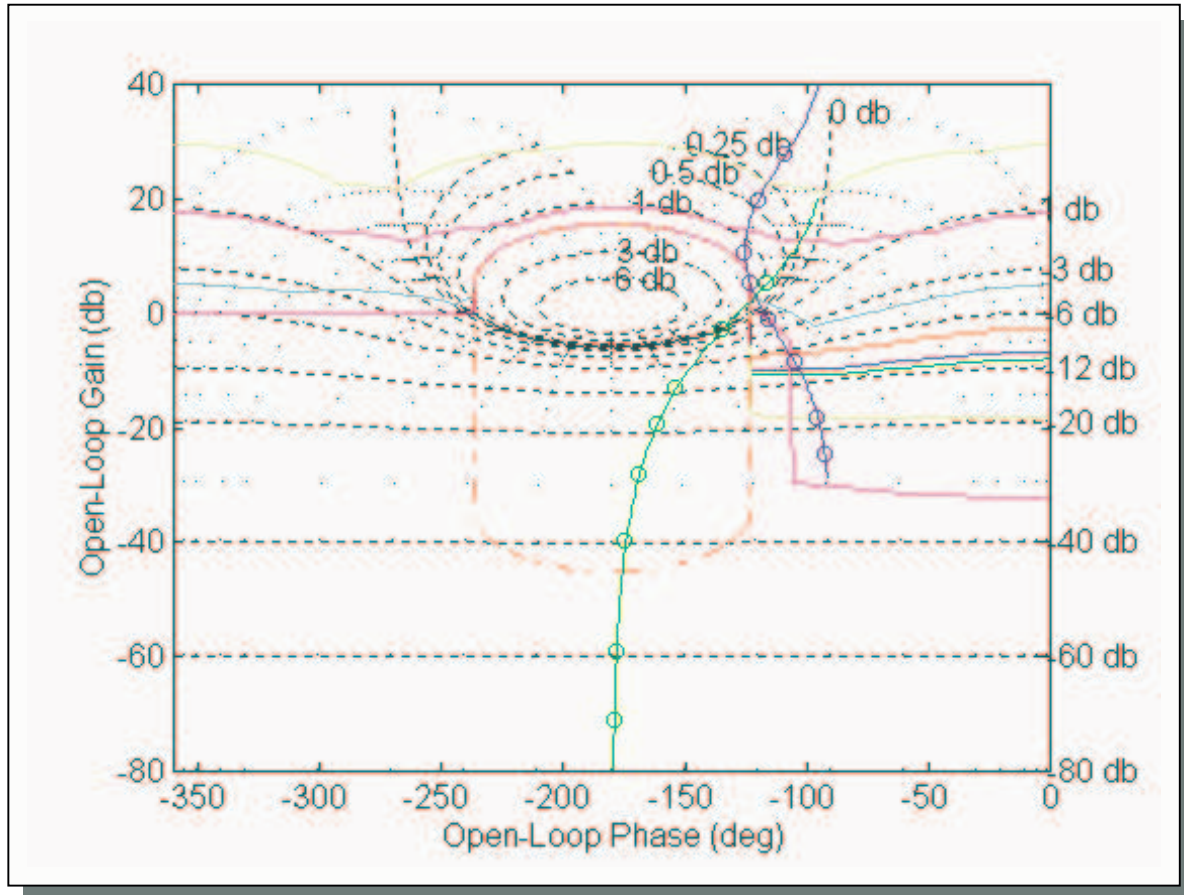
Figure 3.3.2.C: *PD* optimal design (old nominal open loop (green line) and new nominal open loop after the design of the controller (blue line). The circles represent the frequencies of interest)

The optimal *PD* controller obtained is given by:

$$K_{pd\_opt}(s) = 13.3 + 3.53s$$

From figure 3.3.2.C it can be clearly seen that at low frequencies the additional phase lead introduced by K_{pd_opt} is small while at high frequencies rises to almost 90° (the phase of the nominal open loop reaches asymptotically -90° in this example). The shaped open loop system satisfies the tracking/disturbance specifications and is outside the U-contour. At three frequencies (i= 4, 5, 7), $L_o(j\omega_i)$ lies exactly on the corresponding bounds. Figure 3.3.2.D shows the Bode plots of the controller obtained above, where the gain and the phase introduced can be clearly seen (the frequencies of interest are marked with a blue circle):
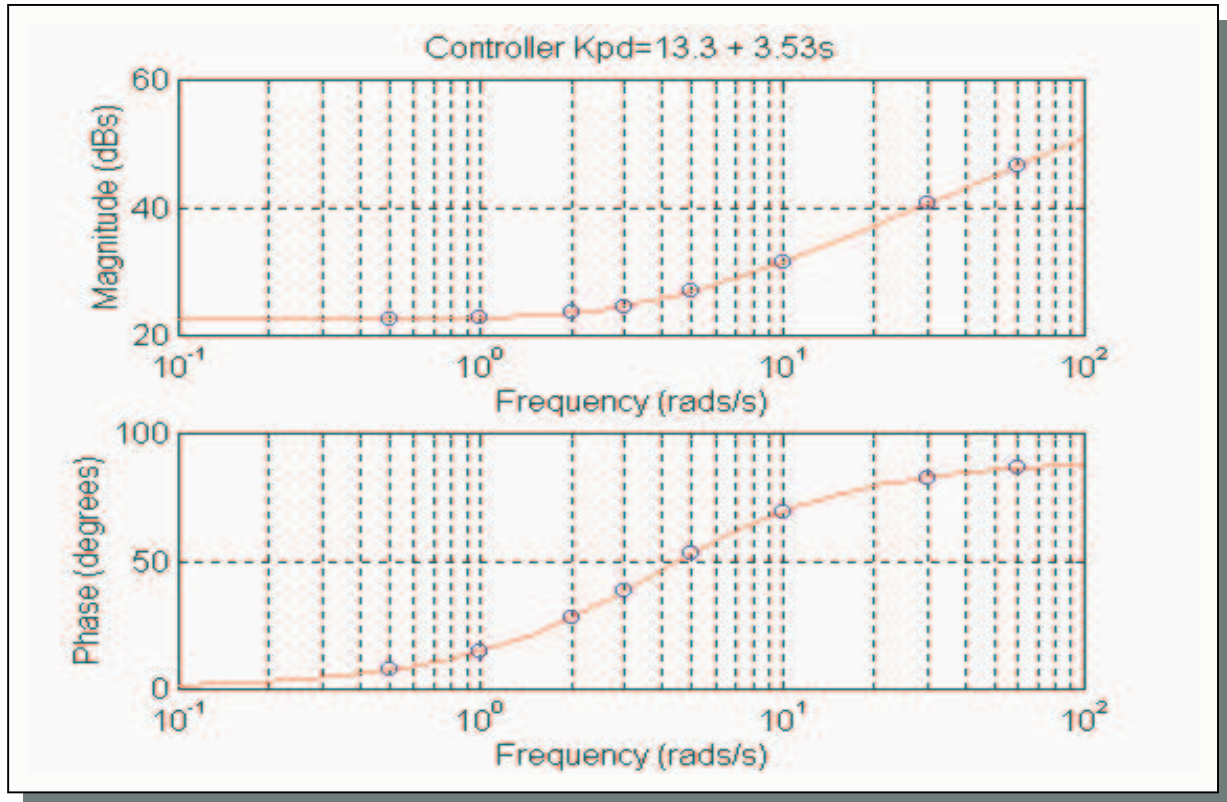
Figure 3.3.2.D: Bode plots of optimal *PD* controller (gain and phase introduced at each frequency)

-Example 2:

Consider the system:

$$G(s) = \frac{a}{s^2}, \quad \text{where } a \in [1,10]$$

(34)

An optimal *PD* controller needs to be designed so that the above system is stabilised and satisfies the tracking specifications given in the previous example (in this case there is no disturbance rejection). Following the procedure of Section 3.3.2, the optimal controller was obtained as:

$$K_{pd\_opt2}(s) = 0.5 + 3.25s$$

Figure 3.3.2.E shows the NC with the nominal open loop, the U-contour, and the corresponding bounds and the new nominal open loop after the design of the optimal *PD*. In this case the phase range is from -180° until -90° because the controller introduces only positive phase with a maximum of 90°:
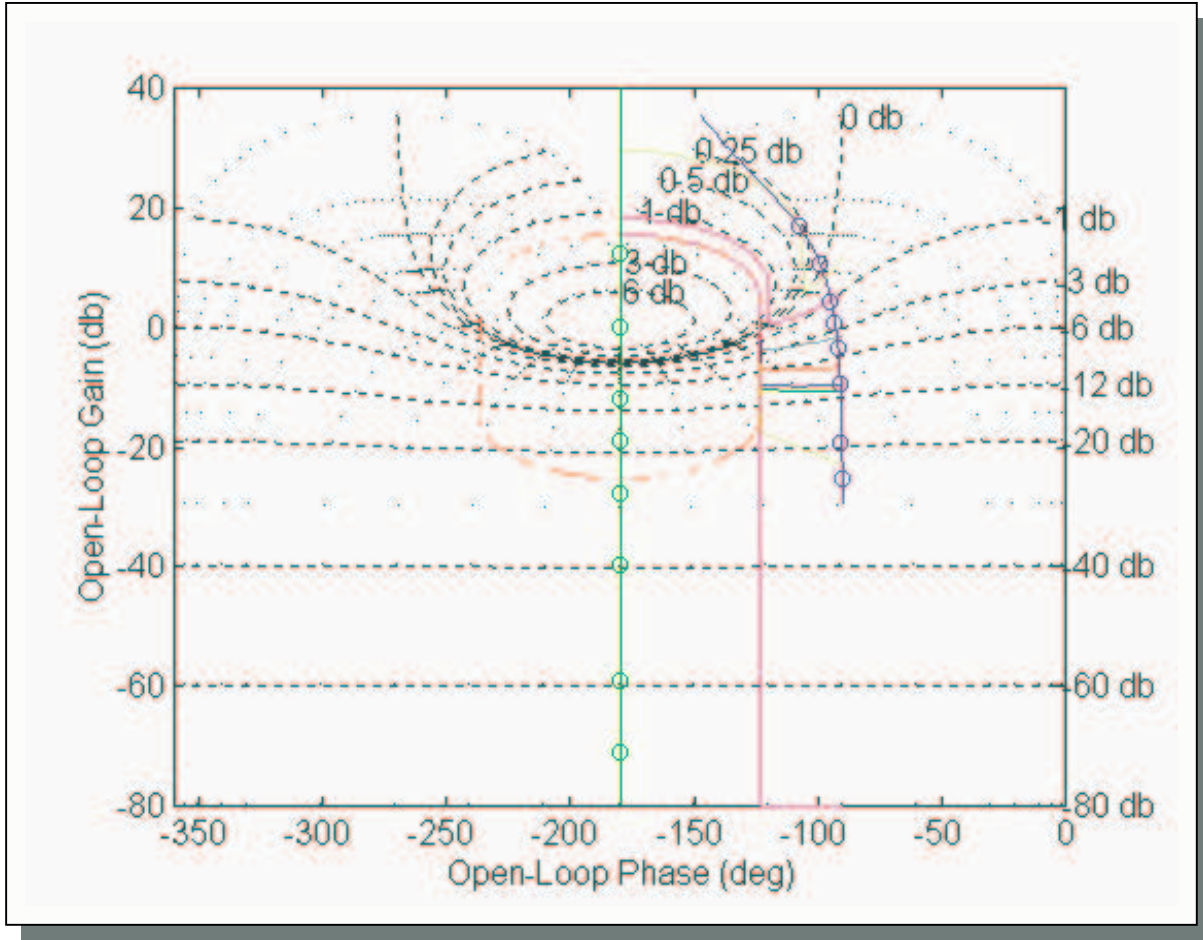
Figure 3.3.2.E: PD optimal design for $G(s) = a/s^2$, where $1 \leq a \leq 10$ (old nominal open loop and frequencies of interest in green, and nominal open loop after designing the controller in blue)

The above examples show that for a realisable system, the design of an optimal *PD* controller following the procedure discussed here is successful. A similar procedure can be followed in order to design a *PI* controller which has the following transfer function:

$$K_{pi}(s) = k_p + \frac{k_i}{s} \tag{35}$$

Both the error and its integral are used for control. The action of a *PI* controller is to reduce the steady state errors by increasing the type of the system by 1, and its use is very common in process control or regulating systems. The next section presents the procedure to design an optimal *PID* controller.

3.3.3 Proportional plus Integral plus Derivative (PID) Controller

PID controllers, also known as *three term* or *process controllers*, are one of the most common type of controllers used commercially. The transfer function of a *PID* controller is the following:

$$K_{pid}(s) = k_p + \frac{k_i}{s} + k_d s \qquad (36)$$

The aim is to adjust the three gain factors (proportional, integral and derivative control) according to the dynamics of the plant, so that both the degree of error reduction (if not error elimination) and the dynamic response will be acceptable. In the frequency domain the *PID* controller introduces phase lag to the nominal open loop (reaching almost $-90°$) at low frequencies due to the dominance of the integral term and phase lead (reaching almost $90°$) at high frequencies due to the dominance of the derivative term. In intermediate frequencies the introduced phase is either negative (due to integral term) or positive (due to derivative term), the proportional term having $0°$ phase introduces only gain [Ref.5,7]. To illustrate, figure 3.3.3.A shows the Bode plots of a *PID* controller with the following transfer function:

$$K_{pid}^{1}(s) = 1 + \frac{2}{s} + 3s$$
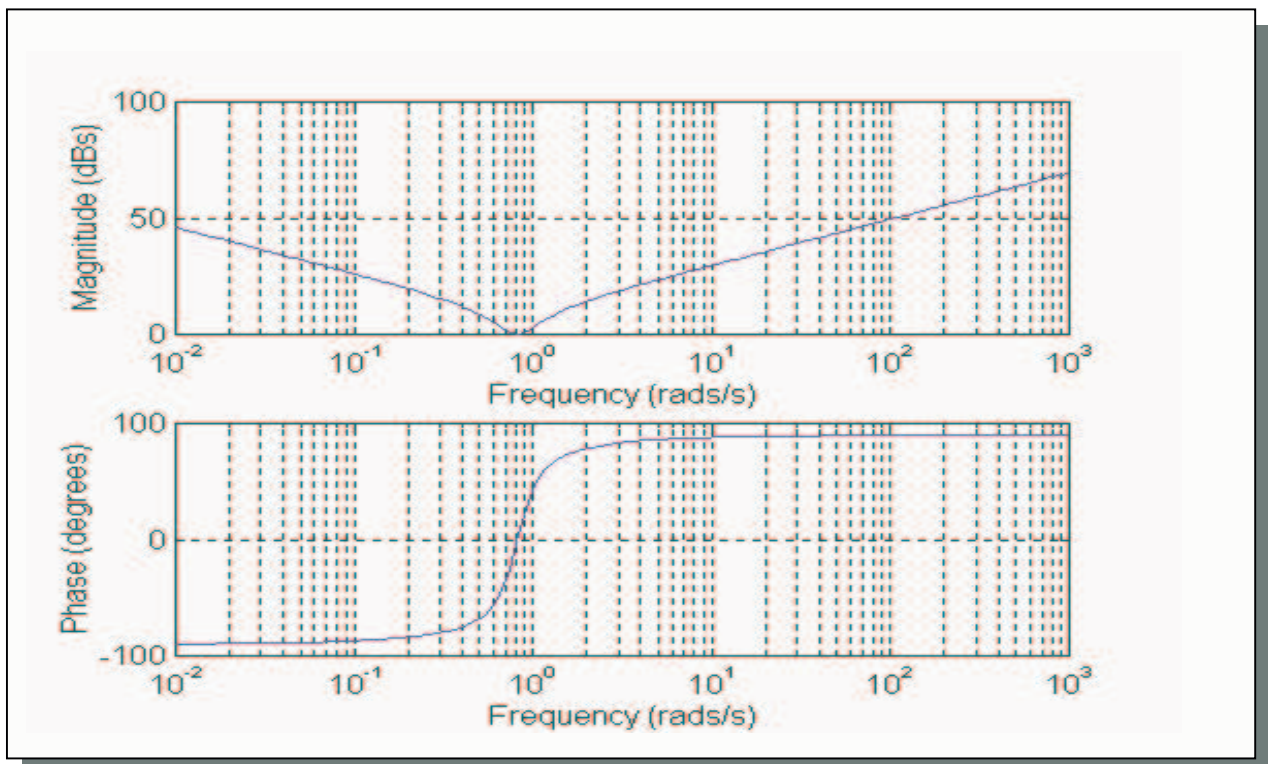
Figure 3.3.3.A: Bode plots of a *PID* controller

In the context of this project, the design constraints that the *PID* controller has to satisfy are:

> 2. $|L(j\omega_i)|_{dB} \geq f(\omega_i)$, for all *i=1,2,3,......,N*
>
> 2. $L(j\omega) \notin B$,   for all *i=1,2,3,......,N*

As in the case of the *PD* controller, the open loop gain must be a minimum (subject to satisfying the above constraints, see Section 3.3.2). The asymptotic gain of the nominal open loop is given by:

$$\lim_{\omega \to \infty} \left\{ \left| \left(k_p + \frac{k_i}{j\omega} + k_d\, j\omega \right) \times G_o(j\omega) \right| \right\} \tag{37}$$

Suppose that:

$$|G_o(j\omega)| \sim \frac{A}{\omega^p}$$

at very high frequencies. (Assume that $p \geq 2$, where *p* is the pole/zero excess of the nominal plant). Then the asymptotic gain of the nominal open loop is:

$$|L_o(j\omega)| \sim \frac{A}{\omega^{p-1}} \times |k_d|$$

at high frequencies. Since *A* and *p* are fixed from the plant, $|L_o(j\omega)|_{\omega=high}$ is minimised by minimising $|k_d|$. Hence the following optimisation problem is formulated:

> Minimise $|k_d|$ subject to the following constraints:
>
> $$|L(j\omega_i)| \geq f(\omega_i, \psi_i), \text{ for all } i{=}1,2,3,......,N$$
>
> $$\text{(where } \psi_i = \angle L(j\omega))$$
>
> $$\text{AND} \quad L(j\omega_i) \notin B, \quad \text{for all } i{=}1,2,3,......,N$$

The frequency response ($s=j\omega$) of the controller (from equation (36)) is:

$$K_{pid}(j\omega) = k_p + \frac{k_i}{j\omega} + k_d\, j\omega$$

or

$$K_{pid}(j\omega) = k_p - j\frac{k_i}{\omega} + k_d\, j\omega \tag{38}$$

In terms of magnitude (linear):

$$\left|K_{pid}(j\omega)\right| = \sqrt{k_p^2 + \left(k_d\omega - \frac{k_i}{\omega}\right)^2} \tag{39}$$

In terms of phase:

$$\angle K_{pid}(j\omega) := \phi(\omega) = \tan^{-1}\left(\frac{k_d\omega - \dfrac{k_i}{\omega}}{k_p}\right) \tag{40}$$

Note that the sign of the phase $\varphi(\omega)$ can be either positive or negative (always $\varphi \in [-90, 90]$) and this depends on the three terms (i.e. it depends on the dominance of the derivative or the integral term, provided that all terms have the same sign).

In contrast to the *PD* controller, the phase of the *PID* controller will be fixed at any two specified frequencies i.e. ω_1 and ω_2. The phase of the controller at all other frequencies will then also be fixed according to the combination of the two fixed phases at the two specified frequencies. Using equation (40), φ_r (fixed phase for ω_1) is given by:

$$\phi(\omega_1) := \phi_r = \tan^{-1}\left(\frac{k_d\omega_1 - \dfrac{k_i}{\omega_1}}{k_p}\right)$$

Then,

$$\tan(\phi_r) = \frac{k_d \omega_1 - \dfrac{k_i}{\omega_1}}{k_p}$$

or

$$k_d \omega_1 - \frac{k_i}{\omega_1} = k_p \tan(\phi_r)$$

which implies

$$k_d \omega_1 - \frac{k_i}{\omega_1} - k_p \tan(\phi_r) = 0$$

Thus

$$k_d - \frac{k_i}{\omega_1^2} - \frac{k_p \tan(\phi_r)}{\omega_1} = 0 \qquad (41)$$

Similarly, ϕ_j (the fixed phase for ω_2) is given by:

$$\phi(\omega_2) := \phi_j = \tan^{-1}\left(\frac{k_d \omega_2 - \dfrac{k_i}{\omega_2}}{k_p}\right)$$

then

$$k_d - \frac{k_i}{\omega_2^2} - \frac{k_p \tan(\phi_j)}{\omega_2} = 0 \qquad (42)$$

Equation (41) and (42) can be arranged in the form of a matrix as $A_{(2x3)} \times \underline{k}_{(3x1)} = \underline{0}$:

$$\begin{bmatrix} 1 & \dfrac{1}{\omega_1^2} & -\dfrac{\tan(\phi_r)}{\omega_1} \\ 1 & \dfrac{1}{\omega_2^2} & -\dfrac{\tan(\phi_j)}{\omega_2} \end{bmatrix} \times \begin{bmatrix} k_d \\ k_i \\ k_p \end{bmatrix} = \underline{0} \qquad (43)$$

Provided that the first frequency ω_1 is not equal to the second frequency ω_2, the rank of matrix A is equal to 2. Equation (43) then implies that the vector $[\ k_d\ \ k_i\ \ k_p\ ]^{\mathrm{T}}$ lies in the (one dimensional)

Kernel of matrix A, i.e. that the three gains k_d, k_i and k_p are fixed (up to scaling). Asimple method of calculating the *Kernel* of A is provided by the *Singular Value Decomposition* (SVD) [Appendix C].

Applying the SVD to matrix A in equation (43), we get

$$A = \begin{bmatrix} U_1 & | & U_2 \end{bmatrix} \times \left[\begin{array}{cc|c} \sigma_1 & 0 & 0 \\ 0 & \sigma_2 & 0 \end{array} \right] \times \begin{bmatrix} V_1^T \\ V_2^T \end{bmatrix} \tag{44}$$

where the range of A ($\mathcal{R}(A)$) is equal to the range of U_1 ($\mathcal{R}(U_1)$) and the kernel of A ($Ker(A)$) is equal to the range of V_2 ($\mathcal{R}(V_2)$). It is also known that,

$$A \times \underline{k} = \underline{0} \tag{45}$$

where

$$\underline{k} = \begin{bmatrix} k_d \\ k_i \\ k_p \end{bmatrix}$$

and $\underline{k} \in Ker(A)$ which is equal to $\mathcal{R}(V_2)$. Then, vector $\underline{k}$ can be expressed as:

$$\underline{k} = \underline{V_2} \times \lambda$$

$$\begin{bmatrix} k_d \\ k_i \\ k_p \end{bmatrix} = \begin{bmatrix} V_{21} \\ V_{22} \\ V_{23} \end{bmatrix} \times \lambda$$

where λ is an adjustable gain factor. Moreover, k_d, k_i and k_p can be associated with V_{21}, V_{22} and V_{23} respectively. Thus the magnitude and the phase of the controller from equations (39) and (40) can be written as:

Magnitude (linear):

$$|K_{pid}(j\omega)| = |\lambda|\sqrt{V_{23}^2 + \left(V_{21}\omega - \frac{V_{22}}{\omega}\right)^2} \qquad (46)$$

Phase:

$$\angle K_{pid}(j\omega) = \tan^{-1}\left(\frac{V_{21}\omega - \dfrac{V_{22}}{\omega}}{V_{23}}\right) \qquad (47)$$

Note that equation (47) implies that the phase of the controller (and thus also the phase of the nominal open loop) is now fixed at every frequency ω. Clearly, $|k_d|$ will be minimised when $|\lambda V_{21}|$ is minimum. The optimal value $|k_d|$ (subject to the constraints given in page 41 and $\varphi(\omega_1)=\varphi_r$ and $\varphi(\omega_2)=\varphi_j$ can be found from the following consideration.

The robust performance objectives are satisfied if[7]

$$|L_o(j\omega)|_{dB} \geq f(\omega_i, \psi_i), \text{ for all } i=1,2,3,\ldots,N$$

where

$$|L_o(j\omega_i)|_{dB} = |G_o(j\omega_i)|_{dB} + |K_{pid}(j\omega_i)|_{dB}$$

Thus

$$|K_{pid}(j\omega_i)|_{dB} \geq f(\omega_i, \psi_i) - |G_o(j\omega_i)|_{dB} \text{ for all } i=1,2,3,\ldots,N$$

Here N is the number of frequencies of interest. Substituting from equation (46),

$$20\log_{10}(|\lambda|) \geq f(\omega_i, \psi_i) - |G_o(j\omega_i)|_{dB} - 10\log_{10}\left(V_{23}^2 + \left(V_{21}\omega_i - \frac{V_{22}}{\omega_i}\right)^2\right)$$

for all $i=1,2,3,\ldots\ldots,N$, which is equivalent to

$$20\log_{10}(|\lambda|) \geq \max_{i \in \{1,2,3,\ldots,N\}}\left\{f(\omega_i, \psi_i) - |G_o(j\omega_i)|_{dB} - 10\log_{10}\left(V_{23}^2 + \left(V_{21}\omega_i - \frac{V_{22}}{\omega_i}\right)^2\right)\right\}$$

or

---

[7] Note that constraint L(jωi) ∈ B can also be formulated in the form $|L(j\omega_i)| > \tilde{f}(\omega_i, \psi_i)$.

$$|\lambda| \geq 10\text{^}\left(\frac{\displaystyle\max_{i\in\{1,2,3,...,N\}} f(\omega_i,\psi_i) - \left|G_o(j\omega_i)\right|_{dB} - 10\log_{10}\left(V_{23}^2 + \left(V_{21}\omega_i - \frac{V_{22}}{\omega_i}\right)^2\right)}{20}\right)$$

Multiplying both sides of the above equation with $|V_{21}|$,

$$\left|\lambda V_{21}\right| \geq \left|V_{21}\right|10\text{^}\left(\frac{\displaystyle\max_{i\in\{1,2,3,...,N\}} f(\omega_i,\psi_i) - \left|G_o(j\omega_i)\right|_{dB} - 10\log_{10}\left(V_{23}^2 + \left(V_{21}\omega_i - \frac{V_{22}}{\omega_i}\right)^2\right)}{20}\right)$$

This equation says that provided $|k_d|$ is chosen to be larger than the RHS term, the constraints are satisfied. Hence the optimal $|k_d|$ is given by,

$$\left|k_{d\_min}\right| = \left|V_{21}\right|10\text{^}\left(\frac{\displaystyle\max_{i\in\{1,2,3,...,N\}} f(\omega_i,\psi_i) - \left|G_o(j\omega_i)\right|_{dB} - 10\log_{10}\left(V_{23}^2 + \left(V_{21}\omega_i - \frac{V_{22}}{\omega_i}\right)^2\right)}{20}\right) \quad (48)$$

Note that throughout this analysis, the phases of $\angle L_o(j\omega_1)$ and $\angle L_o(j\omega_2)$ are fixed as,

$$\psi_1 = \angle L_o(j\omega_1) = \varphi_r$$

and

$$\psi_2 = \angle L_o(j\omega_2) = \varphi_j$$

Clearly, the overall optimal value of $|k_d|$ (i.e. the minimum value of $|k_d|$ which satisfies the robust performance constraints) can be obtained by taking the minimum over *all combinations* of phases $\angle L_o(j\omega_1)$ and $\angle L_o(j\omega_2)$ as these vary within their allowable ranges.

The following algorithm, which obtains the optimal PID controller, was implemented in *MATLAB*:

Algorithm PID₁

1. *Find the phase of the nominal open loop ($K(s)=1$), for the first frequency ω_1.*

2. *Find the phase of the nominal open loop, for the second frequency ω_2.*

3. *Set the range of the first fixed phase φ_r for ω_1 (due to the action of the PID controller in the interval $[-90^o+\angle L_o(j\omega_1),90^o+\angle L_o(j\omega_1)]$).*

4. *Set the range of the second fixed phase φ_j for ω_2 (again due to the action of the PID controller in the interval $[-90+\angle L_o(j\omega_2),90+\angle L_o(j\omega_2)]$).*

5. *Initialise arrays to store the optimal values of k_d, k_i, k_p for all combinations of ψ_2 for fixed ψ_1.*

6. *Initialise arrays to store the optimal k_d, k_i, k_p for all combinations of phases (ψ_1 and ψ_2).*

7. *Outer loop (runs n times, where n is the number of discretised points for the first fixed phase φ_r).*

   7.1 *Intermediate loop (runs k times, where k is the number of discretised points for the second fixed phase φ_j).*

   7.1.2 *Perform SVD for matrix A (for each combination of φ_r and φ_j).*

   7.1.3 *Hold the values of vector $\underline{V}_2$.*

   7.1.4 *Initialise matrix to store the phase of the nominal open loop for all frequencies of interest (it initialises each time a SVD is performed).*

   7.1.5 *Initialise arrays to store local minimum k_d and corresponding k_i and k_p for each time the inner loop runs (these initialise each time the combination of phases change).*

   7.1.6 *Inner loop (runs N times, where N is the number of frequencies of interest).*

7.1.6.1 For the first two frequencies (i=1,2), the phase of the nominal open loop is fixed by assumption.

7.1.6.2 For the rest of the frequencies find the phase of the nominal open loop using:

$$\psi_i = \angle G_o(j\omega_i) + \angle K_{pid}(j\omega_i), \qquad \text{for all } i = 3,4,\ldots,N$$

These are fixed because every time the loop runs the phase of the nominal plant is fixed and known and the phase of the controller is also known (via the SVD). For all frequencies of interest the magnitude of the bounds is obtained approximately via linear interpolation.

7.1.6.3 For each i find the gain λ using equation (48) that satisfies the requirements and temporary store it. Then find k_d, k_i and k_p by multiplying them with the associated element of $\underline{V_2}$ (force k_p positive so that the phase of the controller will always be in the interval [-90°,90°]).

End of Inner loop.

7.1.7 Find the local minimum of k_d for the current combination of phases and store it, store also the corresponding k_i and k_p.

End of Intermediate loop.

7.2   Find the minimum k_d of all minima obtained in 7.1.7 and store it. Also store the corresponding k_i and k_p.

End of Outer loop.

8. Find the global minimum k_d and also the corresponding k_i and k_p.

End of Algorithm

The above algorithm (was implemented in Matlab function **pid_op2()**), works as expected and finds the optimal PID controller which gives the solution to the design problem. In order to get the 'best' controller, which gives the solution the following considerations were made:

(1). The above procedure is followed only when the all elements of vector $\underline{V}_2$ have the same sign. This implies that all controller gains (k_d, k_i, k_p) will be positive and the phase of the controller will always be in the range [-90°, 90°]. The controller will introduce phase lag at low frequencies and phase lead at high frequencies as desired.

(2). If the elements have different sign, then all gains are set to infinity (and so they are discarded when the minimum is chosen).

(3). It is a good practice to fix the phase of the nominal open loop at the first and the last frequency of interest. By following this approach the sensitivity of the solution is improved. This also allows the phase in the last frequency vary in a range outside the U-contour, which means that the number of combinations is reduced.

(4). The two fixed phases are independent and as a result different number of discretisation points can be used for each one. This helps to determine the magnitude of the bounds more accurately via linear interpolation.

-Example 1:

Consider the plant given in equation (1). Here a PID controller is needed in order to help the system meet the tracking and disturbance rejection specifications given in Sections 2.3 and 2.7. Figure 3.3.3.B shows the nominal open loop with the selected frequencies, the U-contour and the corresponding maximum bounds. Moreover, it shows the new nominal open loop corresponding to the optimal PID controller.
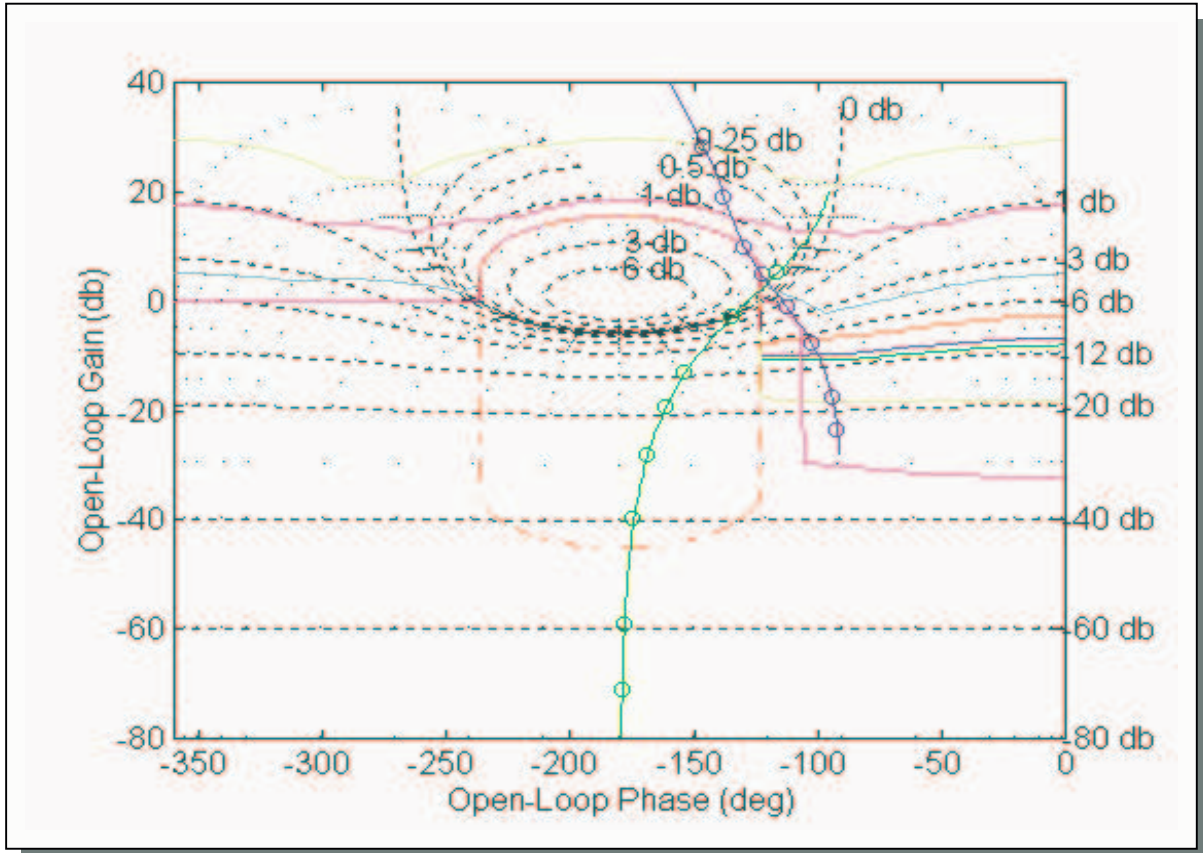
Figure 3.3.3.B: *PID* optimal design (initial nominal open loop (green line) and new nominal open loop after the design of the controller (blue line). The circles represent the frequencies of interest

The optimal PID controller obtained is given by:

$$K_{pid\_opt}(s) = 12.5 + \frac{4.53}{s} + 3.9s$$

From figure 3.3.3.B it can be seen that at low frequencies due to the dominance of the integral term, phase lag is introduced to the nominal open loop while at high frequencies due to the dominance of the derivative term, phase lead is introduced. Note also that the shaped optimal open loop lies on or above the bounds, with four frequencies of interest (i=1,3,4,6) lying exactly on the bounds. To illustrate the action of the PID controller, figure 3.3.3.C shows its Bode plots (gain and phase introduced by the controller). The frequencies of interest are marked with a circle.
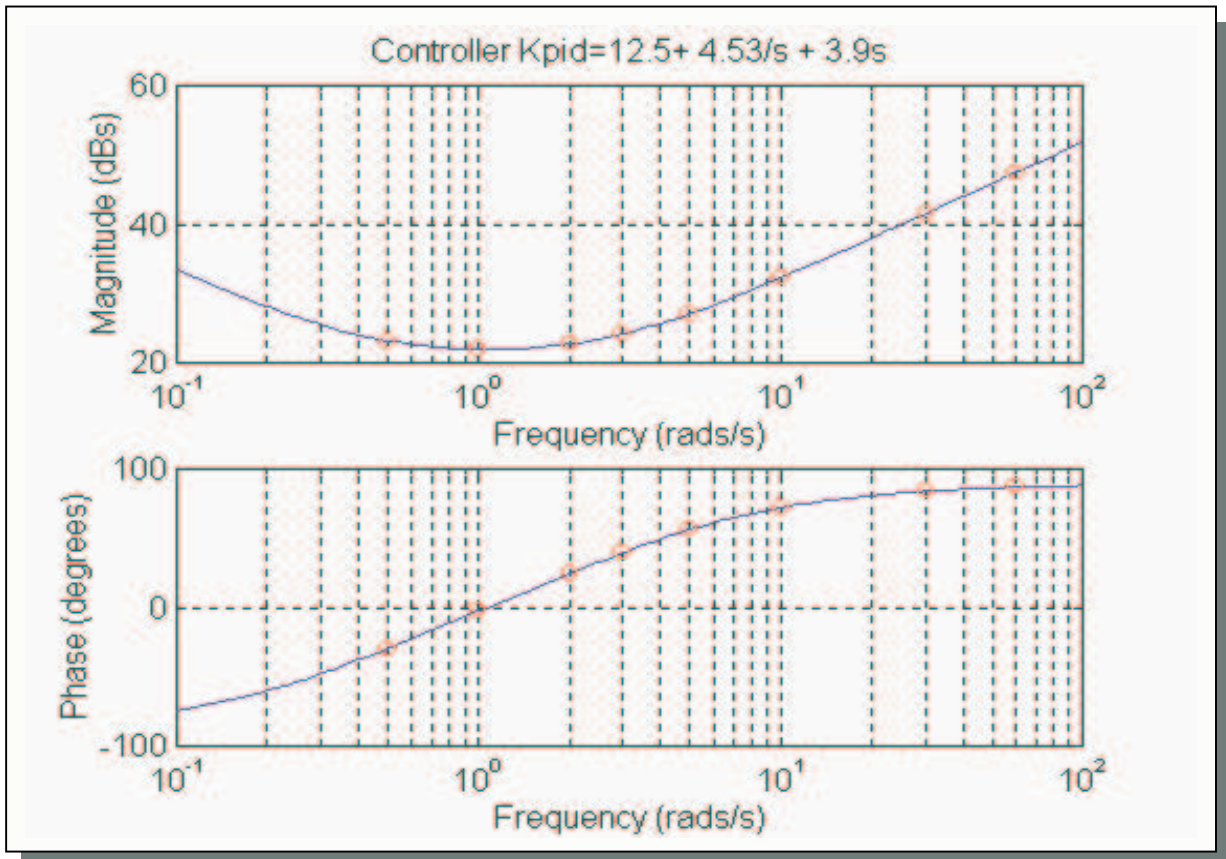
Figure 3.3.3.C: Bode plots of optimal *PID* controller (gain and phase introduced)

-Example 2:

Consider the system:

$$G(s) = \frac{k}{(s+a)(s+b)}, \qquad \text{where } k \in [1,4], \ a \in [1,5] \text{ and } b \in [1,4]$$

The design of an optimal PID is needed so that the system will satisfy the tracking specifications given in the previous example (there is no disturbance rejection included). Moreover, in this case the chosen frequencies are ω={0.1, 0.5, 1, 2, 3, 5, 10, 60} rads/s. The optimal controller was designed following the procedure of Section 3.3.3. Figure 3.3.3.D shows the NC with the nominal open loop, the U-contour, and the Horowitz templates (which are the corresponding bounds) and the new nominal open loop after the design of the optimal PID controller.
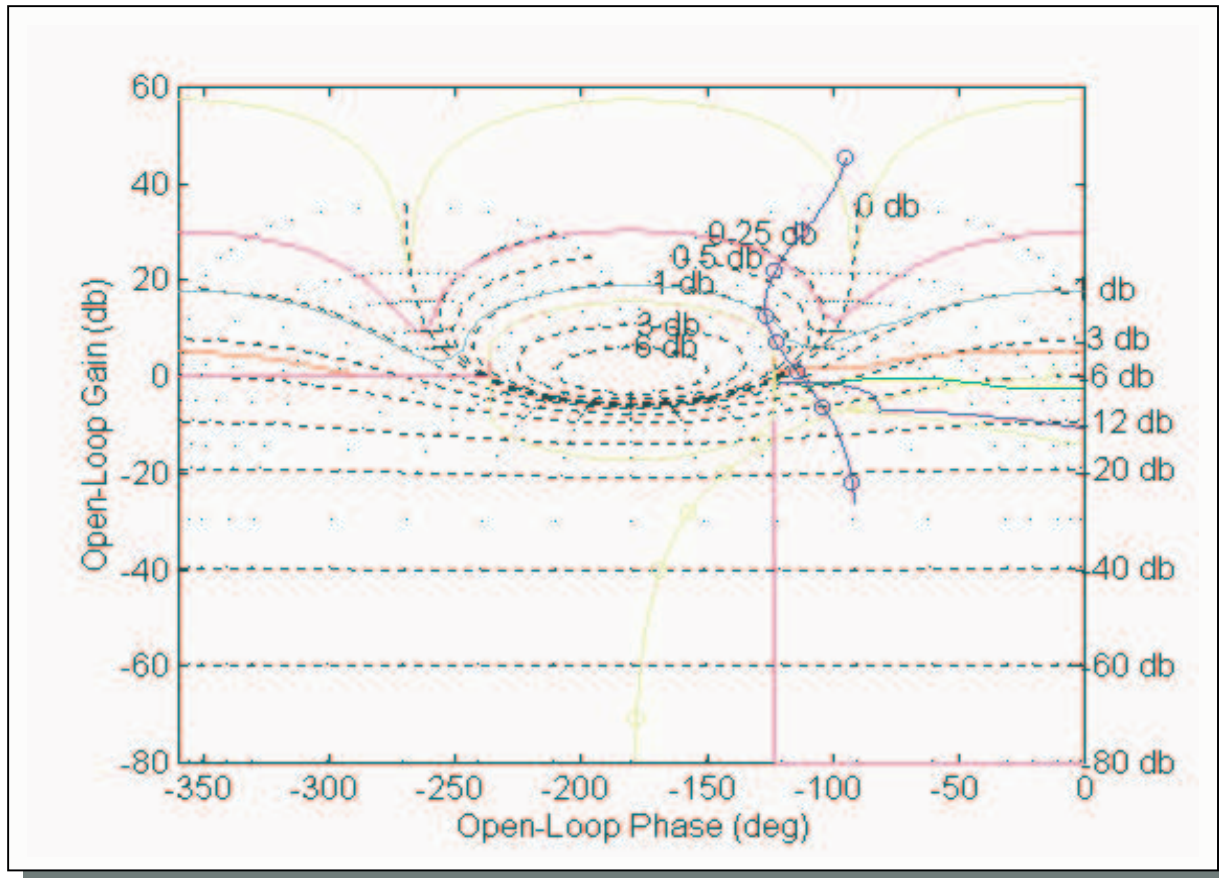
Figure 3.3.3.D: *PID* optimal design for *G(s)=k/(s+a)(s+b)*, where the nominal open loop before the design of the controller is in green and the new nominal open loop after the design of the controller is in blue, the frequencies of interest are represented by circles.

From the above examples, the design of an optimal PID controller for realisable systems following the procedure discussed in this section was successful. In order to complete the design procedure, an appropriate pre-filter will be designed. This is discussed in the next chapter.

CHAPTER FOUR

PRE-FILTER DESIGN

4.1 Introduction

The design of an appropriate nominal open loop $L_o(j\omega)$ guarantees only that the variation ('spread') of the magnitude response of the control ratio $|T_R(j\omega_i)|$ is within the allowed specifications (i.e. less or equal than $\delta_R(j\omega_i)$) [Ref.1]. The role of a *pre-filter* in a control system is to place

$$LmT(j\omega_i) = \frac{L(j\omega_i)}{1 + L(j\omega_i)}$$

within the given specifications in the frequency domain (see Section 2.3, figure 2.3.B). That is, the variation of $|T_R(j\omega_i)|$ must lie within the bounds B_u and B_l. Figure 4.1.A shows the bounds B_u and B_l with the variation of $|T_R(j\omega_i)|$ for the example considered in equation (1) with parameter range of $k=\{1,5,10\}$ and $a=\{1,5,10\}$. Note that in order to find the maximum spread of the variation of $|T_R(j\omega_i)|$, the minimum and maximum values for each uncertainty parameter must be included, i.e. the 'best' and the 'worst' case-combination.
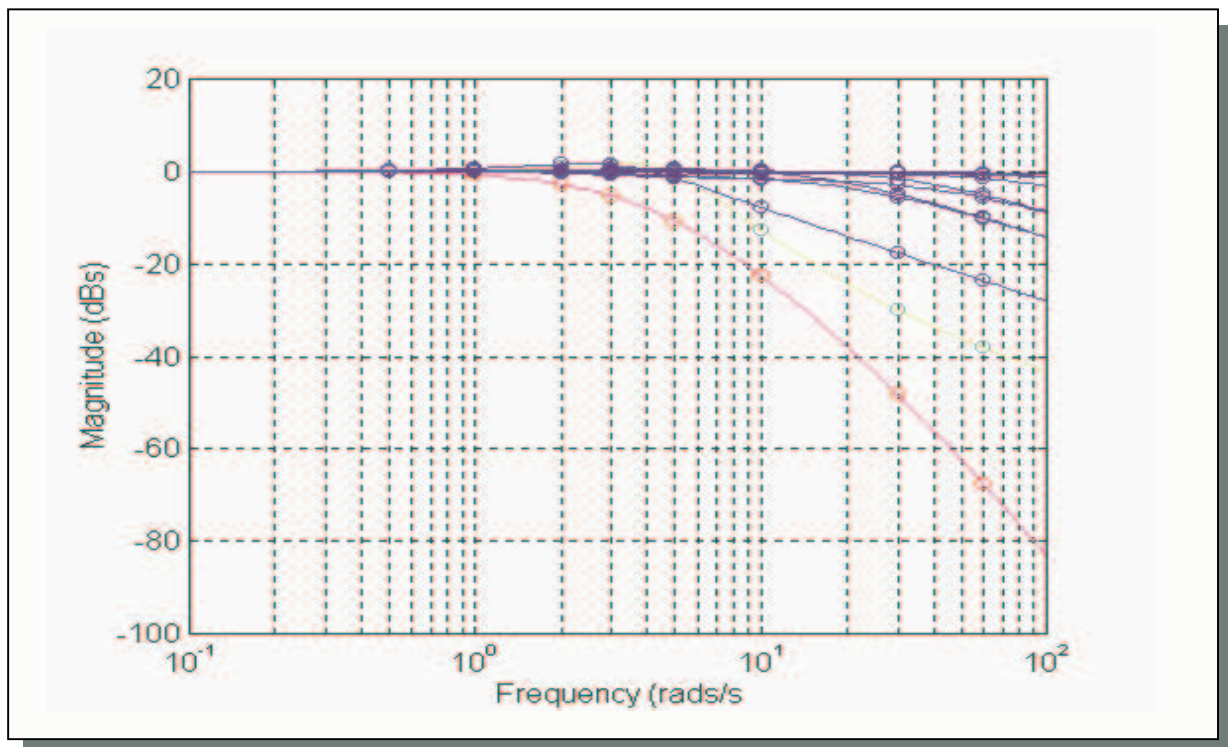

Figure 4.1.A: Frequency responses of CL system without pre-filter and the desired range of acceptable CL frequency responses

The next section discusses the design procedure of an appropriate *pre-filter*, which will adjust the CL system responses within the desired range.

4.2 Pre-filter Design

1. First, the CL system responses without the pre-filter are determined by taking various combinations of the uncertainty parameters of the plant (including at least the maximum and the minimum values of each of the parameters to ensure maximum spread).

2. From the responses determined in step 1, the maximum and minimum bounds are obtained (their difference gives the maximum spread). Figure 4.2.A, shows the desired range of bounds and the maximum spread of the CL system responses.
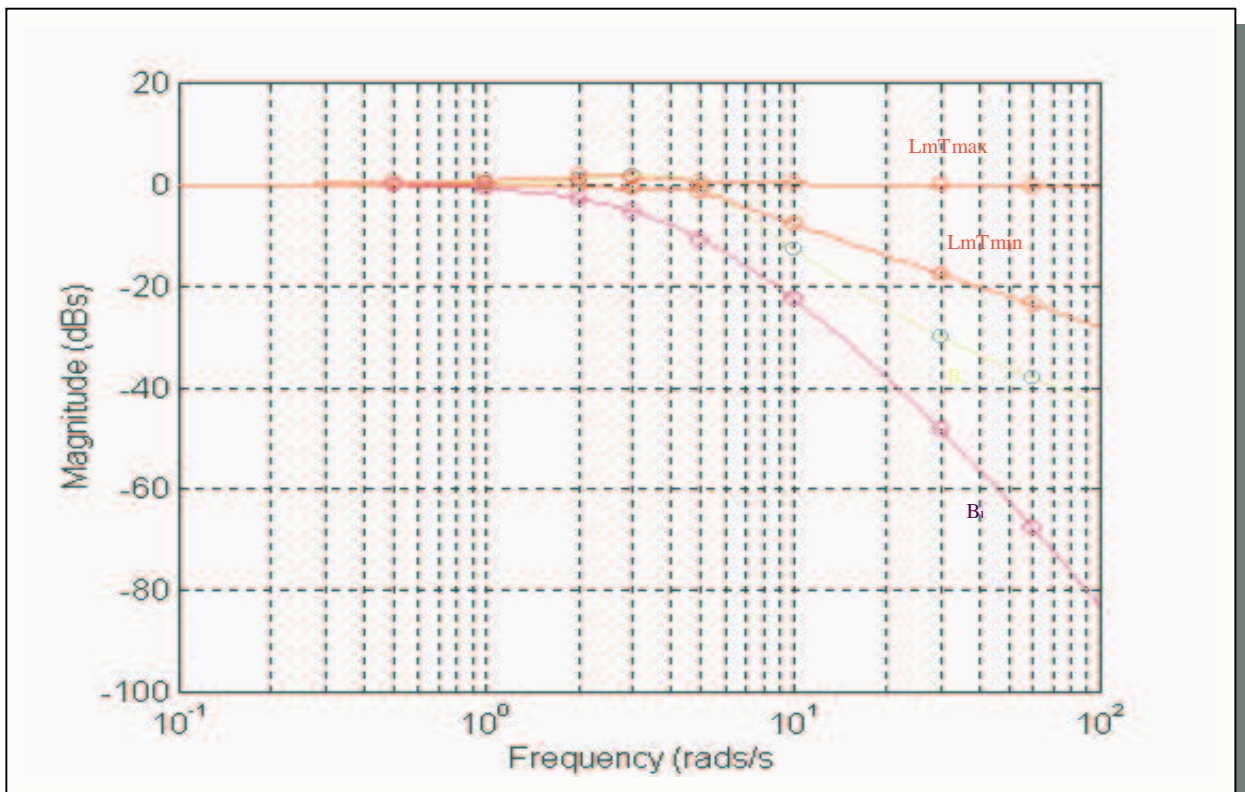

Figure 4.2.A: Desired range of bounds and maximum spread of CL system responses without the *pre-filter*

3. From steps 1 and 2 above, we obtain the differences $[B_u - LmT_{max}]$ and $[B_l - LmT_{min}]$. These differences represent the maximum acceptable bound and the minimum acceptable bound of the magnitude frequency response of the *pre-filter*. Figure 4.2.B shows the range in within the bound of the pre-filter must lie in order to satisfy that the CL system responses will lie within the given specifications.
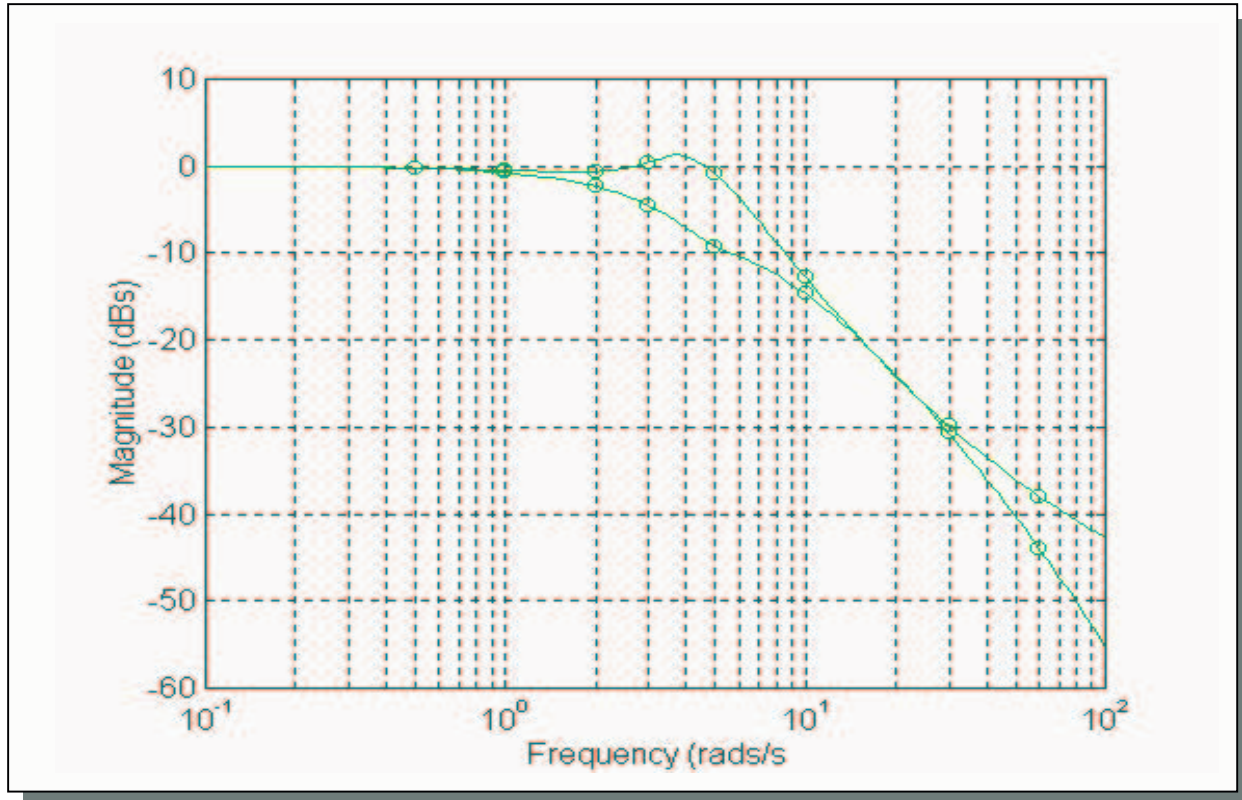
Figure 4.2.B: Allowable frequency response (magnitude) range of pre-filter

4. Using straight-line approximations (usually by inspection from the graphs), *F(s)* can be synthesised such that *LmF(jω)* will lie within the range of allowable bounds from step 3. Moreover for step forcing functions,

$$\lim_{s \to 0}\{F(s)\}=1$$

  is enforced so that the s.s.e to step inputs is zero.

5. The *pre-filter F(s)* obtained from above procedure ensures that the CL system responses lie within the specified range shown in figure 4.2.A (B_u - B_l), for all combinations of the uncertain parameters [Ref.1].

Note that for this example, as can be seen from figure 4.2.B the frequency response of *F(s)* at certain frequencies can vary more than at other. This can be verified from figure 4.2.A where we can see that at frequencies $ω_{4,5}$ the CL system responses have a greater range of adjustment because the specifications are not tight. In addition in frequencies $ω_{1,2,6,7}$ the specifications are very tight and therefore the pre-filter bounds are limited (i.e. only one straight-line approximation can be chosen).

4.3 Types of Pre-filter

Usually a second order pre-filter suffices; this has the following transfer function:

$$F(s) = \frac{A_g}{\left(1 + \dfrac{s}{\omega_{c_1}}\right)\left(1 + \dfrac{s}{\omega_{c_2}}\right)} \tag{49}$$

where, A_g is an adjustable gain (usually 1), ω_{c_1} and ω_{c_2} are the first and second cut-off frequencies, respectively. These constants can be found via the procedure presented in Section 4.2.

Higher order *pre-filters* can be used in order to give a more accurate result. Nevertheless, higher order *pre-filters* are more complex and thus the minimum-order possible *pre-filter* is desired.

4.4 Design example (for PID controller)

The design of an appropriate *pre-filter* is the same for all types of controllers, i.e. *phase lead/lag cascade networks*, *PDs*, *PIDs*. For illustration purposes of the procedure, the system described in equation (1) and the optimal *PID* controller, obtained in Section 3.3.3.

Figure 4.1.A shows the desired range of tracking bounds and the CL system responses without the *pre-filter*, and figure 4.2.A shows the maximum spread of the CL responses without the *pre-filter* and the given specifications. Moreover figure 4.2.B, shows the allowable range of bounds, within which the response of the designed *pre-filter* has to lie.

By inspection, an appropriate 2$^{\text{nd}}$ order *pre-filter* for this system was found to be:

$$F(s) = \frac{1}{\left(1 + \dfrac{s}{2.5}\right)\left(1 + \dfrac{s}{11.3}\right)} \tag{50}$$

Its magnitude frequency response can be seen in figure 4.4.A. Clearly this lies within the allowable range given in figure 4.2.B.
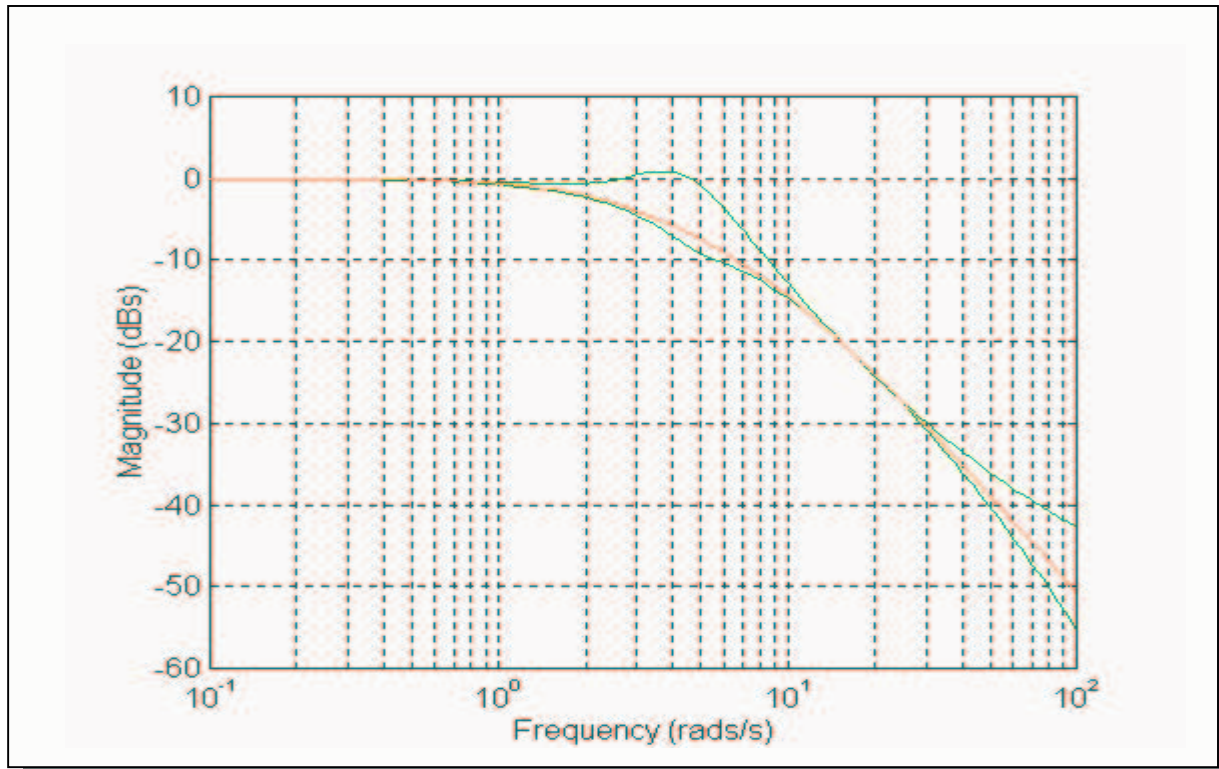
Figure 4.4.A: Magnitude frequency response of designed *pre-filter F(s)*

Figure 4.4.B shows that by using the designed pre-filter -from equation (50)- the CL responses lie within the range of allowed specifications.
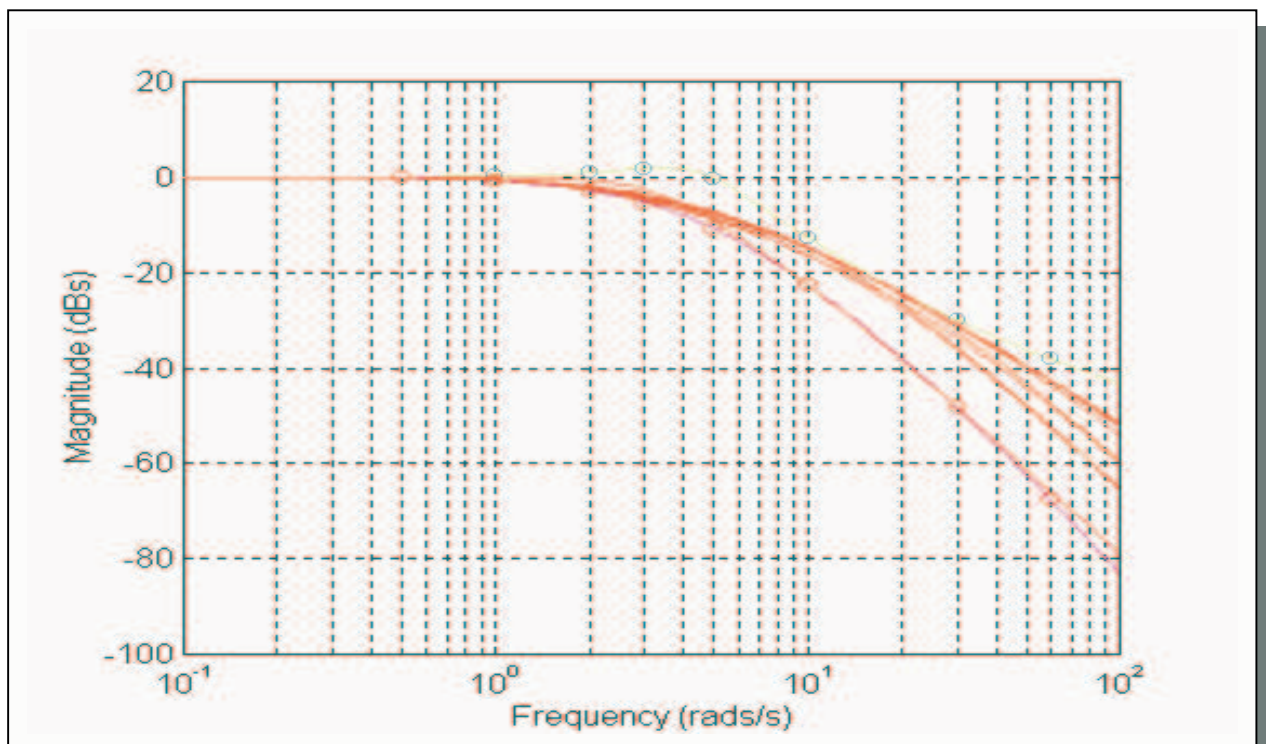

Figure 4.4.B: CL bounds after the introduction of the designed *pre-filter F(s)*

57

From the above, it follows that the system will meet both the given tracking specifications and also the disturbance rejection specifications. This can be seen in the next Chapter, which includes the simulation results of the system, described in equation (1), for the three types of controllers used in this project.

CHAPTER FIVE

SIMULATION RESULTS

5.1 Introduction

This chapter presents the simulation results of the overall system including the phase lead/lag cascaded networks (from the graphical design), the *PD* controller, and the *PID* controller, which were obtained in this project. Note that the *pre-filter* for each one of the overall systems was designed by following the procedure of Section 4.2. The system, which was used to illustrate the final results of the design, is given in equation (1).

5.2 Tracking Performance-Simulations

First the tracking performance of the system was obtained for each controller and appropriate *pre-filter*. Figure 5.2.A shows the tracking response (step responses for certain combinations of the uncertain parameters) of the system including the *phase lead/lag* cascaded networks.
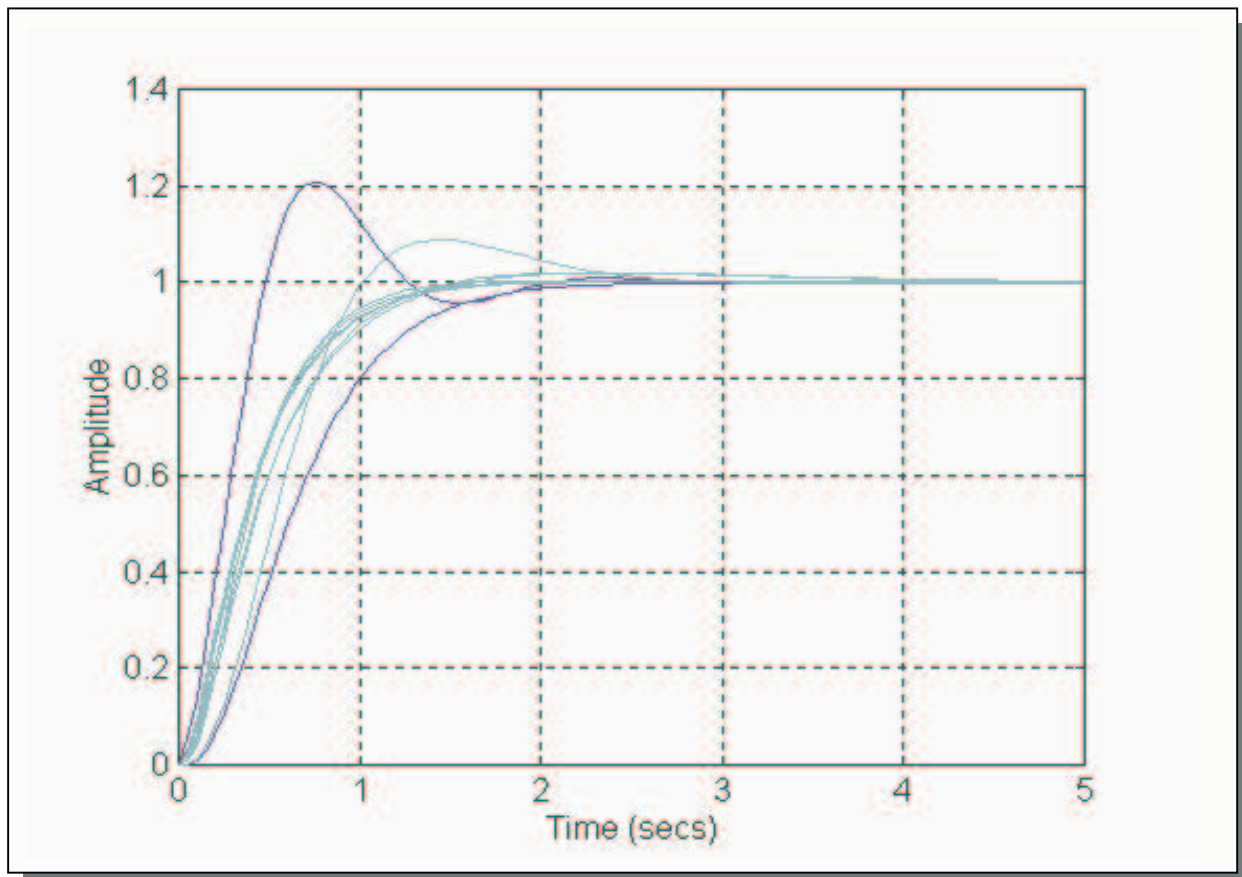

Figure 5.2.A: Step responses of CL system with appropriate pre-filter including phase lead/lag cascaded networks.

Figure 5.2.B shows the step responses of the CL system including the *PD* controller.
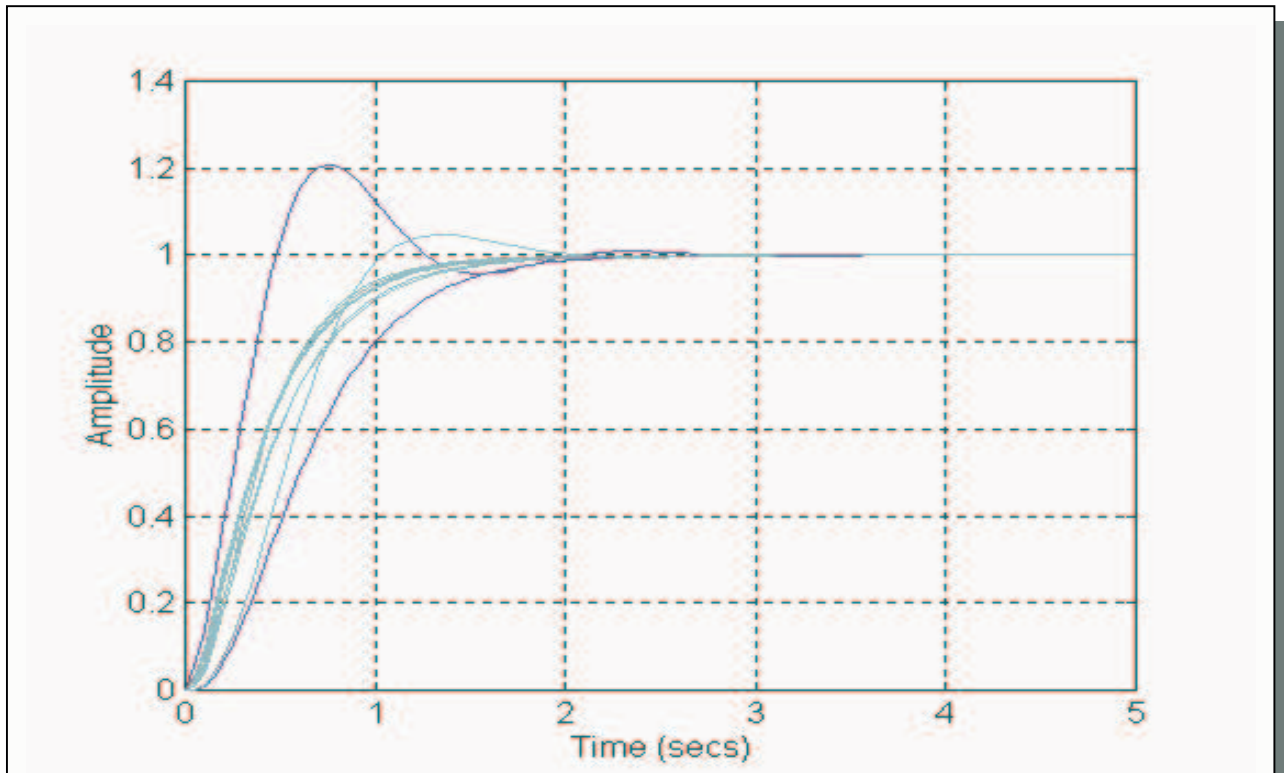

Figure 5.2.B: Step responses of CL system with appropriate pre-filter including *PD* controller.

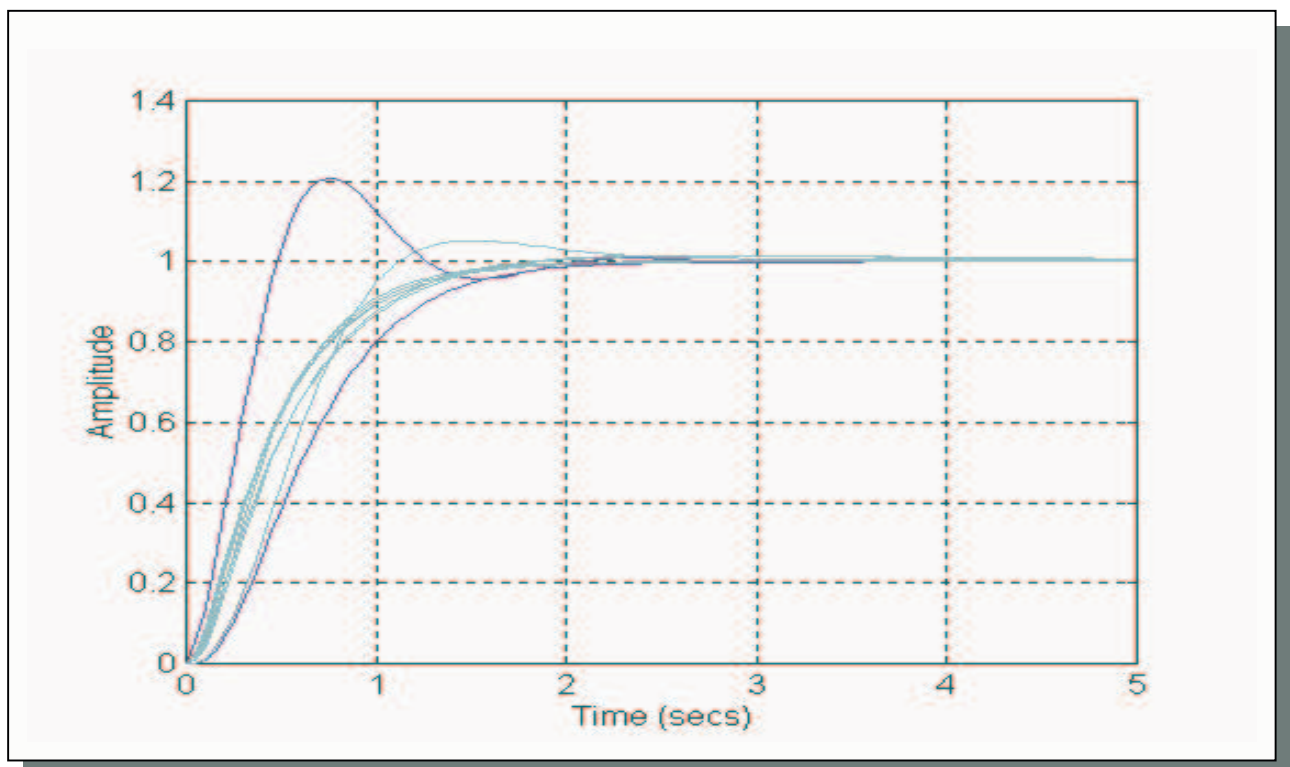Finally, figure 5.2.C shows the step responses of the CL system incorporating the *PID* controller.

Figure 5.2.C: Step responses of CL system with appropriate pre-filter including *PID* controller.

From the figures above it can be seen that the step responses of the system for all controllers designed were acceptable. The system responses to a unit reference input lie within the given specifications in all cases. Thus, its behaviour will be within the specified allowable range.

5.3 Disturbance rejection-Simulations

The system must also satisfy the disturbance rejection specifications (given in section 2.7). Figure 5.3.A illustrates the response of the system with the phase lead/lag cascaded networks to a unit step disturbance at the output of the plant *G(s)*.
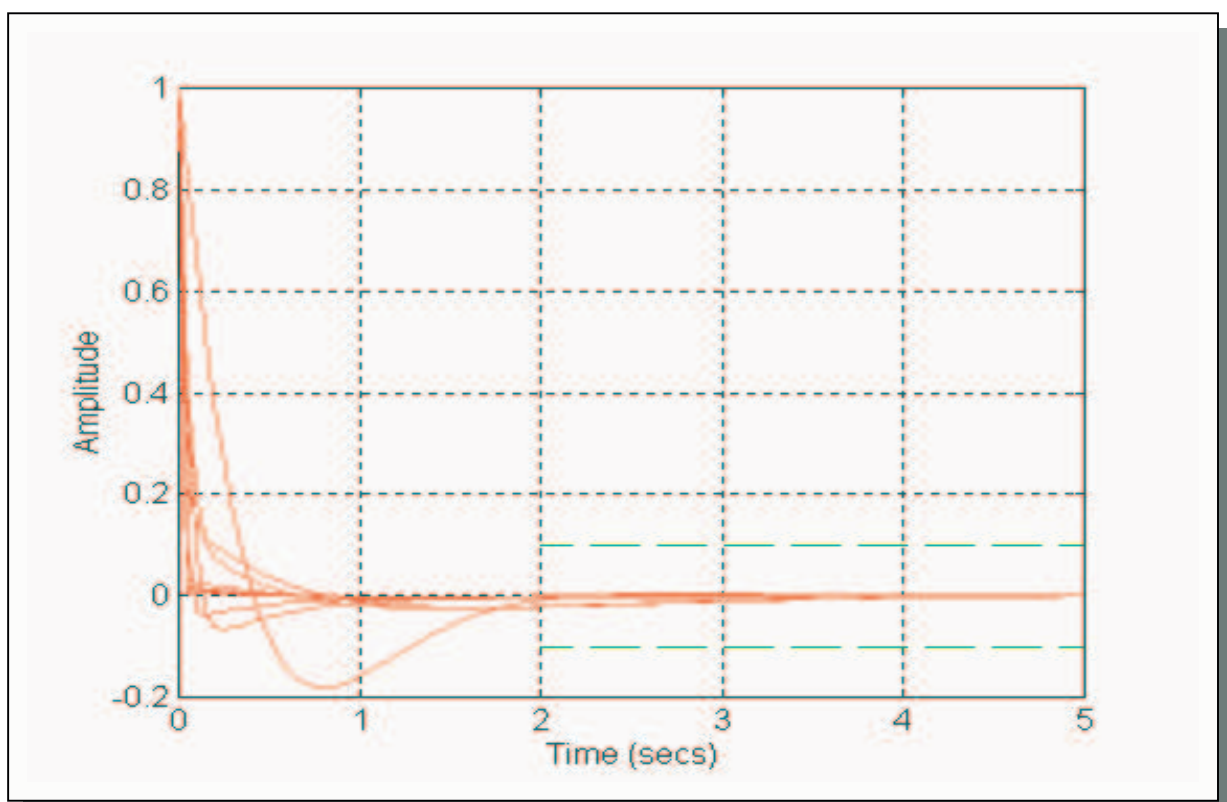

Figure 5.3.A: Disturbance rejection of system with phase lead/lag networks in cascade

Figure 5.3.B shows the response of the system using the *PD* controller to a unit step disturbance input at the output of the plant.
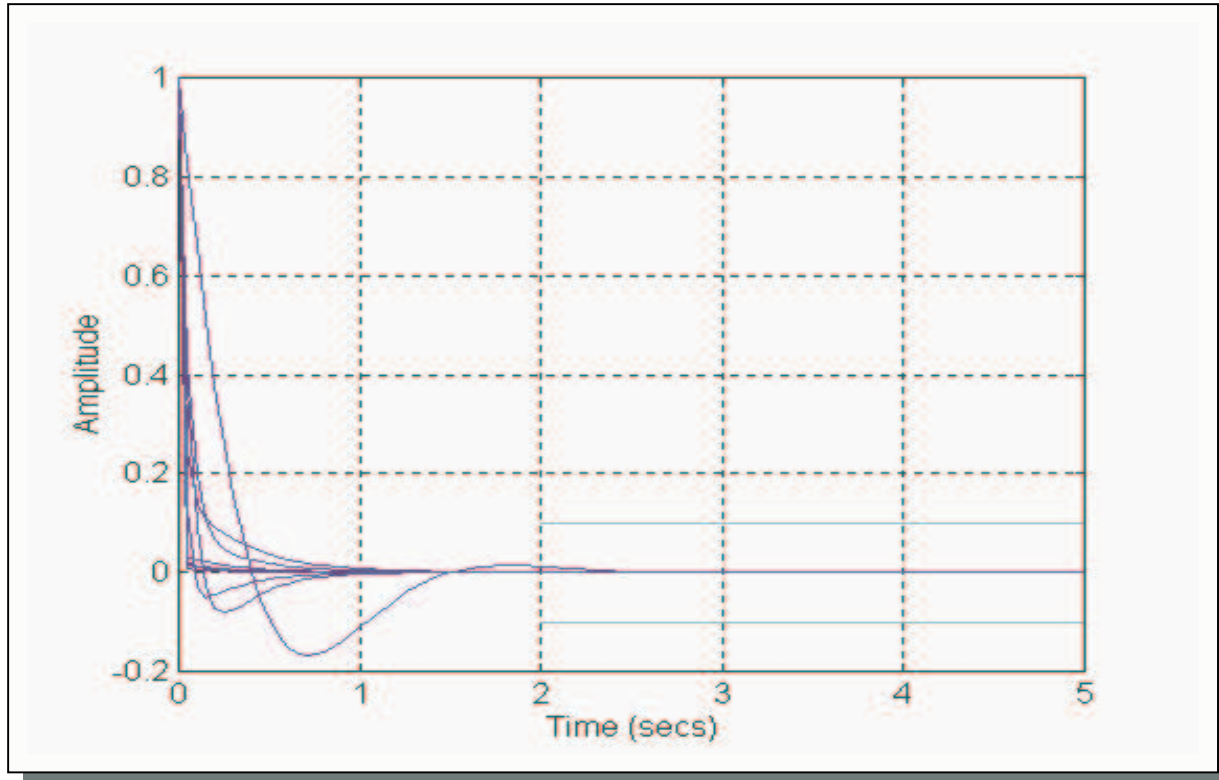
Figure 5.3.B: Disturbance rejection of system with *PD* controller

Finally, figure 5.3.C shows the response of the system incorporating the *PID* controller to a unit step disturbance input at the output of the plant.

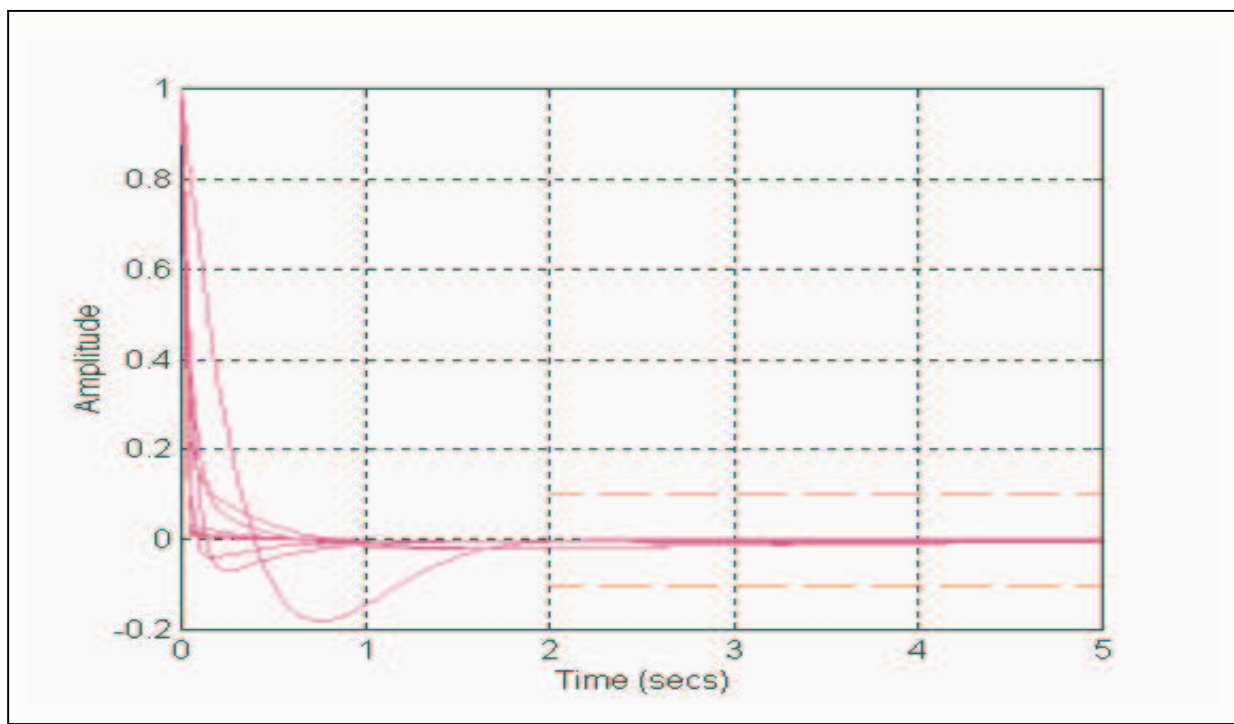**Figure 5.3.C:** Disturbance rejection of system with *PID* controller

Thus, the system satisfies the disturbance rejection for all values of uncertain parameters of the plant in all cases of controllers.

Overall, it has been seen from the tracking and disturbance simulation results that all designs met both the tracking and the disturbance rejection specifications.

CONCLUSIONS

This project report includes the full work done on the design of a system characterised by a large uncertainty due to the variation of uncertain parameters of the plant. The work involved familiarisation with Matlab and extensive reading on QFT theory, software design and design examples. The frequency responses and the simulation results have shown that the design of a SISO system (including external disturbance inputs) proved to be successful for all controllers obtained. Thus, the least complex controller can be chosen as it satisfies the given specifications.

Future work includes implementation of the software with the use of GUIs and user interface menus. This design can be also extended to MIMO systems with large uncertainty. Moreover, the optimisation techniques can be applied for the design of more complex optimal controllers and also for the design of an optimal pre-filter.

The tracking specifications (in the form of bounds in the frequency domain) are obtained from the tracking control ratio, which is found from the desired tracking performance specifications usually for a step reference input. These characteristics are divided into *transient* (settling time t_s, peak overshoot M_p, and the peak time t_p, and the *steady-state* characteristics (gain A) [Ref.1,5].

The control ratio usually is approximated by simple first or second order models (*over-damped* or *under-damped* depending on the type of the response in the time domain). The transfer function of a second order system is:

$$M(s) = \frac{\omega_n^2}{s^2 + 2\zeta\omega_n s + \omega_n^2}$$

where ω_n and ζ can be obtained from the peak and settling time, i.e.

$$t_s = \frac{4}{\zeta\omega_n}$$

and

$$t_p = \frac{\pi}{\omega_n\sqrt{1-\zeta^2}}$$

Note that even if there are four input characteristics (t_s, M_p, t_p, A) only two parameters need to be found, thus if the above equations do not suffice to derive ω_n and ζ the following equation can be also used:

$$M_p = 1 + \exp\left(\frac{-\pi\zeta}{\sqrt{1-\zeta^2}}\right)$$

Of course, the derived tracking control ratio must be such that will satisfy the set requirements. In addition, the spread of the maximum and minimum tracking bound in the frequency domain at high frequencies has to be wide, such that the specifications will be met (the spread of the tracking bounds has to be larger than the actual variation at the plant at high frequencies) [Ref.1]. Thus either a zero or a pole has to be inserted in the control ratio (the zero to the upper tracking control

ratio and the pole at the lower tracking control ratio). To illustrate, consider the following two second order models:

$$M_{upper}(s) = \frac{x}{s^2 + ys + c}$$

and

$$M_{lower}(s) = \frac{r}{s^2 + ls + f}$$

Because the two models are 2nd order they have the same slope at high frequencies (*40 dBs*). To modify the asymptotic characteristics at high frequencies, they can be transformed to the following models, so that the variation of the system at high frequencies can be fit within the bounds, i.e.

$$M_{upper}(s) = \frac{x(s + x_1)}{s^2 + ys + c}$$

and

$$M_{lower}(s) = \frac{r}{(s^2 + ls + f) \times (s + r_1)}$$

where x_1 is a zero which reduces the asymptotic attenuation rate of the upper model and r_1 is a pole which increases the attenuation rate of the lower model. As a result the spread between the two corresponding bounds will become wider at high frequencies and it will tend to infinity as $\omega \to \infty$ (see figure below).

Before introduction of poles/zeros   After introduction of poles/zeros
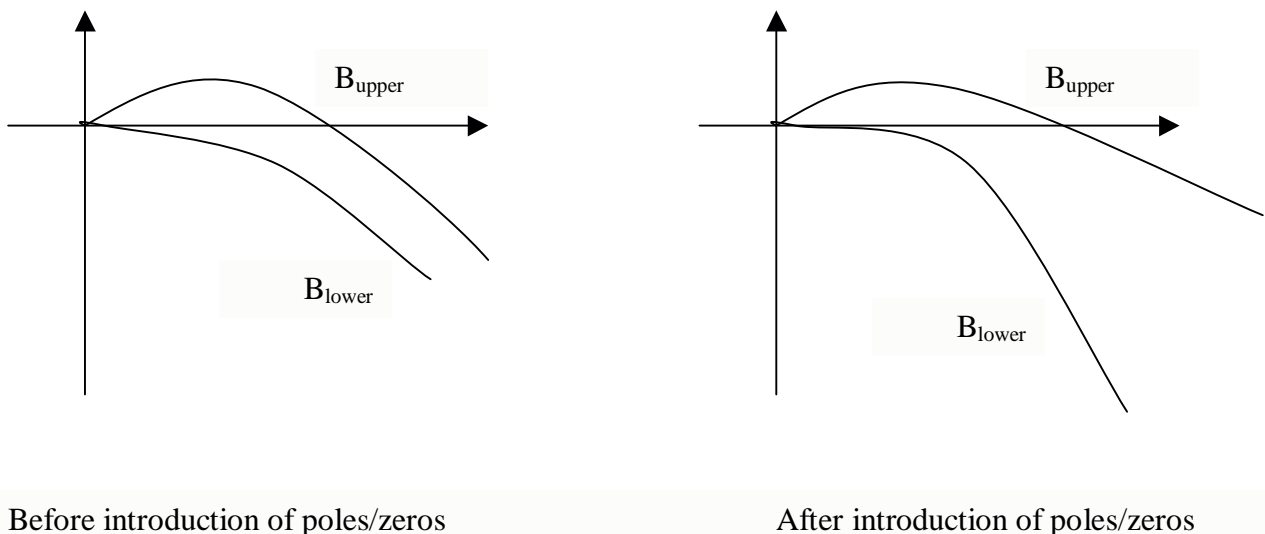
Figure A.1: Comparison of spread before and after the introduction of poles/zeros in the models

Note that the derived models have to be consistent with the degrees of the numerator and the denominator of the uncertain plant used (i.e. have to be realisable)[Ref.1]. Thus in certain occasions a suitable first or second order system cannot be found in order to satisfy simultaneously all specifications. In this case a higher order model control ratio is desired and usually it is given according to the input specifications (e.g. see the tracking specifications in Section 2.3) [Ref.1]. The analysis and design of high order model control ratios is not a purpose of this project.
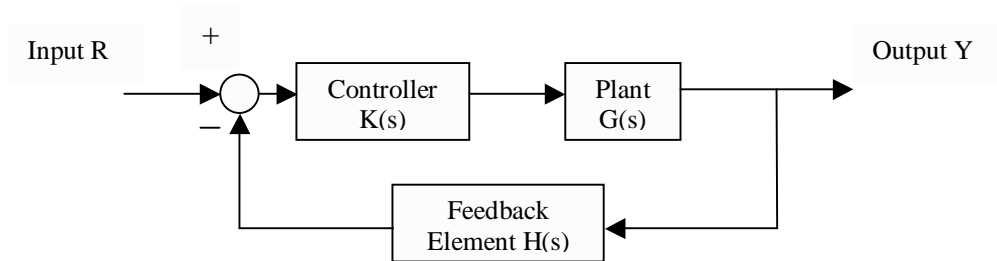
Consider the feedback system in figure B.1,

Figure B.1: Feedback (negative) system

The CL transfer function between the input (reference) and the output signal is:

$$T(s) = \frac{G(s)K(s)}{1 + G(s)K(s)}$$

Note that *H(s)* is usually unity (i.e. *H(s)*=1). The frequency response of *T(s)* is given by,

$$T(j\omega) = \frac{G(j\omega)K(j\omega)}{1 + G(j\omega)K(j\omega)}$$

The magnitude of *T(jω)* is then given as,

$$|T(j\omega)| = \left| \frac{G(j\omega)K(j\omega)}{1 + G(j\omega)K(j\omega)} \right|$$

The locus of all points where,

$$|T(j\omega)| = M$$

is known as *M-circles* of values *M*.

The equations of *M-circles* in the Nyquist plane are given below:

D

Let $G(j\omega)K(j\omega)=x+jy$ (complex co-ordinates description on the NP). Thus,

$$\left|T(j\omega)\right| = \left|\frac{G(j\omega)K(j\omega)}{1+G(j\omega)K(j\omega)}\right| := M$$

or

$$M = \frac{\sqrt{x^2 + y^2}}{\sqrt{(1+x)^2 + y^2}}$$

Taking squares of both sides,

$$M^2 = \frac{x^2 + y^2}{(1+x)^2 + y^2}$$

which can written,

$$M^2\left[(1+x)^2 + y^2\right] = x^2 + y^2$$

Rearranging,

$$x^2\left(1-M^2\right) + y^2\left(1-M^2\right) - 2xM^2 = M^2$$

Dividing by $(1-M^2)$ we have,

$$x^2 + y^2 - 2x\frac{M^2}{\left(1-M^2\right)} = \frac{M^2}{\left(1-M^2\right)}$$

and adding the term $\left[\dfrac{M^2}{\left(1-M^2\right)}\right]^2$ to both sides,

$$x^2 + y^2 - 2x\frac{M^2}{\left(1-M^2\right)} + \left[\frac{M^2}{\left(1-M^2\right)}\right]^2 = \frac{M^2}{\left(1-M^2\right)} + \left[\frac{M^2}{\left(1-M^2\right)}\right]^2$$

which can be written,

E

$$\left(x-\frac{M^2}{1-M^2}\right)^2 + y^2 = \left(\frac{M}{1-M^2}\right)^2 \qquad \text{(b.1)}$$

This equation represents a circle on the Nyquist plane with centre at point $\left(\frac{M^2}{1-M^2},0\right)$ and radius

$\frac{M}{1-M^2}$. In figure B.2 various circles of *M*-values are plotted. Note that the circles to the left of

point $g=\left(-\frac{1}{2},0\right)$ have values *M*>1 and the circles to the right of point *g* have values *M*<1. In the

case of *M*=1 the circle becomes a straight line ('circle with infinite radius') as can be seen from
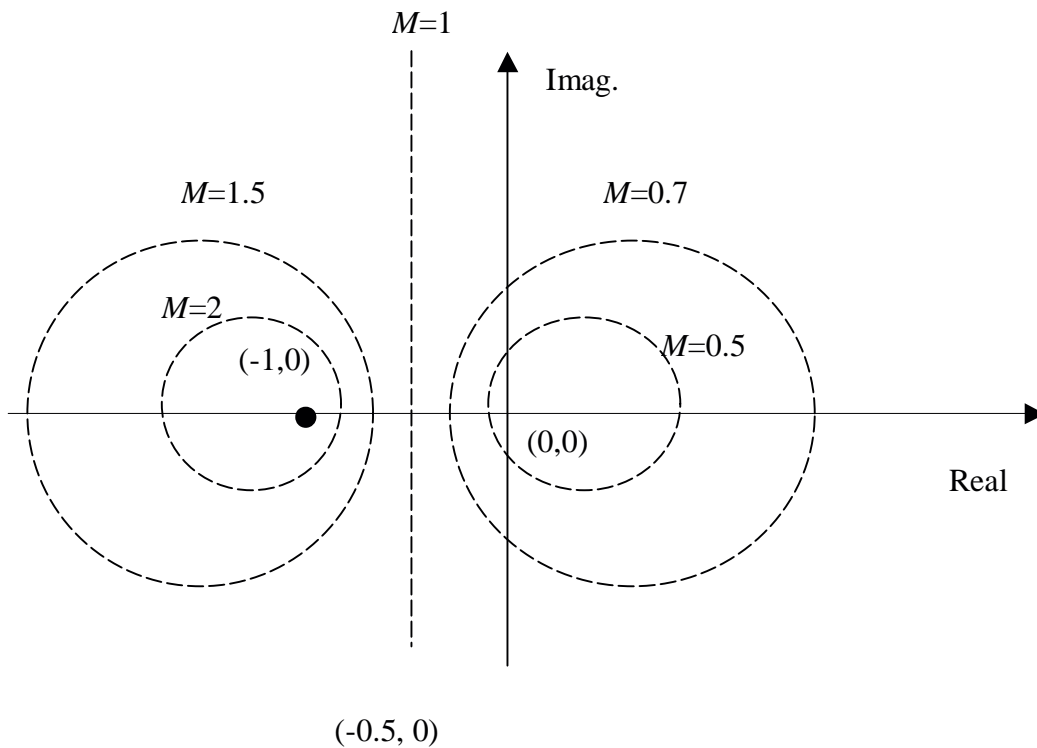
equation (b.1) [Ref.5].

Figure B.2: Nyquist Plane with constant M-circles

Unlike the representation of *M-circles* on the Nyquist plane, the representation on the Nichols chart

is different. *M-circles* on the NC depend on their *M-value*, i.e. when *M*>1 the *M-circles* on the NC

are closed contours while for *M*<1 they are open contours tending to straight lines as *M* decreases.

In the case of *M*=1 the *M-circle* is an open contour which tends to infinity. Figure B.3 shows the NC with various *M-circles*.
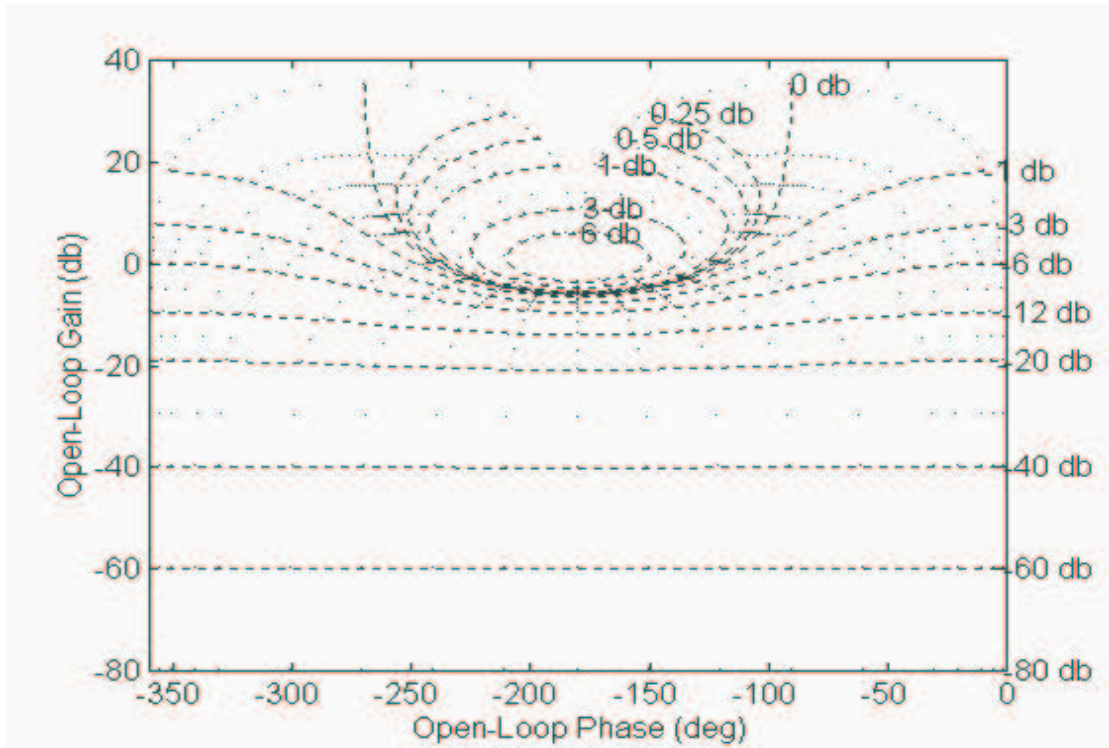

Figure B.3: NC with a range of M-circles

In order to convert the constant *M-circles,* defined at given phases, from the Nyquist plane to the NC, functions **m_cir()** and **m_grid1()** are used. The procedure followed is the following.

In order to represent the *M-circles* in the NC we have to solve simultaneously two equations,

$$\left(x - \frac{M^2}{1-M^2}\right)^2 + y^2 = \left(\frac{M}{1-M^2}\right)^2 \tag{b.2a}$$

and

$$y = \gamma\, x \tag{b.2b}$$

where γ is the slope of the line $y = \gamma\, x$ for each angle of the phase vector (-360,0). The phases rotate anticlockwise.

In order to find a solution to the above set of equations, the line in (b.2b) must be either a tangent to the circle (then there is a double solution $x_1=x_2$ and it is real), or it must cross the circle (then there

G

are two real solutions $x_1 \neq x_2$). In the case where x_1 and x_2 are complex the line is neither tangent nor crosses the circle.

There are three possibilities for the *M-circles*:

(1) *M*>1

In this case the *M-circle* is a closed contour in the NC because it does not contain the origin (0,0) and there are solutions only for a given range of slopes γ. Figure B.4 shows such an *M-circles*.

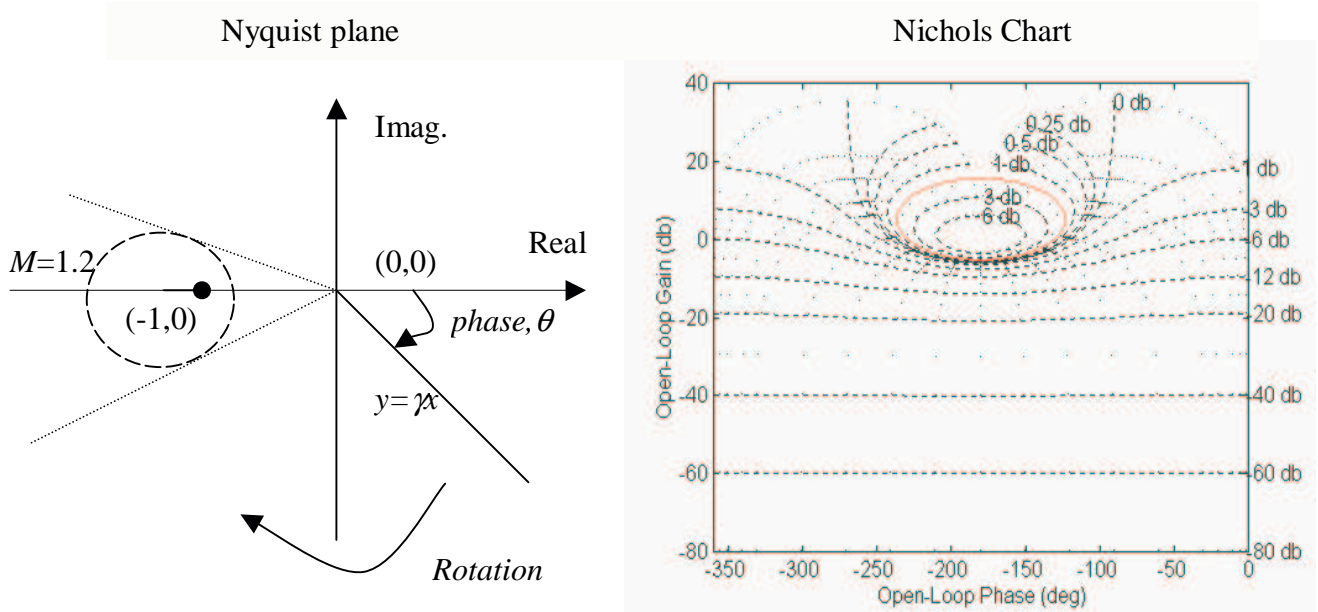**Figure B.4:** Conversion of M-circle (M>1) from NP to NC

(2) *M*<1

The resulting *M-circles* in the NC are open contours and tend to straight lines as *M* decreases. Note that since the origin lies within the circle in the Nyquist domain, there exists a unique magnitude for each phase (i.e. a directed straight line through the origin intersects the *M-circle* at a unique point). As a consequence the *M-circles* in the NC are open contours.

Nyquist plane   Nichols Chart

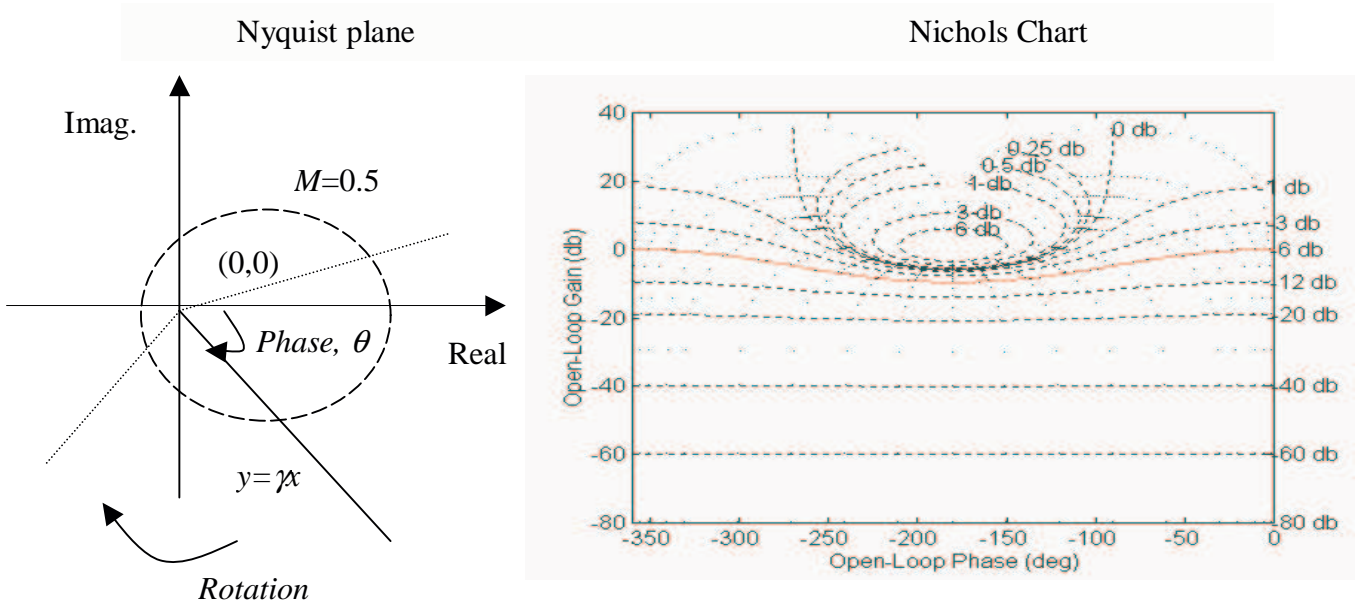**Figure B.5:** Conversion of M-circle (M<1) from NP to NC

(3) $M=1$

In the case $M=1$ the *M-circle* is a straight line in the NP with real part $x= -0.5$. The resulting M-circle in the NC is an open contour which tends asymptotically to infinity at phases $–270^o$ and $–90^o$. This is because (as can be seen from figure. B.6) the phase of the *M-circle* in this case is always in the interval $(-270^o,-90^o)$.

Nyquist plane   Nichols Chart
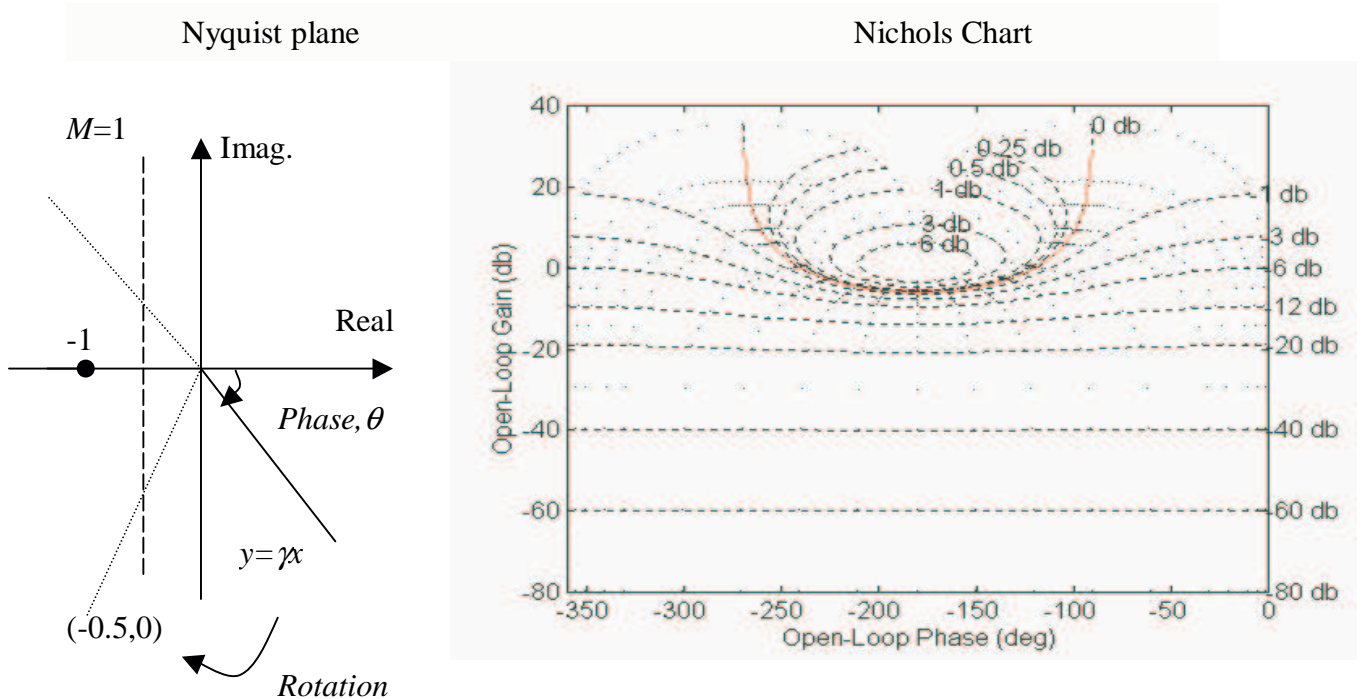

Figure B.6: Conversion of M-circle (M=1) from NP to NC

A matrix $A \in \mathbf{R}^{n \times m}$, i.e. A is an $n \times m$ matrix (n rows and m columns where $n < m$) with real elements, can be written as:

$$A = \begin{bmatrix} a_{11} & a_{12} & \ldots & \ldots & a_{1m} \\ . & . & a_{ij} & . & . \\ a_{n1} & \ldots & \ldots & \ldots & a_{nm} \end{bmatrix}$$

The range of A, $\mathcal{R}(A)$, is defined as,

(1)
$$R(A) = \left\{ Ax \,\middle|\, x \in \mathbf{R}^m \right\} \subseteq \mathbf{R}^n$$

Then $\mathcal{R}(A)$ is a subspace of $\mathbf{R}^n$. To see this take any two vectors y_1 and y_2 in $\mathcal{R}(A)$, i.e. let

$$y_1 \in R(A), \text{ where } y_1 = Ax_1, \text{ for some } x_1 \in \mathbf{R}^m$$

and

$$y_2 \in R(A), \text{ where } y_2 = Ax_2, \text{ for some } x_2 \in \mathbf{R}^m$$

Then it follows that,

$$ay_1 + \beta y_2 = A(ax_1 + \beta x_2) \in \mathbf{R}^m$$

(2)
$$Ker(A) = \left\{ x \,\middle|\, Ax = \underline{0}_n \right\} \subseteq \mathbf{R}^m$$

$Ker(A)$ is a subspace of $\mathbf{R}^m$. To see this take any x_1 and x_2 in $Ker(A)$, so that

$$Ax_1 = 0, Ax_2 = 0$$

Then

$$A(ax_1 + \beta x_2) = Aax_1 + A\beta x_2 = 0$$

which means that $ax_1 + ax_2 \in Ker(A)$ [Ref.8].

J

We can also define the following:

(a) If $S \subseteq \boldsymbol{R}^{\,m}$, we define $S^{\perp}$ as the set,

$$\mathbf{S}^{\perp} = \left\{z \,\middle|\, z^T y = 0 \text{ for all } y \in \mathbf{S}\right\} \subseteq \mathbf{R}^{m}$$

This also is a subset of $\boldsymbol{R}^{\,m}$.

(b) For the matrix $A_{n \times m}$, it can be shown that

$$\left[R(A)\right]^{\perp} = Ker(A^T) \subseteq \mathbf{R}^{n}$$

and also

$$R(A^T) = \left[Ker(A)\right]^{T}$$

Singular Value Decomposition (SVD)

Any matrix $A_{n \times m}$ where, $A \in \boldsymbol{R}^{\,n \times m}$ can be expressed as,

$$A = \begin{bmatrix} U_1 & U_2 \end{bmatrix} \begin{bmatrix} \Sigma_{\rho,\rho} & 0 \\ 0 & 0 \end{bmatrix} \begin{bmatrix} V_1^T \\ V_2^T \end{bmatrix}$$

in which $U=[U_1 \; U_2]$ and $V=[V_1 \; V_2]$ are orthogonal and $\Sigma_{\rho,\rho}$ is a diagonal matrix with positive diagonal entries (these are known as the *singular values* of A) [Ref. 8].

A, can be written alternatively as,

$$A = U_1 \Sigma V_1^T$$

The Range and Kernel of A can be easily obtained from relations:

$$R(A) = R(U_1)$$

and

$$Ker(A) = R(V_2)$$

In Matlab the *singular value decomposition* can be performed by using function **svd()** which has the following form, $[U,S,V]$=svd(A).

K

LIST OF REFERENCES

[1]. D'Azzo, J J, Houpis, C H, *'Linear Control Analysis and Design: conventional and modern'*, 1995, McGraw-Hill

[2]. Maciejowski, J M, *'Multivariable Feedback Design'*, 1989, Addison-Wesley

[3]. Horowitz, I M, *'Quantitative Feedback Theory'*, IEEE proceedings, Vol. 129, part D, no. 6, pp 215-226, November 1982

[4]. Bryant, G F, Halikias, G D, *'Optimal loop-shaping for systems with large parameter uncertainty via linear programming'*, 1995, Int. J. Control, Vol. 62, no. 3, pp 557-568

[5]. Dorf, R C, Bishop, H B, *'Modern Control Systems'*, 7th Edition, 1995, Addison-Wesley

[6]. Fletcher, R, *'Practical Methods of Optimisation: Unconstrained Optimisation'*, Vol.1, 1980, Wiley & Sons

[7]. Saadat, H, *'Computational Aids in Control Systems using Matlab'*, 1993, McGraw-Hill

[8]. Horn, R A, Johnson, C R, *'Matrix Analysis'*, 1990, Cambridge University Press

CONFIRMATION OF WORK

I confirm that the work submitted is my own and appropriate references have been made to the work of others.

Argyrios Zolotas